

First Interim Technical Report

CONSTRICTED HIGH ENTHALPY ARC HEATER DESIGN AND
PERFORMANCE DATA, INCLUDING CALCULATIONS FOR A
10 MW DESIGN

Prepared for
NASA Manned Spacecraft Center
Structures and Mechanics Division
Entry Environment Simulation Branch
2101 Webster-Seabrook Road
Houston, Texas 77058

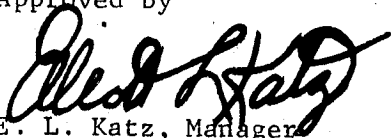
Contract No. NAS 9-3564

EOS Report 6320-2Q-1

27 August 1965

Prepared by
Robert Richter
Rolf D. Buhler
Gary L. Marlotte

Approved by


E. L. Katz, Manager
FLUID PHYSICS DIVISION

ELECTRO-OPTICAL SYSTEMS, INC., - PASADENA, CALIFORNIA
A Subsidiary of Xerox Corporation

CONTENTS

1.	INTRODUCTION	1-1
2.	SOME GENERAL TRENDS AND SCALING RULES	2-1
	2.1 General Comments	2-1
	2.2 Method of description for the Evolution of Simple Scaling Rules and Trends	2-2
	2.3 Small, Conduction-Governed Tube Arcs	2-4
	2.4 Large, Radiation-Governed Open Arcs (without Cross Flow)	2-6
	2.5 High Powered Tube Arcs	2-10
	2.6 Constricted Arc Gas Heaters	2-14
3.	COMPUTER CALCULATIONS	3-1
	3.1 Plasma Property Formulation	3-1
	3.2 Comparison of Cases	3-5
	3.2.1 Calculations for a 0.5 cm Diameter Constrictor	3-5
	3.2.2 Calculations for a 2.0 cm Diameter Constrictor Comparing "Yos-like" and "Maecker-like" Properties	3-11
	3.2.3 Calculations Showing Pressure Dependence for a 2.0 cm Diameter Constrictor	3-14
	3.2.4 Calculations Showing Current Dependence for a 2.0 cm Constrictor	3-14
	3.3 Calculations for a Large High-Power Device	3-22
4.	ONE MEGAWATT HEATER - BRIEF REVIEW OF PERFORMANCE DATA	4-1
	4.1 Correlation Between Total Enthalpy, Constrictor Exit Pressure, and Mass Flow Rate for Choked Flow Conditions	4-1

CONTENTS (contd)

4.2	Electric Parameters	4-8
4.3	Energy Transfer to the Constrictor Wall	4-20
4.4	Heater Efficiency	4-23
5.	EXTRAPOLATION TO LARGE SIZE CONSTRICTED ARC HEATERS	5-1
5.1	A Combined Analytical and Experimental Approach to the Design of Large Diameter Constricted Arc Heaters	5-2
5.2	Design and Performance Calculations for a 10 Megawatt Constricted ARC Heater	5-6
6.	CONCLUSIONS	6-1

ACKNOWLEDGEMENTS

This program is being carried out under Contract NAS 9-3564 under the technical direction of Mr. D. Greenshields and Mr. John Grimaud, Structures and Mechanics Division, NASA Manned Spacecraft Center. Their guidance through technical discussions is gratefully acknowledged. The writers are also indebted to numerous associates, both in and outside this company for valuable suggestions and discussions.

The staff of the Magneto Plasmadynamics Branch of the NASA Ames Research Center under Mr. Howard Stine supplied considerable assistance and information for this project, at the request of the Technical Monitor. This includes the computer runs listed and much other pertinent experimental and theoretical information supplied by Messrs. C. Shepard and V. Watson from their own arc heater studies. The writers wish to express their thanks for this important assistance, and hope that this most fruitful exchange of information will continue in the future.

1. INTRODUCTION

The purpose of this report is to present procedures for the design analysis and performance predictions of constricted (coaxial flow) arc air heaters for materials testing and atmospheric entry simulation. This design and performance analysis is to be based on comparisons of theoretical and experimental results covering constricted arc gas heaters and arc research cascades of various sizes. The experimental heater results cover a power range from about 30 to 1000 kw. The theoretical and semi-empirical heater calculations are carried up to the 10 MW level.

A range of heater enthalpies is covered, with emphasis on the "high enthalpy" regime ($\sim 20,000 - 50,000$ Btu/lb or $4.6-11.6 \times 10^7$ J/kg). This covers the most critical portions of the Appollo and similar Lunar parabolic earth return entry trajectories, and the lower half of the Mars return Earth entry spectrum.

This report summarizes, combines and compares the results of the following study phases:

- i) experimental measurements made with the $\frac{1}{2}$ cm internal diameter research arc cascade apparatus
- ii) theoretical calculations carried out for this program by the NASA Ames Research Center staff, using the Stine-Watson Constricted Arc Computer program
- iii) design calculations made for the 1 MW (2 cm diameter) constricted arc heater
- iv) measurements made with the 2 cm diameter (1 MW) Laboratory Model Arc Heater
- v) various scaling rules, theoretical and experimental results on arc columns and heaters obtained by different authors on other research programs (as referenced).

- vi) preliminary design calculations for a 10 MW high enthalpy constricted arc heater, based on the above results.

Since the time when this work and this report were first started, the outlook and the emphasis have shifted considerably, as a result of the experimental findings. When this report was first planned, it was expected that the theoretical and the experimental results on the 1 MW level would be in at least fair agreement. It was therefore planned to base the design procedures for the 10 MW case primarily on the theoretical calculations and scaling rules, with "minor" adjustments to bring about agreement with a few early test results from the 1 MW Laboratory Model heater. As the work progressed, it became apparent that the experimental results showed very different trends, as well as values, than the theoretical (computer) calculations.

Consequently it became necessary to accumulate and cross correlate a much larger body of experimental data from the 1 MW heater than originally anticipated before reasonably reliable design predictions and extrapolations to the 10 MW level could be made. Thus the shift in emphasis in this report is toward much more experimental information, empirical correlations and trends as the basis for extrapolation and design of large heaters. The size of the chapter on the 1 MW heater performance data reflects this.

At the same time, the portions on the theoretical calculations and the scaling rules based on these have been deemphasized. Clearly the heater theory will need much further basic study and improvements before it can be relied upon for design. This work is beyond the scope of the current program which is primarily concerned with the heater design and development.

The material of this report is organized as follows:

Section 2, contains general considerations of the scaling parameters and functional relationships between these parameters for constricted arc gas heaters.

Section 3, summarizes the pertinent results of the computer integrations carried out at the NASA Ames Research Center. These results are also compared (as far as is possible) with earlier numerical results on the asymptotic large arc column obtained by Yos and cross correlated here by Marlotte.

Section 4, covers a review of the experimental results obtained to date with the 1 MW Laboratory Model Heater, and cross plots which can form the basis for extrapolations and design calculations for larger heaters. The results from the $\frac{1}{2}$ cm (~ 100 kw) research arc cascade tests were not reproduced here because they no longer appear pertinent for the large heaters of interest though these results were very helpful in the design of the 1 MW heater.

Section 5, summarizes the design calculation procedures based on the (mostly empirical) results of Section 4. Typical design estimate numbers are given for a 10 MW high enthalpy constricted arc heater. These results are briefly compared with those from a computer integration for the same size. The engineering feasibility of this heater is briefly discussed.

2. SOME GENERAL TRENDS AND SCALING RULES

2.1 General Comments

Before discussing the detailed theoretical and experimental results on arc heaters in the three size ranges (100, 1000, 10,000 kw), it may be helpful to review those general scaling rules and other trends for arcs and arc heaters which are known. This background should serve both for the interpretation and correlation of the theoretical and experimental results (Sections 3 and 4) and for the design rules and extrapolations to be evolved in Section 5 of this report.

Most of the Laboratory research on arcs has been done in the past few years on small, tube confined arc columns at moderate pressures not too far from 1 atmosphere. Such arcs, with or without a superimposed axial gas flow, can be carefully and reproducibly observed in the Maecker type research cascade arc channel apparatus, so that many excellent sets of experimental data exist on such arcs. This regime covers arcs typically up to ~ 500 amp and constrictor channels mostly below 1 cm diameter. Also, for this regime, in which the gas flow can usually be assumed to be laminar and in which radiation and self absorption usually play a secondary role, good approximate theoretical descriptions exist which seem to agree with the experiments to within the uncertainties of the transport properties. For nitrogen and air the theoretical high temperature transport properties are still uncertain to within factors of 2 or 3. Therefore the procedure has been for this laminar regime to use transport property curves obtained by the mathematical inversion of arc measurements ("Maecker-like" properties of Section 3). With these properties consistent "theories" are obtained which seem to adequately describe this regime, including the scaling as far as this has been tested. However, when the same (supposed by empirical) transport properties are used to calculate much larger constricted arcs, large discrepancies arise which are not yet understood.

Much more powerful arcs, both open and enclosed, are extensively used in furnaces, chemical reactors, wind tunnel heaters, as well as for welding and cutting. But such arcs are harder and more expensive to run in laboratory research apparatus, so that for the high power regime really few sets of data exist which are sufficiently complete and controlled to be useful as research information. Theoretical descriptions for the high power, high pressure arc regime are much more difficult due to the possible importance of electro-magnetic forces and instabilities, fluid flow turbulence, radiation and self absorption which have to be taken into account. Therefore, the highpowered arc, while extensively used in practice, is only very poorly understood theoretically or experimentally in a basic way. Nevertheless, it is for this high power, high pressure regime that good engineering predictions and design procedures are most urgently needed, since wind tunnel and materials test jet arc heaters in the 10 to 100 MW regime will be needed in the immediate future. Clearly these high powered devices are too expensive to permit development of a pure "Edisonian" trial and error basis.

2.2 Method of Description for the Evolution of Simple Scaling Rules and Trends

The arc-gas flow interaction in a constricted arc gas heater is, of course, a very complicated three dimensional phenomenon, which is accurately described only by a set of partial differential equations, namely the electromagnetic and the gas dynamic conservation equations for mass, momentum, energy and electric charge. The variables which enter into these equations are local gas properties, electric and gas dynamic intensities, etc., which, even under the assumption of fully axisymmetric conditions, vary with both the radial and the axial coordinates, r and z , throughout the region.

However, to make possible a much simpler, though coarser, kind of analysis and, in particular, to obtain simple scaling and design formulas, we attempt to describe the constricted arc and gas flow

without taking account of detailed radial distributions, (i.e., in the manner of a one-dimensional flow model). This type of description which for the arc is called the wire (or "Kanal") model, brings the description down to the following types of variables:

- a) Integral quantities which are descriptive of the whole arc-gas flow region (or the whole heater), such as
 - I total current
 - V overall voltage
 - M total mass flow
- b) Geometric variables describing the whole heater, such as
 - R constrictor radius (usually constant along the length)
 - L constrictor length
- c) Local intensive or extensive quantities which have been averaged in a suitable manner over the cross section of either the arc or the whole constrictor tube at one axial station. Thus these "representative" local gas properties or other parameters become functions only of the axial coordinate z :
 - $r_1(z)$ effective arc radius
 - $p(z)$ mean gas pressure at the station z
 - $\bar{h}(z)$ mass averaged enthalpy
 - $\bar{\phi}(z)$ mass averaged heat conduction potential
 - $\bar{\rho}(z)$ space averaged density
 - $\bar{w}(z)$ space averaged velocity
 - $\bar{\sigma}(z)$ space averaged electric conductivity
 - $\bar{u}(z)$ space averaged radiation density
 - $E_z(z)$ local (axial) electric field strength

In the following the $\bar{\quad}$ and \sim signs will be omitted, but in the dimensional and other simple equations given the variables are to be regarded as

representative values at one station, in the spirit of the one-dimensional description.

2.3 Small, Conduction-Governed Tube Arcs

When an arc is drawn through a relatively small constrictor tube at modest pressures, the whole physical behaviour is governed by the balance of ohmic heating and thermal conduction. Typically, this applies to nitrogen arcs of a few hundred amperes in a $\frac{1}{2}$ cm radius tube at one atmosphere (i.e., when $pR \leq 250$ Newt/m). For hydrogen this holds up to larger tube sizes and/or higher pressures.

Since the conduction is to the tube wall, the essential length variable in the radial (space like) direction is the tube or constrictor radius R . If we consider first the "infinitely long" constricted laminar arc column (with or without axial flow, i.e., the Heller Elenbaas case), then the essential variables are:

$$r_1, R, I, E, \sigma, \phi, \text{ and possibly } u$$

A set of dimensionless parameters for this case is then:

$$\frac{r_1}{R}, \frac{I^2}{R^2 \sigma \phi}, \frac{E I}{\phi}, \text{ and possibly } \frac{u R^2}{\phi} \quad (2.1)$$

The radiation u and the last parameter of the group (which for this case is much smaller than unity) could have been omitted for this case.

Upon closer examination and integration of the energy balance (Heller Elenbaas) equation, it turns out that

$$E R = f_1(I/R, \text{ gas properties and pressure}) \quad (2.2)$$

$$r_1/R = f_2(I/R, \text{ gas properties and pressure}) \quad (2.3)$$

$$\phi = E I \cdot f_3(\text{gas properties and pressure}) \quad (2.4a)$$

also

$$\phi = f_4(I/R, \text{ gas properties and pressure}) \quad (2.4b)$$

The mean enthalpy h comes out also roughly proportional to the power per unit length, $E I$. By "gas properties" we mean here simply the

relation between σ and ϕ , roughly the effective slope of the σ vs ϕ curve. The dependence on the pressure is weak. The radiation term u , when introduced becomes a small correction which gets larger for higher pressures, channel radii, and currents. The above relations are, of course, compatible with the dimensionless parameters (2.1). In particular, the basic current scaling parameter is always I/R as seen from the second parameter in 2.1. The proportionality between ϕ and $E I$ is seen from the third parameter of 2.1.

The scaling rules (2.2)-(2.4) state that, for a given gas and pressure in this regime the arc temperature, enthalpy, etc. are determined by one parameter, I/R . For a given arc state (I/R) the voltage gradient is then inversely and the current directly proportional to the channel size R , and the power per unit length, $E I$, required to produce this state or mean gas temperature is independent of the size R .

For the subsequent discussion of arc heaters these points are important, which follow immediately from the relations for the "infinitely" long or asymptotic constricted arc column:

The heat loss to the wall per unit length equals $E I$ (the power input). This is proportional to ϕ , and roughly proportional to the enthalpy h . However the wall heat load (per unit of wall surface area) is given by

$$q_w = \frac{E I}{2 \pi R} \propto \frac{\phi}{R} \approx \frac{h}{R} \quad (2.5)$$

Thus in the conduction dominated regime, high enthalpy gas is easier to contain (lower q_w) the larger the constrictor. Also, in a larger constrictor the same enthalpy is obtained with a much lower power

density $\left(\frac{E I}{\pi R^2} \right)$.

2.4 Large, Radiation-Governed Open Arcs (without Cross Flow)

Large open arcs without cross flow have not yet been completely analyzed theoretically. Some work on this is presently being carried out, (e.g., by V. Watson*), but the last word has not yet been written. In particular, it is not yet clear whether such a hypothetical arc (infinitely long, in an atmosphere without gravitational convection) would grow indefinitely with time or with length, though it appears probable that it would mathematically approach a finite asymptotic size. Because of this indefinite size and because self absorption of radiation must become important here, such arcs are much more difficult to describe or analyze in an approximate manner. However dimensional analysis or a simplified (wire model type) energy equation** shows that there is, for large arcs, a radial scaling parameter r_u , given by the dimensionless group $I^2/(\pi^2 \sigma u)$, which is obtainable from the last two parameters in 2.1, by division. The hypothetical radius

$$r_u = \left[\frac{I^2}{\pi^2 \sigma u} \right]^{\frac{1}{4}} \quad (2.6)$$

expresses the fact that a wire model arc of radius r_u would (neglecting self absorption) radiate as much power per unit length as it would dissipate by ohmic heating, since

$$\pi r_u^2 u = I^2 / \left(\pi r_u^2 \sigma \right) = E_u I$$

Thus, if the luminous core reached a radius equal to r_u while still remaining optically thin, it would be in "radiation equilibrium" and could not grow rapidly thereafter. Note that for nitrogen (Yos) the quantity $(\sigma u)^{-\frac{1}{4}}$ remains practically constant above $\sim 15000^\circ\text{K}$ for each pressure but decreases slowly with increasing pressure (Fig. 2.1). Thus the scaling length r_u becomes, for high currents, independent of the temperature per se, but is proportional to $I^{\frac{1}{2}}$, and decreases like $p^{-\frac{1}{2}}$ with

* NASA Ames Research Center, Verbal communication to the writers.

** R. D. Buhler, Technical Note in preparation.

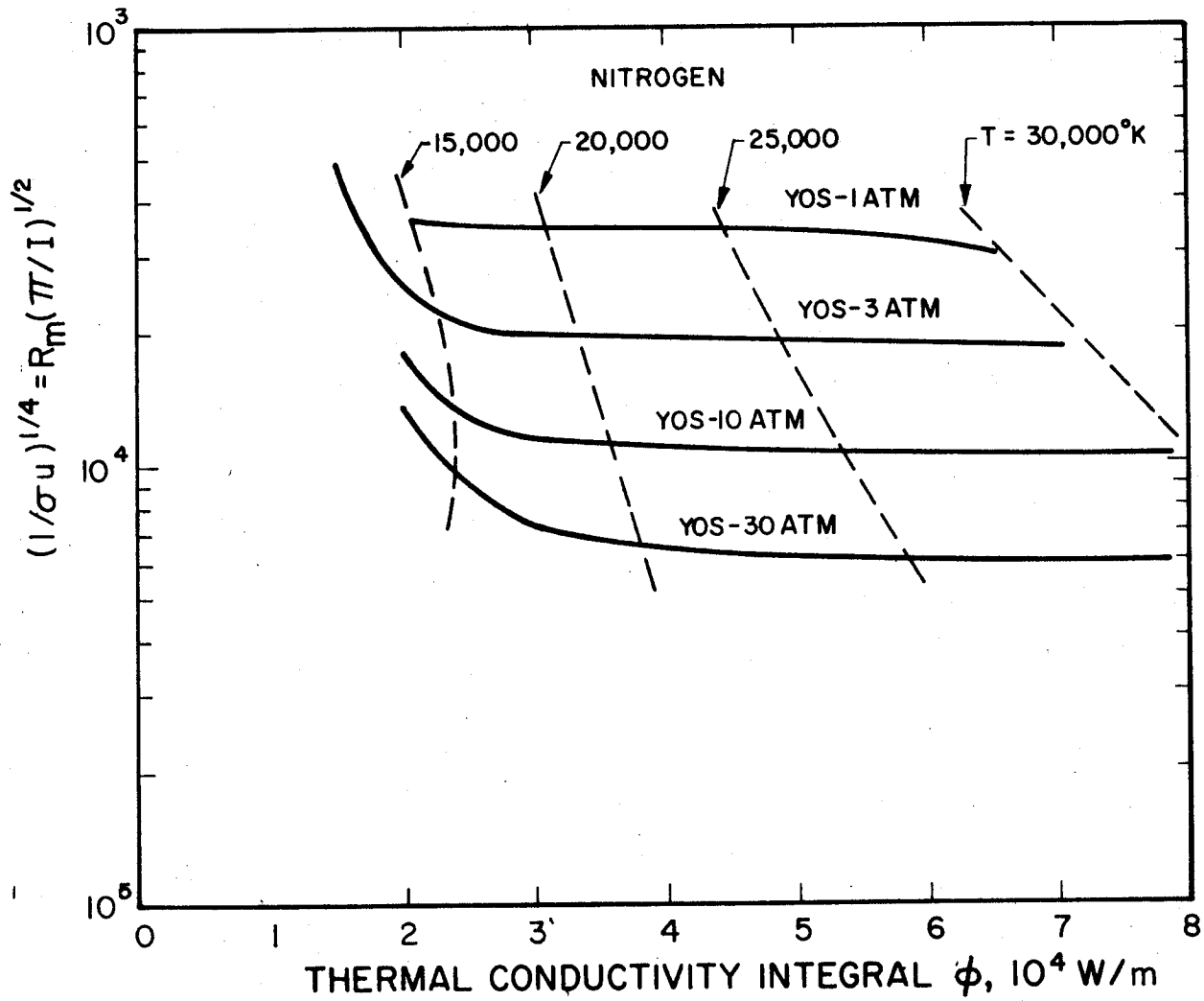


FIG. 2-8 ARC SIZE PARAMETER $(1/\sigma u)^{1/4}$ FOR NITROGEN

increasing pressure. For 1000A at one atmosphere pressure, $r_u \approx 6$ mm, or 7.4 mm at 1500A.

If r_u were the correct asymptotic wire model arc radius, then the corresponding approximate electric field for the open arc would be

$$E = \sqrt{\frac{u}{\sigma}} \quad (2.7)$$

According to the gas properties of Yos (ref. 1) the quantity u/σ becomes nearly independent of the temperature for diatomic gases above a certain temperature, at least for a considerable span of temperatures. For nitrogen (according to Yos) at one atmosphere, $\sqrt{u/\sigma} \sim 8-10$ V/cm for temperatures between 15,000 and 30,000°K. (See Fig. 2.2 which gives σ/u)

From these simple considerations one would expect that the voltage gradient of large, open arcs with minimal convection effects should be substantially independent of the current, and depend only on the pressure (Note that $\sqrt{u/\sigma}$ is a strong function of the pressure, according to Yos. See Fig. 2.2).

Empirically these trends are borne out quite well. King (Ref. 2) states that the voltage gradients of large open arcs in atmospheric air, when convection and electrode effects are small, are always close to 10 V/cm, for all currents above ~ 100 amp which were investigated. Also it is known that this potential gradient increases with the pressure.

$\sqrt{u/\sigma}$ increases like $p^{.85}$ at high temperatures but more slowly

$(\sim p^{.5})$ below 15000°K.

For such arcs the power per unit length, or the power radiated would then be

$$E I \approx I \times f(\text{pressure, gas properties}) \quad (2.8)$$

$$\approx I \sqrt{u/\sigma}$$

The simple considerations given here clearly do not represent an accurate theoretical description of an open arc, since conduction, self absorption, and the temperature profile were totally ignored. However these relations show some of the observed trends and can serve as a rough guide.

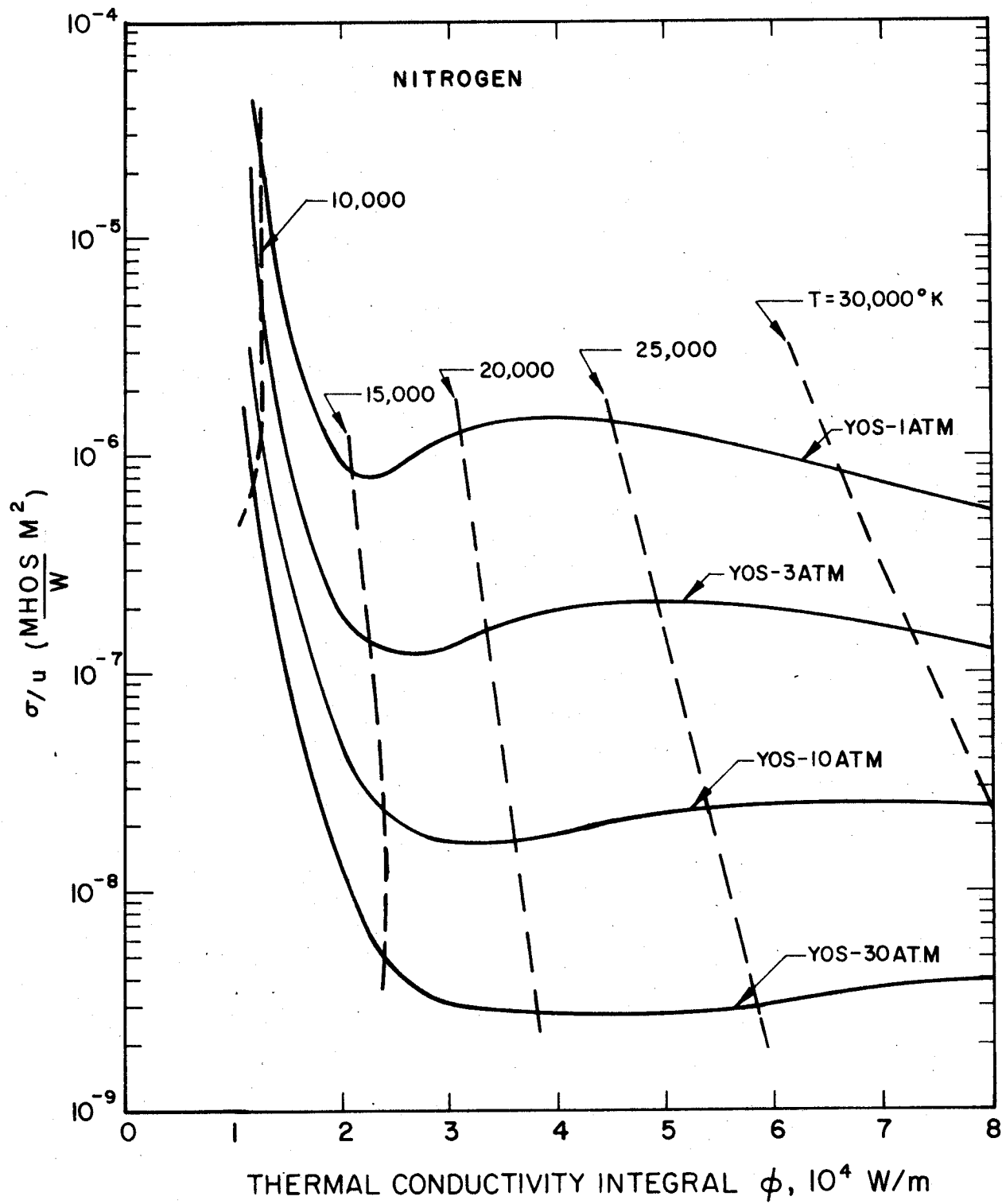


FIG. 2-2 ARC CONDUCTANCE FUNCTION, σ/u ,
FOR NITROGEN

2.5 High Powered Tube Arcs

If the enclosing tube is large compared with r_u , then it is not yet clear whether the tube has appreciable influence on the arc, except for slightly increased thermal conduction. In that case the arc should behave substantially like a large open arc. However, if the constrictor is sufficiently small so that the arc can "fill out" the tube, i.e., if

$$R \lesssim \left(I^2 / \pi^2 \sigma u \right)^{1/2}$$

then the constrictor radius R must become the governing size and an important scaling length.

Let us now assume that the product of arc radius and pressure is large enough that the radiative heat transfer term predominates, i.e.

$$u R^2 / \phi \gg 1, \text{ or better } \frac{u r_u^2}{\phi} = \frac{I}{\phi \pi} \sqrt{\frac{u}{\sigma}} \gg 1$$

but yet, that the arc is still optically thin for practical purposes, i.e., that most of the radiated energy (except that from the far ultra violet region) gets out. Then we will for such arcs have the following trends and scaling rules:

$$E = \frac{I}{\pi R^2 \sigma} \approx \frac{\pi R^2 u}{I} \approx \sqrt{\frac{u}{\sigma}} \quad (\text{neglecting thermal conduction})$$

$$E I = \frac{I^2}{\pi R^2 \sigma} \approx \pi R^2 u + \text{conduction term}^* \quad (2.9)$$

$$\approx I \sqrt{\frac{u}{\sigma}} + \text{conduction term}^*$$

* small correction term

$$\sigma u \approx \left(\frac{I}{R^2 \tau} \right)^2 - \text{conduction term*} \quad (2.10)$$

As before under 2.4 the basic variable which sets the arc temperature etc. is the current density, I/R^2 . Clearly τu is a unique function of the gas temperature and pressure.

Again for these arcs there is a tendency for E to be nearly independent of current, temperature, etc. and to depend primarily on the pressure & gas type, since at high temperatures ($\sim 15,000 - 30,000^\circ\text{K}$). u/σ is practically a constant at each pressure.

It appears from these simple relations that for large values of I/R^2 the conduction term must become more important again. This is seen from the last equation above since τu reaches a stationary value at high temperatures. For example, for nitrogen at 1 atmosphere,

$$\sqrt{\tau u} \approx 800-1100 \text{ amp/cm}^2$$

for all temperatures between $\sim 15,000$ and $30,000^\circ\text{K}$, according to Yos. (Ref. 1) Consequently, at current densities above roughly 800 amp/cm^2 , the conduction term must increase more rapidly than the radiation term, and the ratio of radiation to conduction heat transfer must decrease again with increasing I/R^2 . This peak in the radiation to conduction ratio really does occur, at least in the theoretical arc column calculations of Yos. Marlotte estimates from his crossplots of the Yos results (Ref. 3 Fig. 13) that the ratio of the radiative to the conductive heat transfer has, at one atmosphere a maximum at about 900 amp/cm^2 . Note that the condition $\sqrt{\tau u} \approx I/R^2$ is precisely the same as $r_u \approx R$. Thus when r_u approaches the constrictor size, a "filling out" of the constrictor is observed and the conduction increases more steeply from there on, for larger current densities. For example at $\frac{1}{2}$ atmosphere and 1500A, $r_u \approx 1.04 \text{ cm}$, so that we would expect to find a more rapid increase in convective heat load above that current for the 1 cm radius constrictor, while the radiative heat load should level out. The net result on the total heat load is not yet known for this high current density or wall constricted regime.

Even though the relative value of the conduction term increases again for higher values of I/R^2 , it still can remain relatively small for energy balance calculations, for many cases of interest here. However it is not yet negligible for our 1 MW heater.

It thus seems that, at least for large tube arcs, we should distinguish two regimes:

$$r_u \ll R \quad \text{"quasi open" arc regime}$$

$$r_u \geq R \quad \text{"filled out" or "wall constricted" regime}$$

We may further speculate that, for the "open" arc regime the radiant heat transfer to the wall (per unit length) should increase with the current and the pressure about as

$$\left. \begin{aligned} \dot{Q}_R &\approx E_u I \approx I \cdot \left(\frac{p}{\sigma u} \right)^{\frac{1}{2}} \\ &\approx I \cdot \left(\frac{p}{pa} \right)^{.9} \\ &\leq \pi R^2 u \end{aligned} \right\} \begin{array}{l} \text{for} \\ r_u < R \\ \text{or} \\ I < \pi R^2 \sqrt{\sigma u} \end{array} \quad (2.11)$$

The conductive transfer to the constrictor in this regime should be small.

When the arc fills the constrictor channel, i.e., when $r_u \approx R$, we would expect that the radiant heat transfer will no longer appreciably increase with the current and become a function of the pressure only. The conductive heat transfer, on the other hand, will from that point on increase fairly steeply with the current. Thus we expect the heat loss per unit length to behave roughly as follows:

$$\left. \begin{aligned} \dot{Q}_R &\rightarrow \pi R^2 u (p) \\ \dot{Q}_c &\propto \phi \approx \frac{I E (p)}{R^2} \\ &\approx \frac{I}{R^2} \sqrt{\frac{u}{\sigma}} \end{aligned} \right\} \text{for } I \geq \pi R^2 \sqrt{\pi u} \quad (2.12)$$

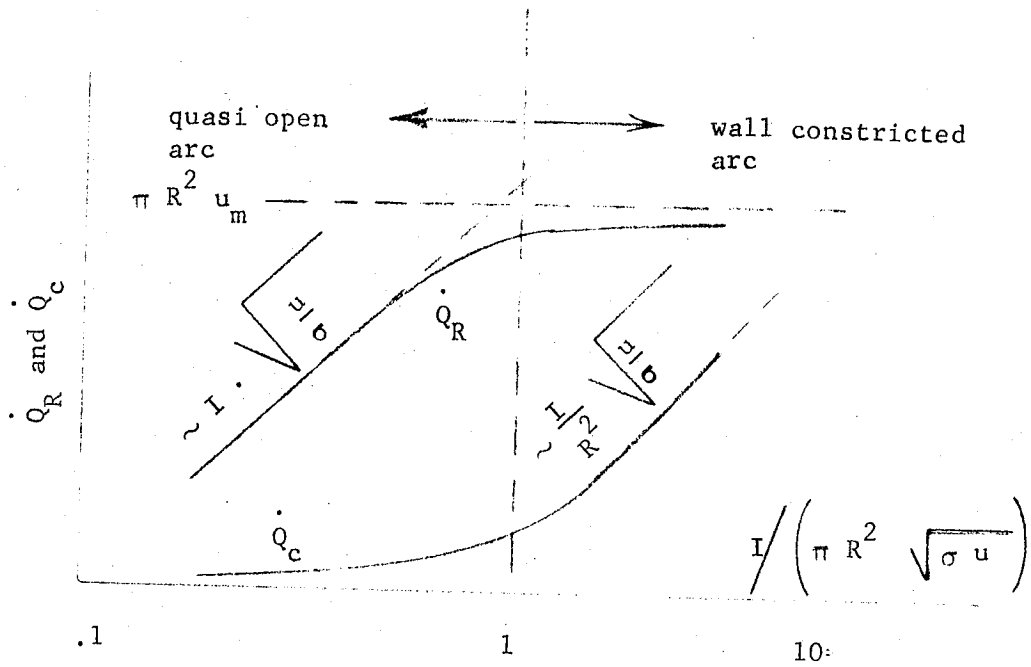


Fig. 2.3 Heat Loss Trends for Large Tube Arcs

(Tentative Postulated Model)

These simple behaviour trends and scaling rules are still partly speculative, but they appear to roughly describe the observed behaviour of such arcs.

2.6 Constricted Arc Gas Heaters

Both theoretical and experimental studies have been made for such heaters in the conduction governed regime (Ref 4 , 5). The theories are all approximations, (Refs 4 , 6 , 7) but extensive "exact" numerical integrations of the conservation equation (for laminar flow) have also been carried out (Ref. 8). Generally good agreement between the numerical solutions and the experiments is observed when the empirically adjusted ("Maecker like") transport properties are used. Even the simple approximate theories predict many of the general trends rather well, including the scaling rules.

The scaling parameters are the same as those for the asymptotic small (conduction dominated) arc column (see 2.2 above) except that one additional important parameter arises. When the arc and flow properties become functions of the axial distance z from some given initial point ($z = 0$), then this coordinate must be taken into the dimensional analysis. z is a time-like coordinate because in the energy equation the growth of the steady arc in the z direction is analogous to the growth of a non steady arc with time (transformation $z = wt$, where w is the axial gas velocity).

The new parameter which enters for the "inlet" or "gas heater" case is an axial heating length parameter first found by Stine and Watson (Ref 4)

$$z_0 = \frac{m \bar{C}_p}{\pi \bar{k}} = \frac{m h_\infty}{\pi \phi_\infty} = \frac{R^2 \bar{\rho} \bar{w} h_\infty}{\phi_\infty} \quad (2.13)$$

where \bar{C}_p and \bar{k} are mean values of the specific heat and the complete thermal conductivity, and h_∞ , ϕ_∞ are representative values of the enthalpy and conduction potential for the corresponding asymptotic

arc column, either both on the centerline or both mass averaged. $\bar{\rho} \bar{w}$ is the mean mass flow density through the heater. Note that z_0 is proportional to R^2 , for given pressure and flow conditions.

The quantity z/z_0 is related to the Péclet number of laminar heat transfer ($Re_z \cdot Pr$) which describes the rate of growth of a thermal boundary layer. Thus

$$\begin{aligned} \frac{z}{z_0} &= \frac{\phi z}{\rho w h R^2} = \frac{k}{u C_p} : \frac{u}{\rho w z} \cdot \frac{z^2}{R^2} \\ &= \left(\frac{1}{Pr} \cdot \frac{1}{Re_z} \cdot \frac{z^2}{R^2} \right) \propto \left(\frac{\text{thermal boundary layer thickness}}{\text{constrictor radius}} \right)^2 \quad (2.14) \end{aligned}$$

This is the pertinent scaling parameter for the growth of a zone heated by cross wise conduction into an axial flow.

However, in the present context the same number can be interpreted in a different way: $\phi_\infty \propto E_\infty I$ which is the heat power conducted to the wall (per unit length) in the asymptotic end state, and is also the electric power dissipated by Ohmic heating in that region. $\dot{m} h_\infty$ is the gas power flow across one station in the asymptotic region. Now, since

$$z_0 \phi_\infty = \dot{m} h_\infty \quad \text{by definition of } z_0 \text{ (see equ 2.13)}$$

$$\propto z_0 E_\infty I \quad \text{by equation 2.4}$$

therefore

$$z_0 \propto \frac{\dot{m} h_\infty}{E_\infty I} = z_H \quad (2.15)$$

z_H is a basic heating length derivable from first principles, namely that distance in which the Ohmic heating $E_\infty I$ would, without losses, produce the final power flow $\dot{m} h_\infty$. The Stine Watson z_0 is thus also proportional to the basic heating length z_H .

The simplified theories for these small constricted arc heaters then predict that all quantities which vary axially become functions of z/z_0 (or of z/z_H). For different operating conditions or different size heaters, points with the same value of z/z_0 are "similar" points. When z/z_0 becomes "large" all quantities must approach the values for the corresponding asymptotic constricted arc column solution.

From physical observations it is believed that in the regime the arc starts as a rather hot, small filament at the tube entrance and grows by conduction to the final size r_1/R , which is a function of I/R and of the gas. The mean enthalpy in the tube rises first steeply, then more slowly to the asymptotic value. The wall heat load rises roughly proportionally to the mean enthalpy except in the very first part of the tube inlet where this heat load is often virtually zero. The electric field is highest at the inlet and drops quickly to the asymptotic level.

The approximate theories mostly describe this general behaviour quite adequately, except for certain anomalies arising from the simplified models used. Moreover, the simple theories do give the right scaling parameters and rules, so that the theoretical results can usually be "doctored up", by empirical fitting of the physical constants (Cf Ref. 5) to give very adequate engineering descriptions for small, low pressure arc heaters.

For higher pressures and higher power levels the approximate theories which exist become generally more complicated, and hence less useful for engineering purposes. The reason appears to be that most of the theories start with the conduction dominated case and introduce the radiation like a perturbation. In this writers opinion it would be better to start with radiation only, i.e., substantially the open arc concept and then introduce conduction to the wall where it becomes important. The limited experimental data which are available to test this point certainly indicate that the conductive and convective heat transfer to the constrictor wall is substantially zero for much of the

constrictor inlet region, for the practically most important cases i.e., where the constrictor is sufficiently large. This indicated schematically in Fig. 2.3. Consequently it appears at present that the open arc scaling rules will be more applicable for the largest part of these higher powered heaters. Unfortunately the open arc scaling rules are not yet firmly established either.

Among the scaling parameters for the radiation governed case, two are useful for engineering correlations. One is the current-radius parameter r_u which was already discussed. The other is the heating length z_H which, for the radiation case becomes

$$z = \frac{\dot{m} h_{\infty}}{E_{\infty} I} = \frac{\dot{m} h_{\infty}}{\pi r_1^2 u} = z_u$$

This has physically the same meaning as discussed previously under z_H . It is thus directly related to the heater length required to produce a given outlet enthalpy.

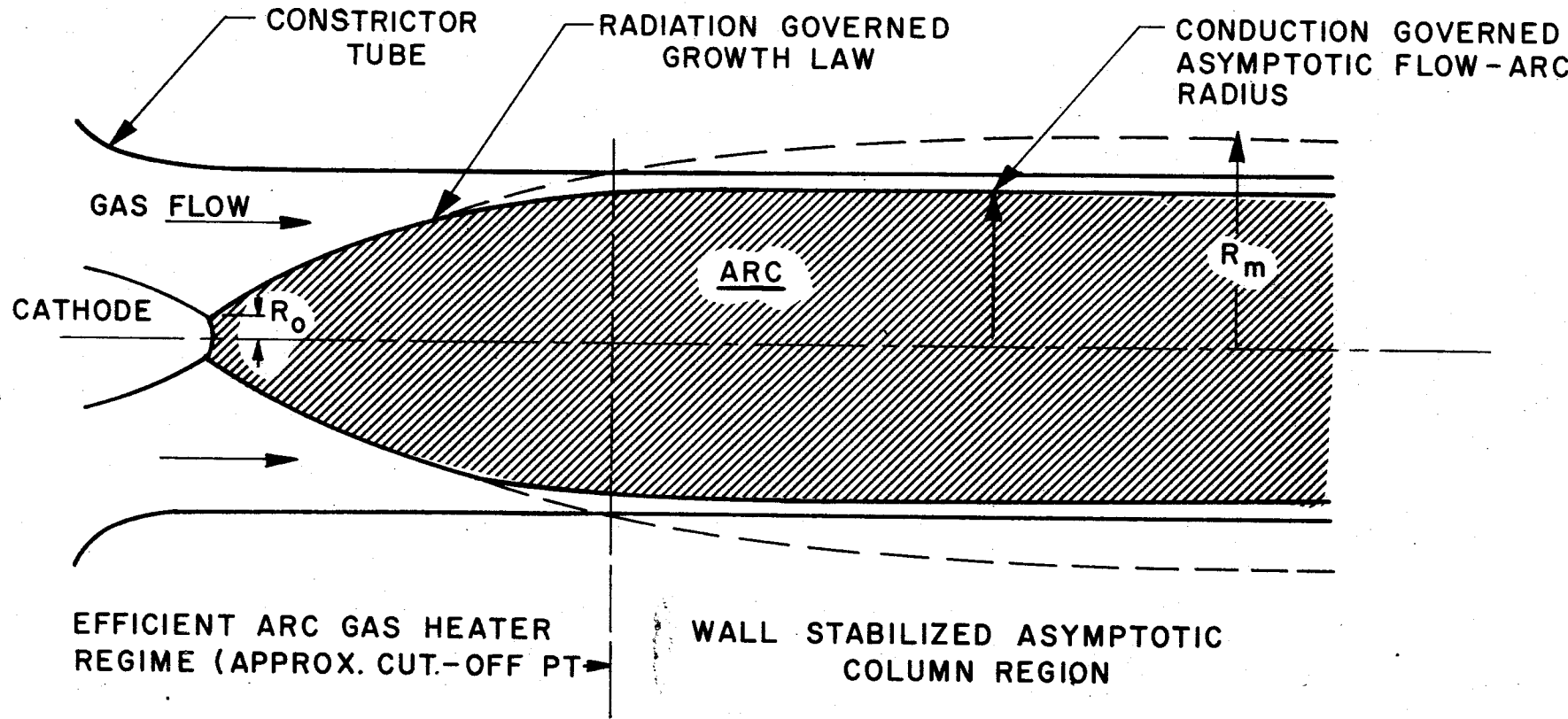


FIG. 2-3 TRANSITION FROM RADIATION TO CONDUCTION GOVERNED FLOW ARC - TYPICAL FOR HIGH ENTHALPY GAS HEATERS AND RESEARCH ARC COLUMNS (SCHEMATIC)

3. COMPUTER CALCULATIONS

Computer calculations were carried out by Velvin R. Watson of NASA/Ames using the Stine-Watson arc heater calculation program reported in Ref. 8 and discussed further in Ref. 9. Various cases defined by current, I , mass-flow, \dot{m} , constrictor radius, R , and stagnation pressure, p , were run. They corresponded to possible operating conditions of the present 2.0 cm I.D. device and others of interest.

In order to run cases using the computer program, it is, of course, necessary to decide what values of the various plasma properties are to be used. This is no trivial matter with nitrogen because of large uncertainties which exist in the properties.

The plasma properties of particular interest are enthalpy, thermal conductivity potential, electrical conductivity, and specific radiated power. Other properties such as viscosity, etc., remained unchanged from the values already incorporated into the program as reported in Ref. 8.

In addition to examining the effects of parameters such as current and pressure, a major objective was to examine the results of using various groups of plasma properties chosen so as to reflect the present uncertainties in the properties.

In order to accomplish this, three groups of properties were defined: "Yos-like", "Maecker-like", and "mixed". These classifications are discussed below.

3.1 Plasma Property Formulation

The work reported in Ref. 10 demonstrated that, if the plasma properties are chosen in a certain manner, the pressure dependency of the properties are approximated exceedingly well by powers

of pressure. Since the computer program is set up so that all properties are evaluated at a given value of enthalpy, h , and pressure, p , the plasma properties are defined as follows.

First, a reference enthalpy at atmospheric pressure, h_a , is obtained from the given values of h and p by the following relationship*:

$$h_a = h \left(\frac{p}{p_a} \right)^x \{h\} \quad (3-1)$$

Then the thermal conductivity integral

$$\phi = \int_0^T K \, dT$$

at the given pressure is determined directly, which yields

$$\phi\{h,p\} = \phi\{h_a\} \quad (3-2)$$

Electrical conductivity is given by

$$\sigma\{h,p\} = \sigma_a\{h_a\} \left(\frac{p}{p_a} \right)^s \{h_a\} \quad (3-3)$$

Similarly, the specific radiated power is given by

$$u\{h,p\} = u_a\{h_a\} \left(\frac{p}{p_a} \right)^t \{h_a\} \quad (3-4)$$

The various curves labeled "Yos-like" in Figs. 3-1 and 3-2 represent the properties of Ref. 1 fitted into the present formulation using powers of pressure.

*In all the equations in this section, functional relationship, e.g., m which is a function of y , will be denoted by $m\{y\}$.

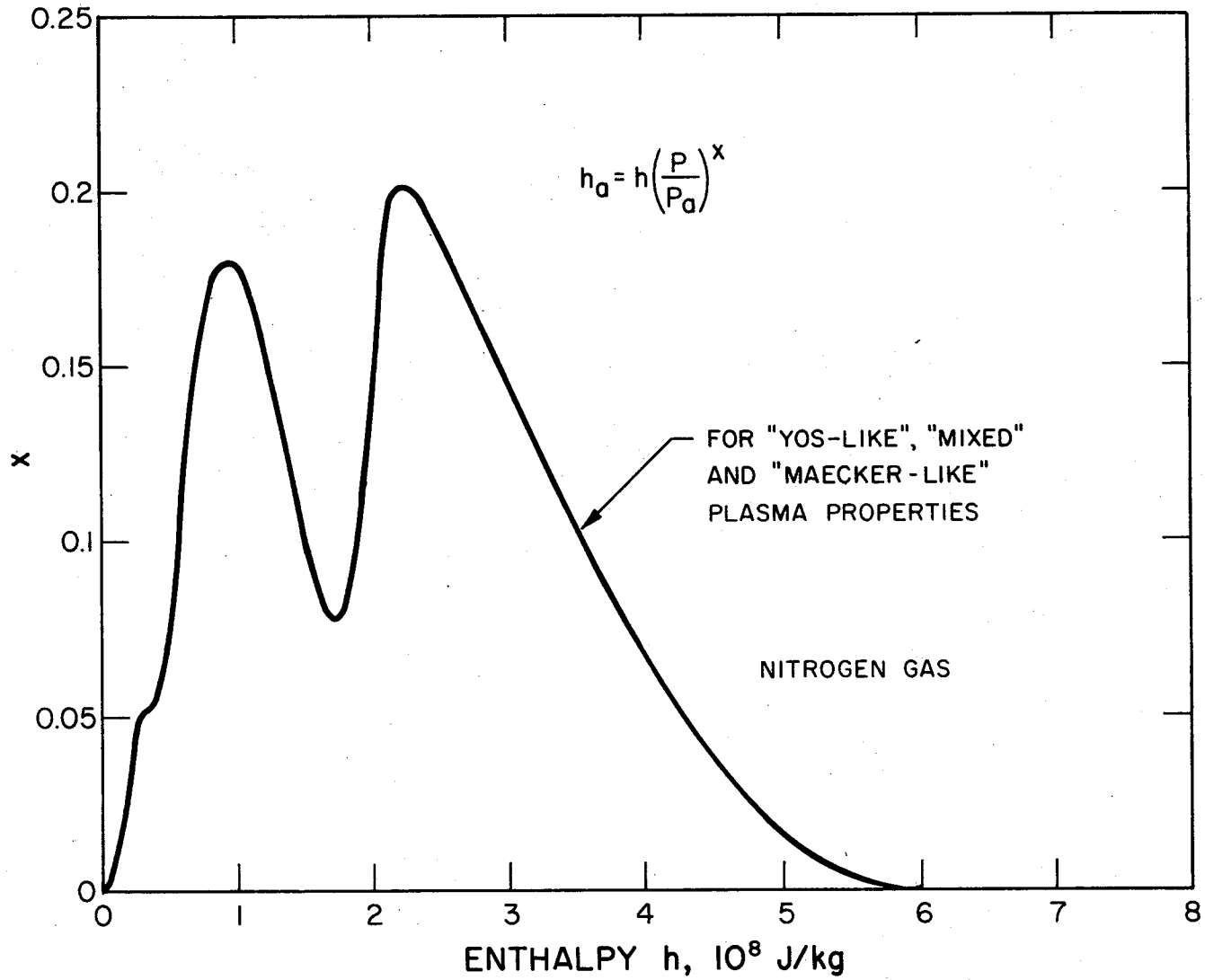


FIG. 3-1 RELATIONSHIP BETWEEN ENTHALPY AND REFERENCE ENTHALPY

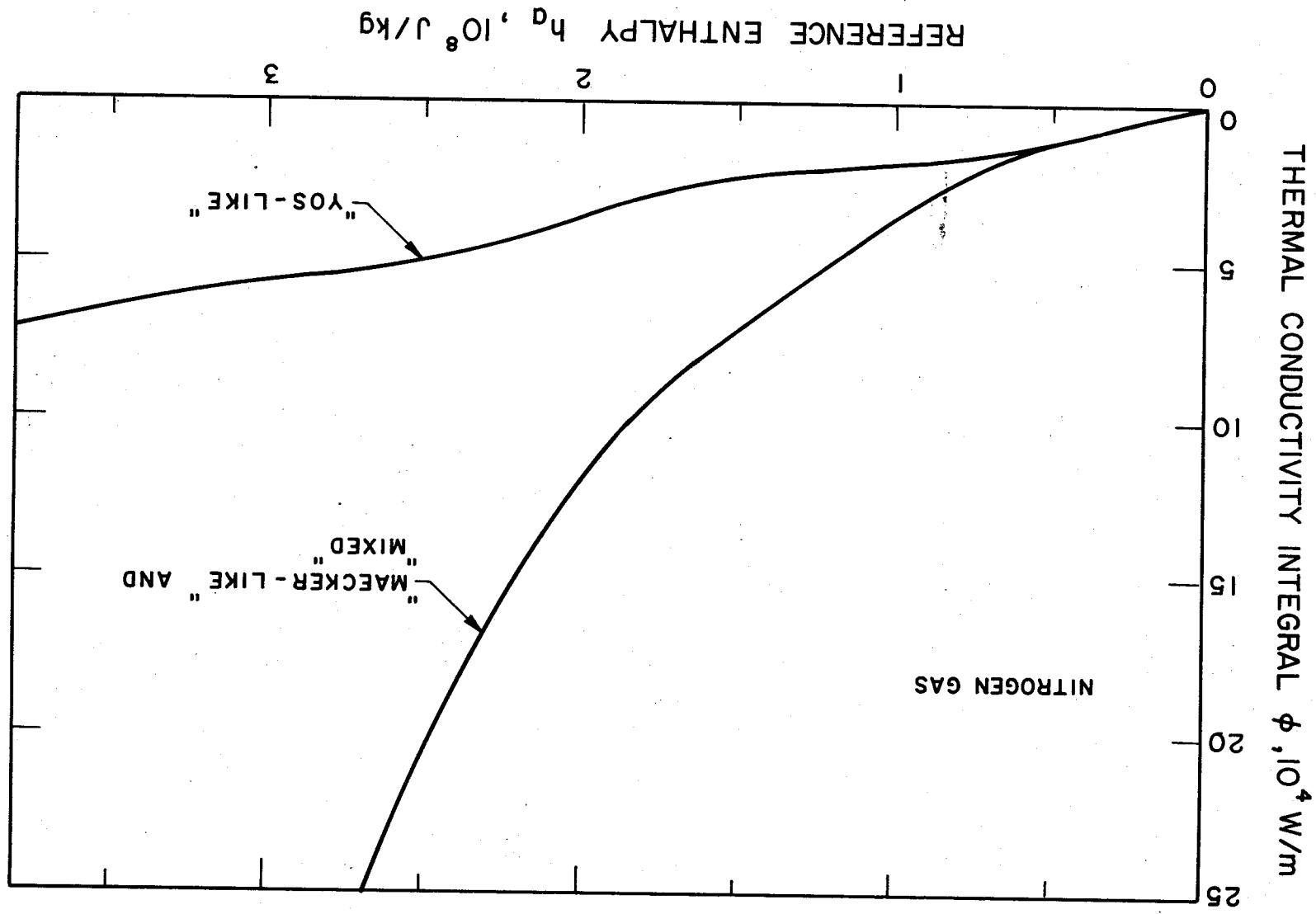


FIG. 3-2 THERMAL CONDUCTIVITY INTEGRAL AS A FUNCTION OF REFERENCE ENTHALPY

Another grouping of nitrogen properties is based upon analytical inversions of measurements made on an arc device 0.5 cm in diameter at atmospheric pressure (Refs. 10 and 11). When these atmospheric pressure nitrogen properties are combined with the previously fitted powers of pressure from the "Yos-like" properties, the complete set of properties is called "Maecker-like". Calculations using these properties are illustrated in Figs. 3-1 through 3-5.

A third group of properties called "mixed" result when the higher radiation values of the "Yos-like" properties are used with the "Maecker-like" properties.

3.2 Comparison of Cases

The various computer cases which were run are listed in Table 3-1. The "skipped" numbers represent cases that were run with plasma properties read into the computer incorrectly. Several groups of related cases will now be discussed individually.

3.2.1 Calculations for a 0.5 cm Diameter Constrictor

Inlet calculations were made using the "Maecker-like" properties for two typical operating conditions of the 0.5 cm research cascade (Refs. 3 and 12). Agreement with experiment was very good for wall heat flux, electric field, and radiation (as it should be, since the basis of "Maecker-like" properties is an inversion of asymptotic measurements on a 0.5 cm device). However, in contrast to the calculations, experimentally determined mass-averaged enthalpies tends to keep drifting higher (Fig. 3-6).

When the "Yos-like" properties were used for the 200-ampere calculations, the following comparisons were indicated. While the axial dependence and fully developed values of mass-averaged enthalpy were almost identical to the "Maecker-like" calculation, the enthalpy profiles were considerably higher (of the order of 80 percent)

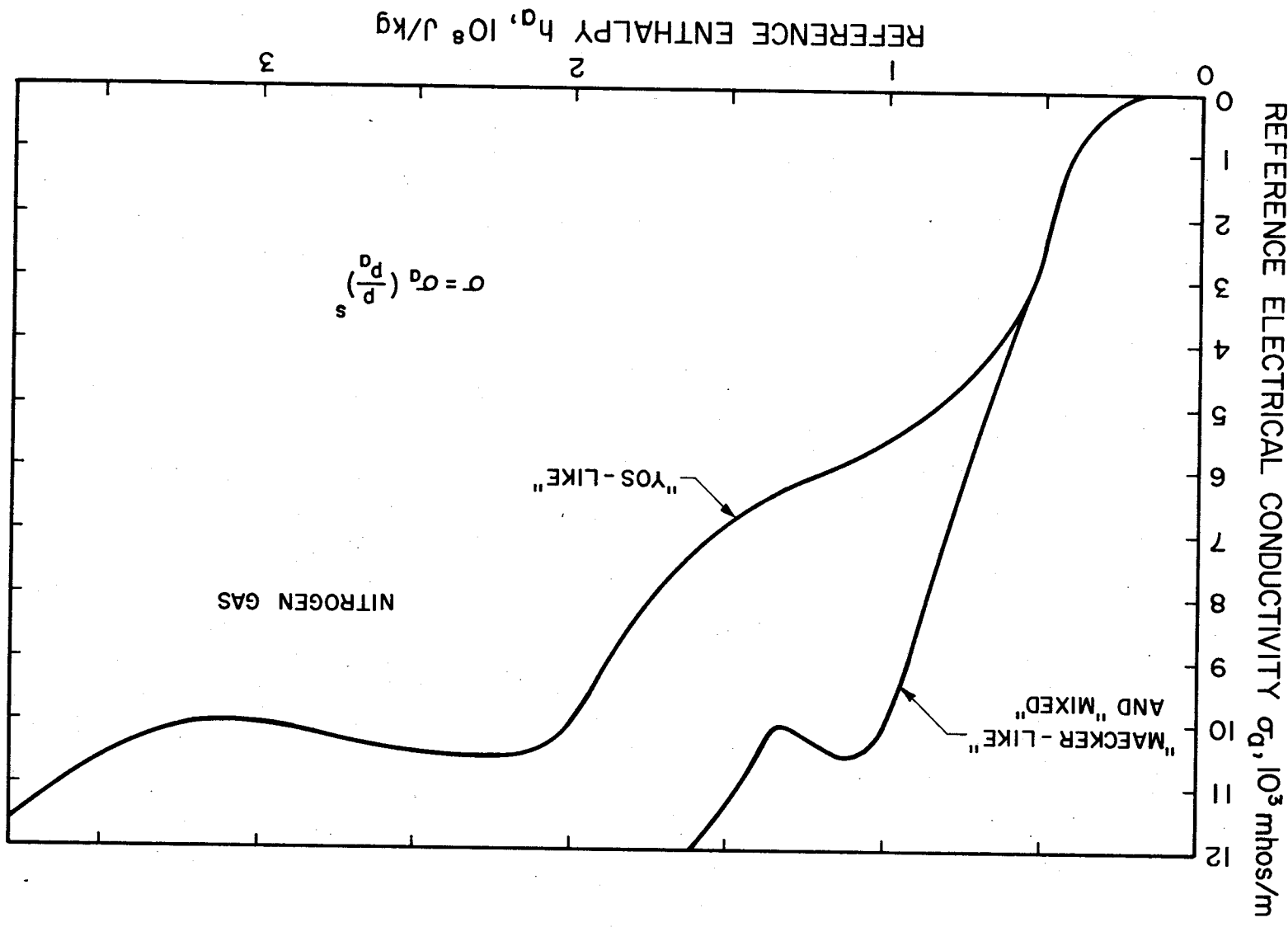


FIG. 3-3 REFERENCE ELECTRICAL CONDUCTIVITY AS A FUNCTION OF REFERENCE ENTHALPY

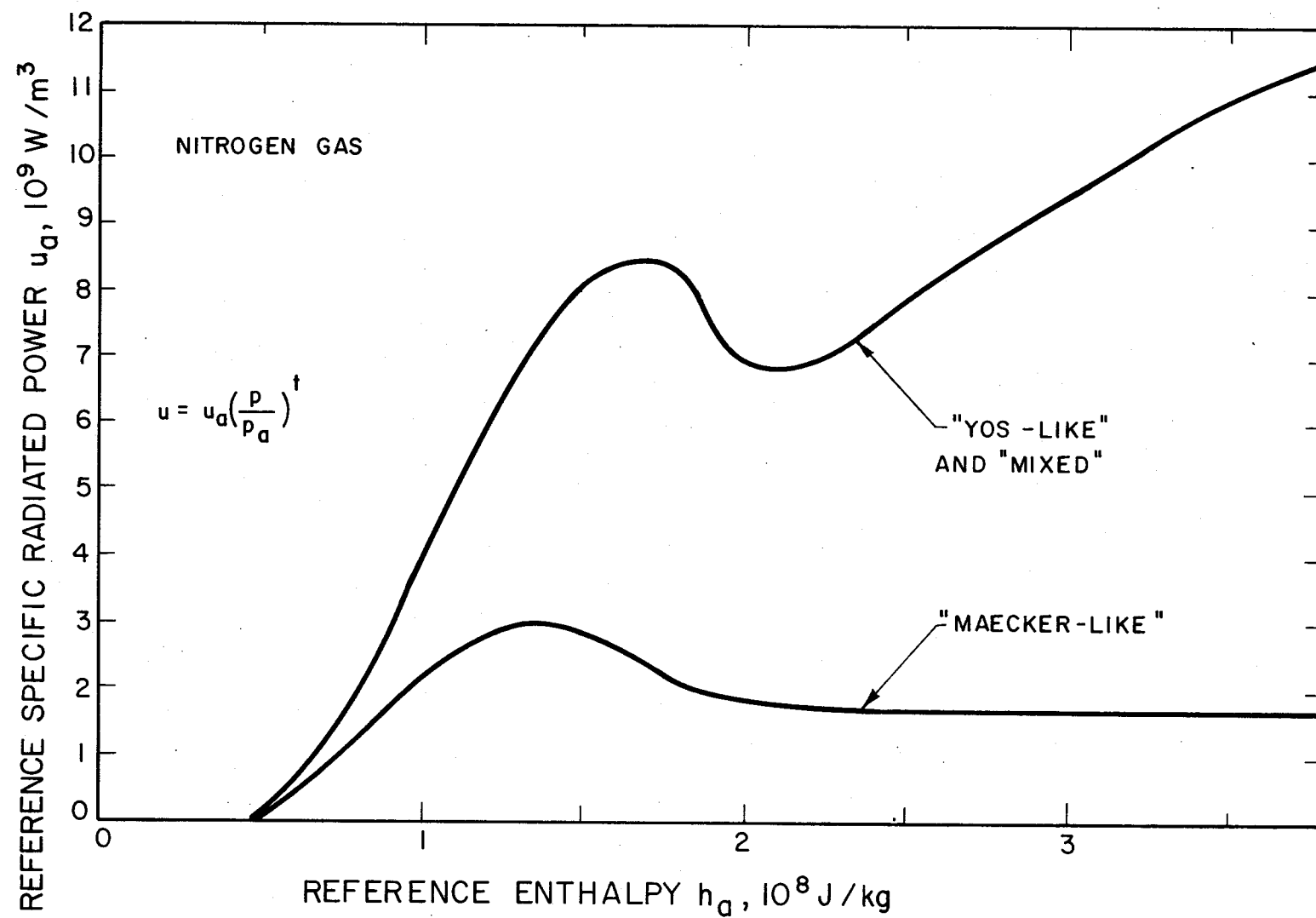


FIG. 3-4 REFERENCE SPECIFIC RADIATED POWER AS A FUNCTION OF REFERENCE ENTHALPY

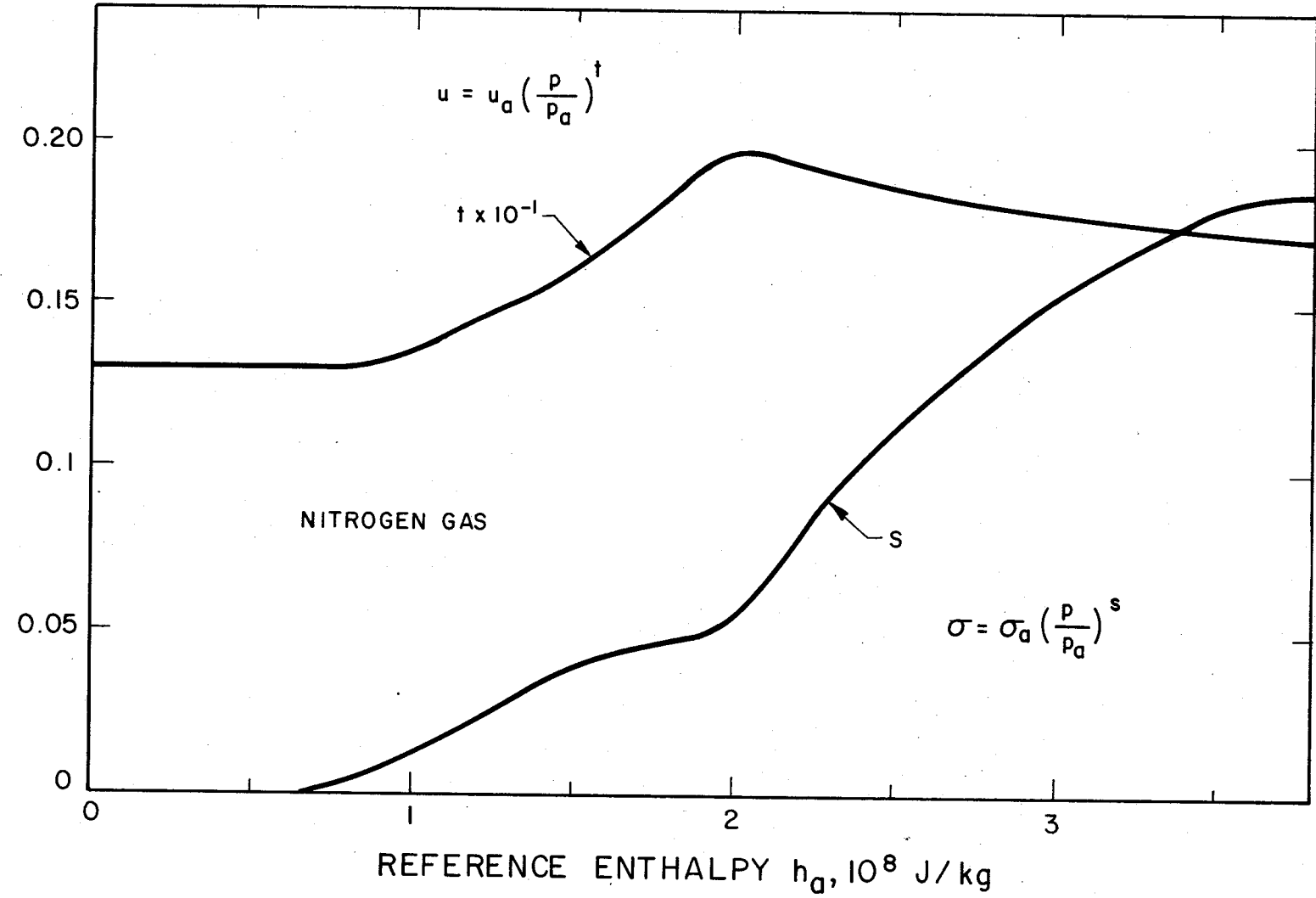


FIG. 3-5 s AND t AS FUNCTIONS OF REFERENCE ENTHALPY

TABLE 3-1
TABLE OF CASES

<u>Case</u>	<u>Diameter (meters)</u>	<u>Current (Amps)</u>	<u>Pressure (Atm)</u>	<u>Flow Rate (kg/sec)</u>	<u>Plasma Properties</u>
1	0.005	200	1.05	0.89×10^{-4}	Yos-like
4	0.02	1400	1.0	0.537×10^{-2}	Yos-like
12	0.005	200	1.02	0.89×10^{-4}	Maecker-like
13	0.005	100	1.02	0.89×10^{-4}	Maecker-like
14	0.005	200	1.05	0.89×10^{-4}	Maecker-like
16	0.02	1400	1.0	0.537×10^{-2}	Maecker-like
17	0.02	1400	2.0	0.537×10^{-2}	Maecker-like
18	0.02	1400	4.0	0.537×10^{-2}	Maecker-like
19	0.02	1600	1.0	0.537×10^{-2}	Maecker-like
20	0.02	1900	1.0	0.537×10^{-2}	Maecker-like
21	0.02	2500	1.0	0.537×10^{-2}	Maecker-like
22	0.02	1500	1.0	0.537×10^{-2}	Mixed
23	0.07	17,000	1.0	0.07	Mixed

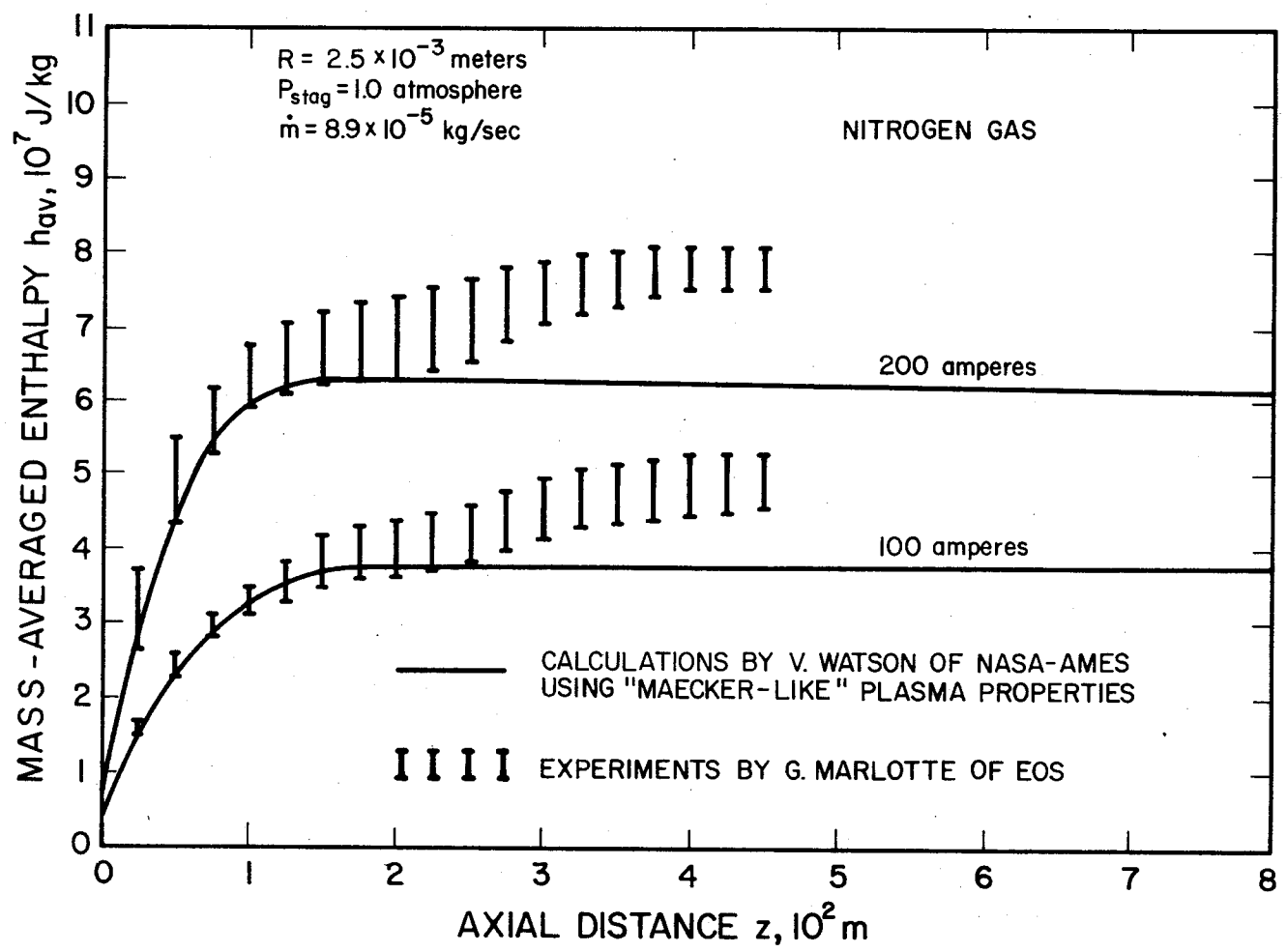


FIG. 3-6 EXPERIMENTAL AND CALCULATED MASS-AVERAGED ENTHALPY AS A FUNCTION OF LENGTH FOR THE 0.5-cm-DIAMETER ARC DEVICE

and the mass flow considerably lower in the center of the discharge. Further, in the "Yos-like" case, the wall heat flux was lower (by 16 percent), radiation much higher (by 320 percent), and the electric field lower (by 16 percent). Hence, the "Yos-like" properties do not agree with the experiments.

3.2.2 Calculations for a 2.0 cm Diameter Constrictor, Comparing "Yos-like" and "Maecker-like" Properties

Cases 4 and 16 demonstrate the effects of using two different groups of plasma properties for a typical operating condition of a 2-cm heater.

The magnitudes and distributions of the various arc-gas flow quantities of interest are quite different for the two cases. Similar tendencies are present as with the smaller diameter calculations with respect to enthalpy, mass flux, and electric field. Now, however, radiation predominates in the wall heat flux and the greatly increased radiation of the "Yos-like" properties gives a "Yos-like" heat flux as much as 290 percent of the "Maecker-like" heat flux. In addition, the "Yos-like" case 4 took a length of almost 90 cm to choke, while the "Maecker-like" case 16 choked in 34 cm. A comparison will now be made dealing with the greatly different radiation values between the two groups of properties. In order to match a particular experimental operating point at 1500 amperes, a comparison was made between case 22, using the "mixed" properties (higher radiation), and the average of cases 16 and 19, using the "Maecker-like" properties (lower radiation). Figure 3-7 shows the total heat fluxes together with the radiation component, while Fig. 3-8 shows the electric field values. On Fig. 3-7, experimental values of heat flux are plotted which tend to substantiate the higher "Yos-like" radiation values.

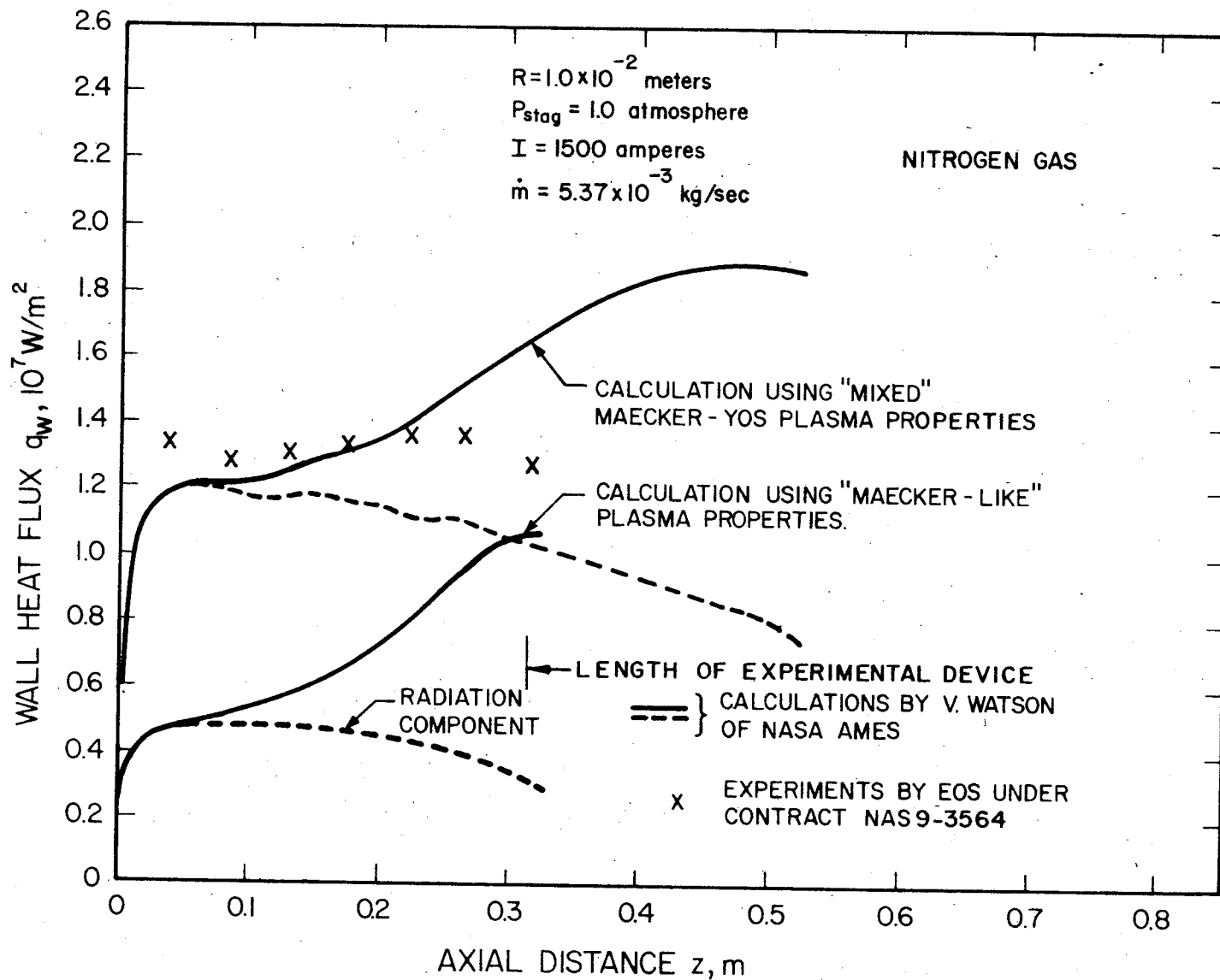
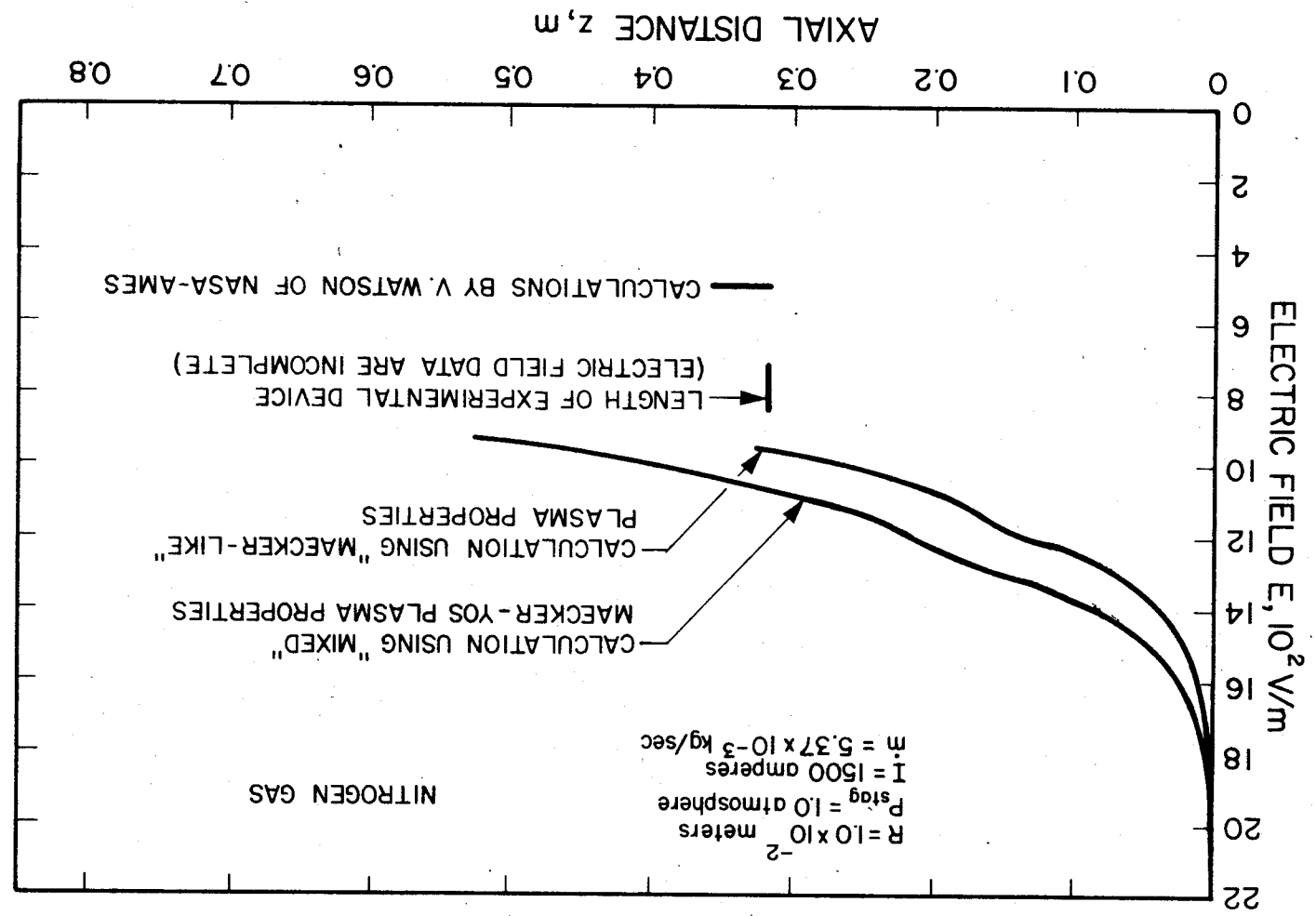


FIG. 3-7 EXPERIMENTAL AND CALCULATED WALL HEAT FLUX AS A FUNCTION OF LENGTH FOR THE 2.0-cm-DIAMETER ARC DEVICE

FIG. 3-8 EXPERIMENTAL AND CALCULATED ELECTRIC FIELD AS A FUNCTION OF LENGTH FOR THE 2.0-cm-DIAMETER ARC DEVICE



3.2.3 Calculations Showing Pressure Dependence for a 2.0 cm Diameter Constrictor

Cases 16, 17, and 18 in Table 3-1 are similar except for a difference in inlet pressure. This particular sequence demonstrates one of the problems of drawing conclusions from the calculations; that is, which parameters should remain fixed to draw meaningful conclusions? Since the mass-flow remained the same in the three cases under discussion, while the inlet pressure was changed, the cases at the higher pressures did not choke in reasonable lengths.

Figure 3-9 shows that values of mass-averaged enthalpy for the higher pressure calculations are reduced at a fixed axial coordinate. Figure 3-10 demonstrates the large pressure dependence of radiation and the large role radiation can have. Of some interest, is the fact that, in the region near the entrance to the heater, where the heat load is predominately radiation, the ratios of the magnitudes of the heat loads are given quite accurately by $(p/p_a)^t$, where $t \approx 1.3$ as may be obtained from Fig. 3-5. Figure 3-11 shows mainly the effect of increased radiation upon the electric field.

3.2.4 Calculations Showing Current Dependence for a 2.0 cm Constrictor

Cases 16, 19, 20, and 21 may be compared in order to examine current effects. The results are fairly self-explanatory and are given on Figs. 3-12 through 3-14. Some experimentally obtained electric fields at lower currents are also shown on Fig. 3-14. Since the "Maecker-like" (low radiation) properties were used for this series of comparisons, the higher values for the experimental electric fields may be substantially due to higher radiation being present in the experiments.

Figure 3-15 shows the calculated pressure drops for the four currents. The curves on Fig. 3-15 indicate that, for the experimental currents of interest, a linear pressure drop is a good approximation.

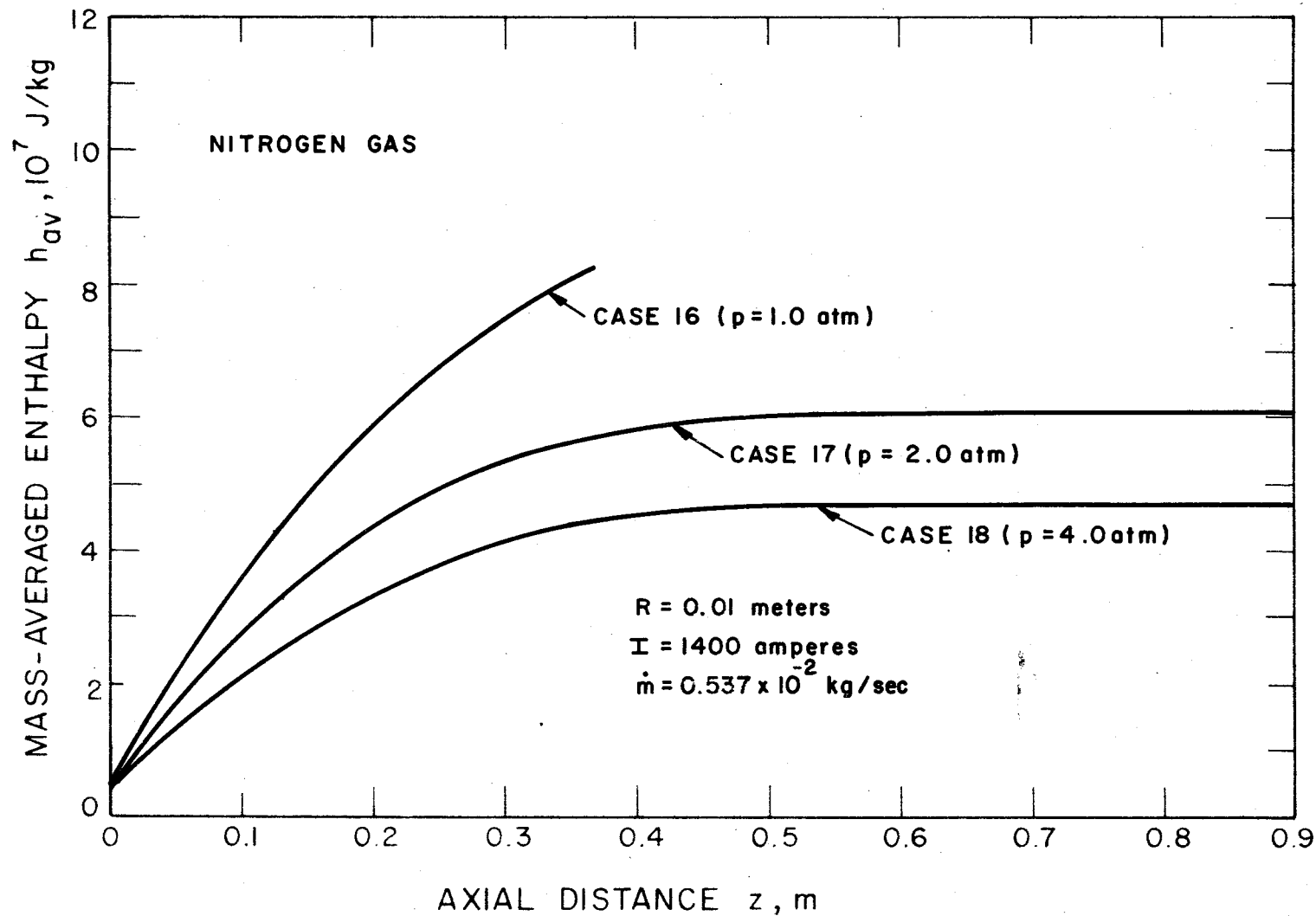


FIG. 3-9 CALCULATIONS SHOWING PRESSURE DEPENDENCE OF MASS-AVERAGED ENTHALPY FOR A 2.0-cm-DIAMETER CONSTRICTOR

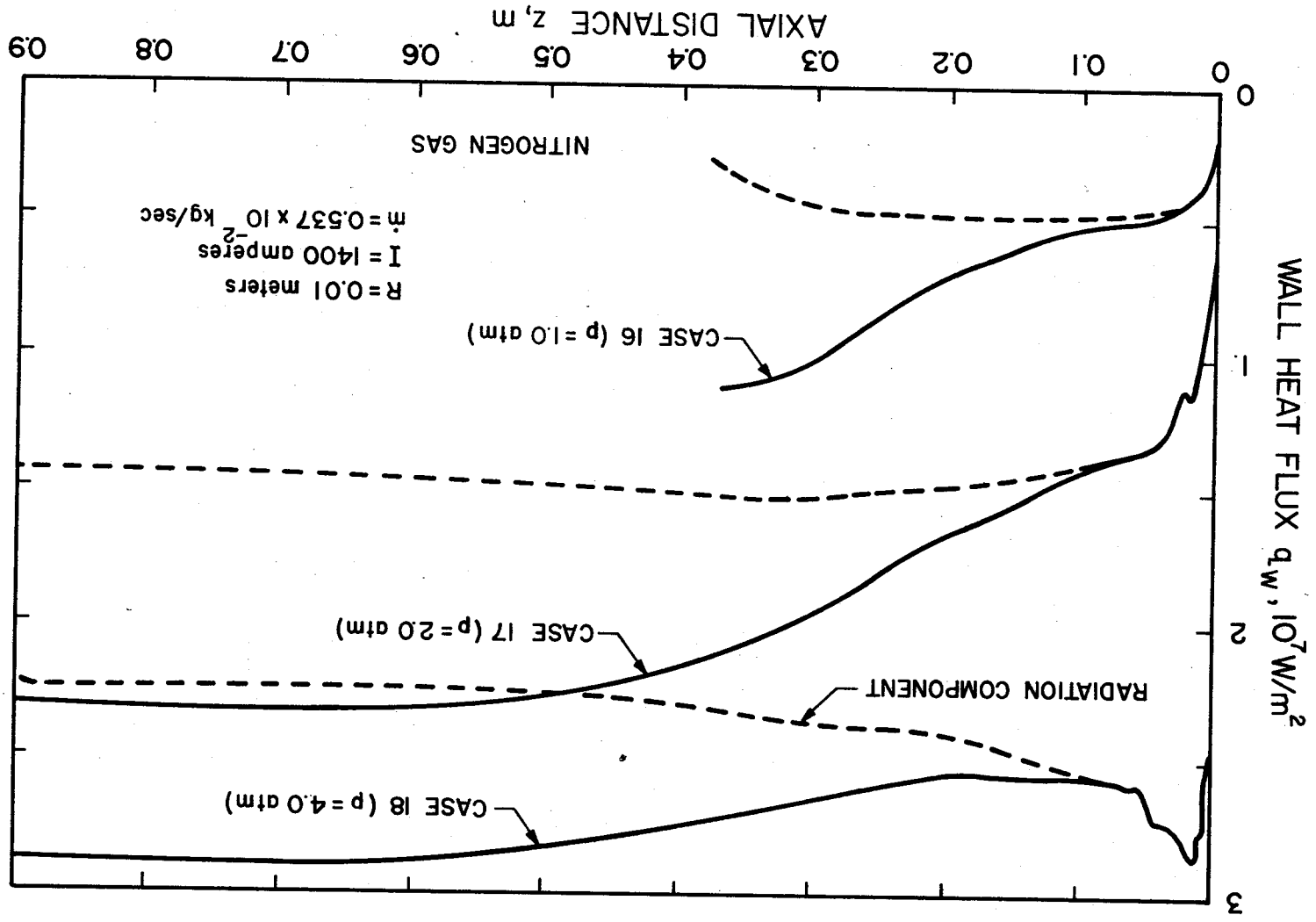


FIG. 3-10 CALCULATIONS SHOWING PRESSURE DEPENDENCE OF WALL HEAT FLUX FOR A 2.0-cm-DIAMETER CONSTRICTOR

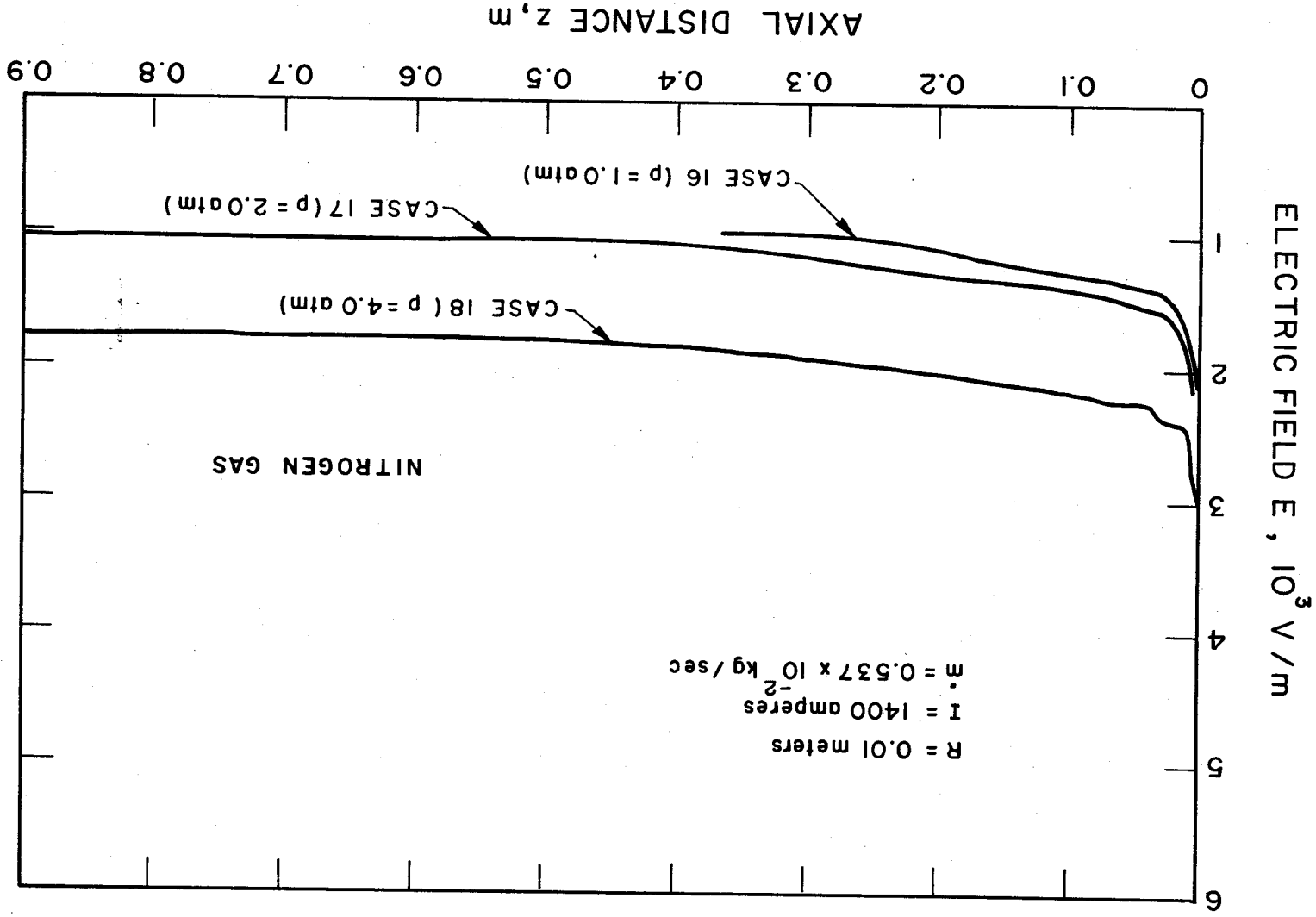


FIG. 3-11 CALCULATIONS SHOWING PRESSURE DEPENDENCE OF ELECTRIC FIELD FOR A
 2.0-cm-DIAMETER CONSTRUCTOR

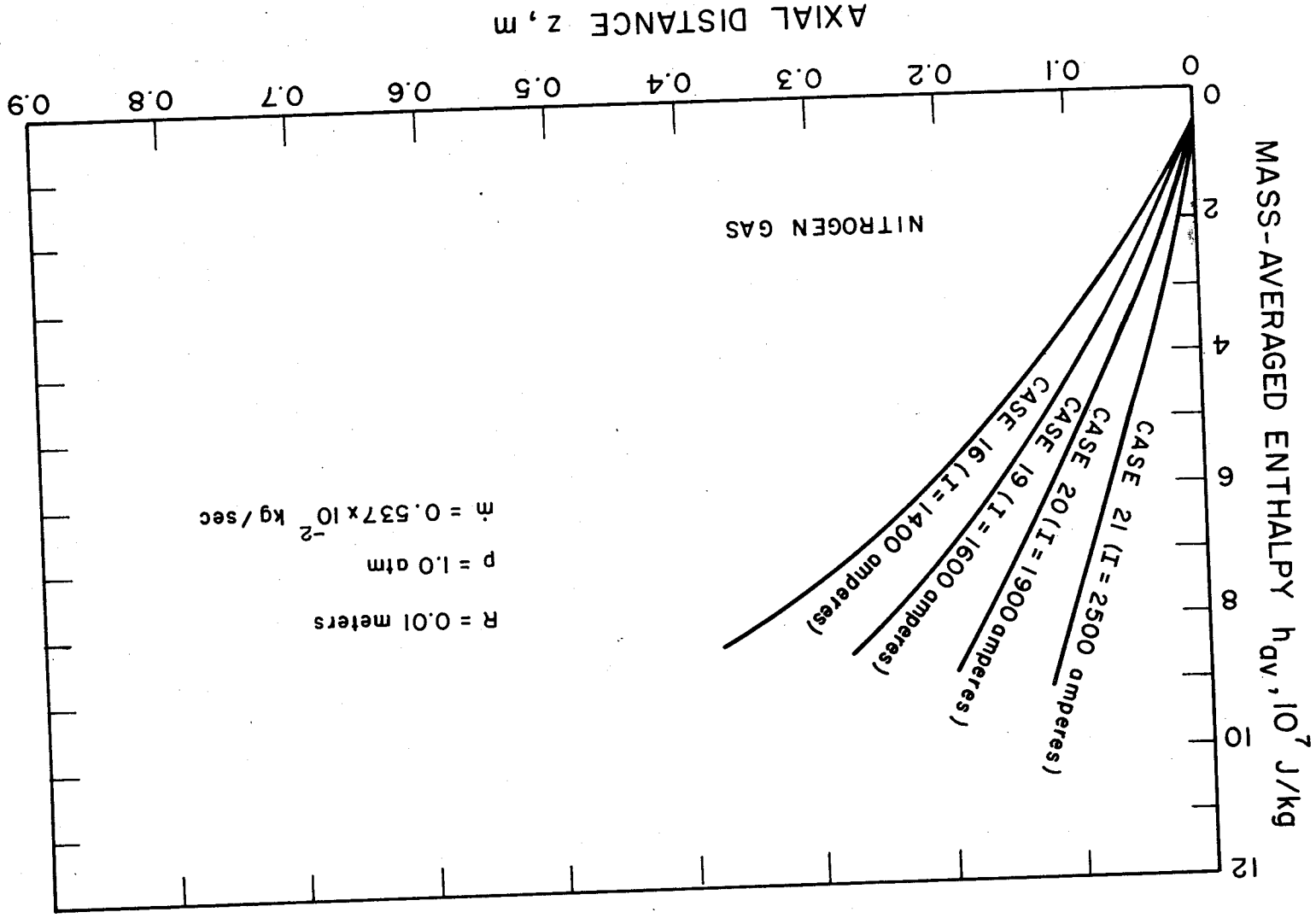


FIG. 3-12 CALCULATIONS SHOWING CURRENT DEPENDENCE OF MASS-AVERAGED ENTHALPY FOR A 2.0-CM-DIAMETER CONSTRICTOR

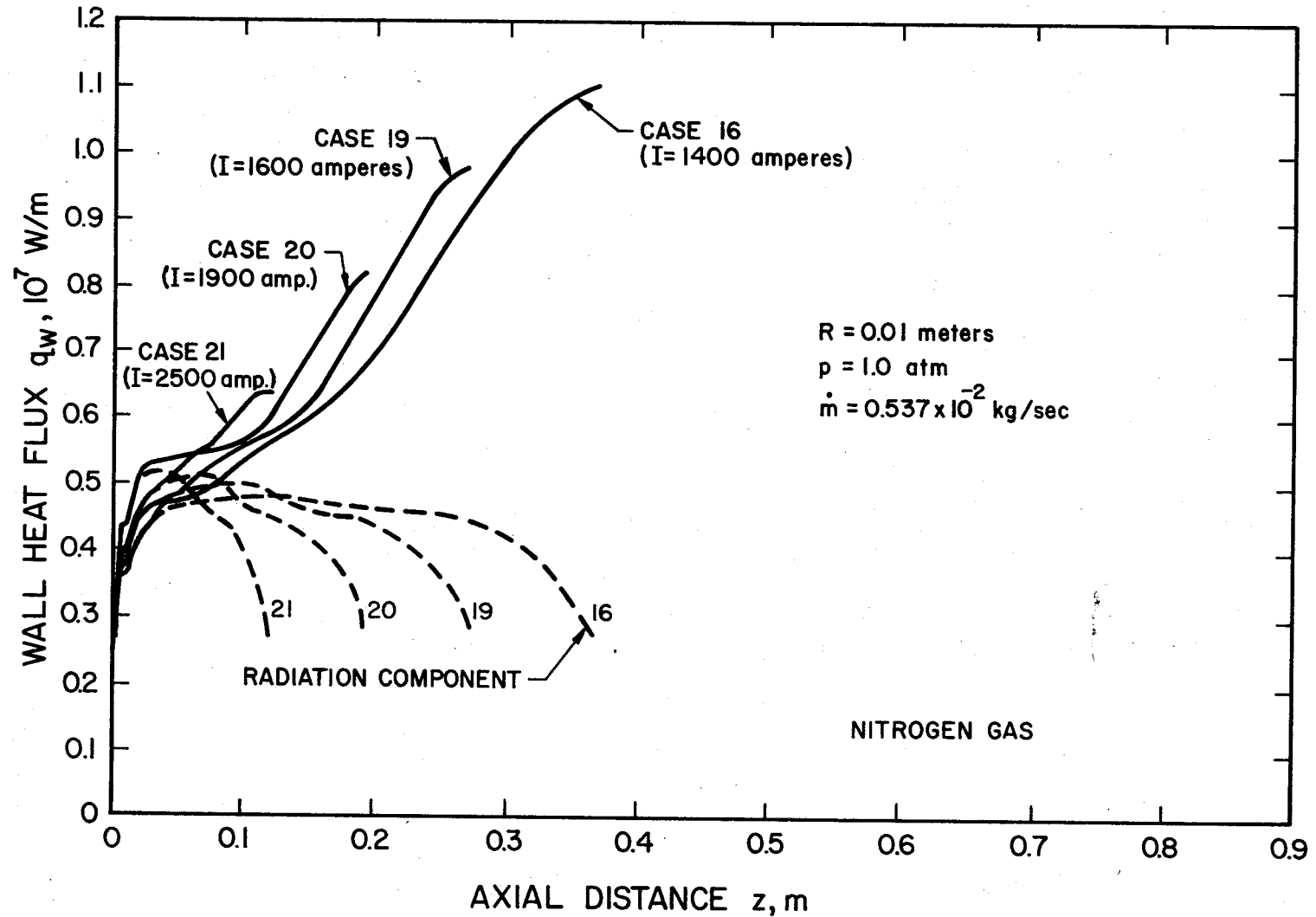


FIG. 3-13 CALCULATIONS SHOWING CURRENT DEPENDENCE OF WALL HEAT FLUX FOR A 2.0-cm-DIAMETER CONSTRICTOR

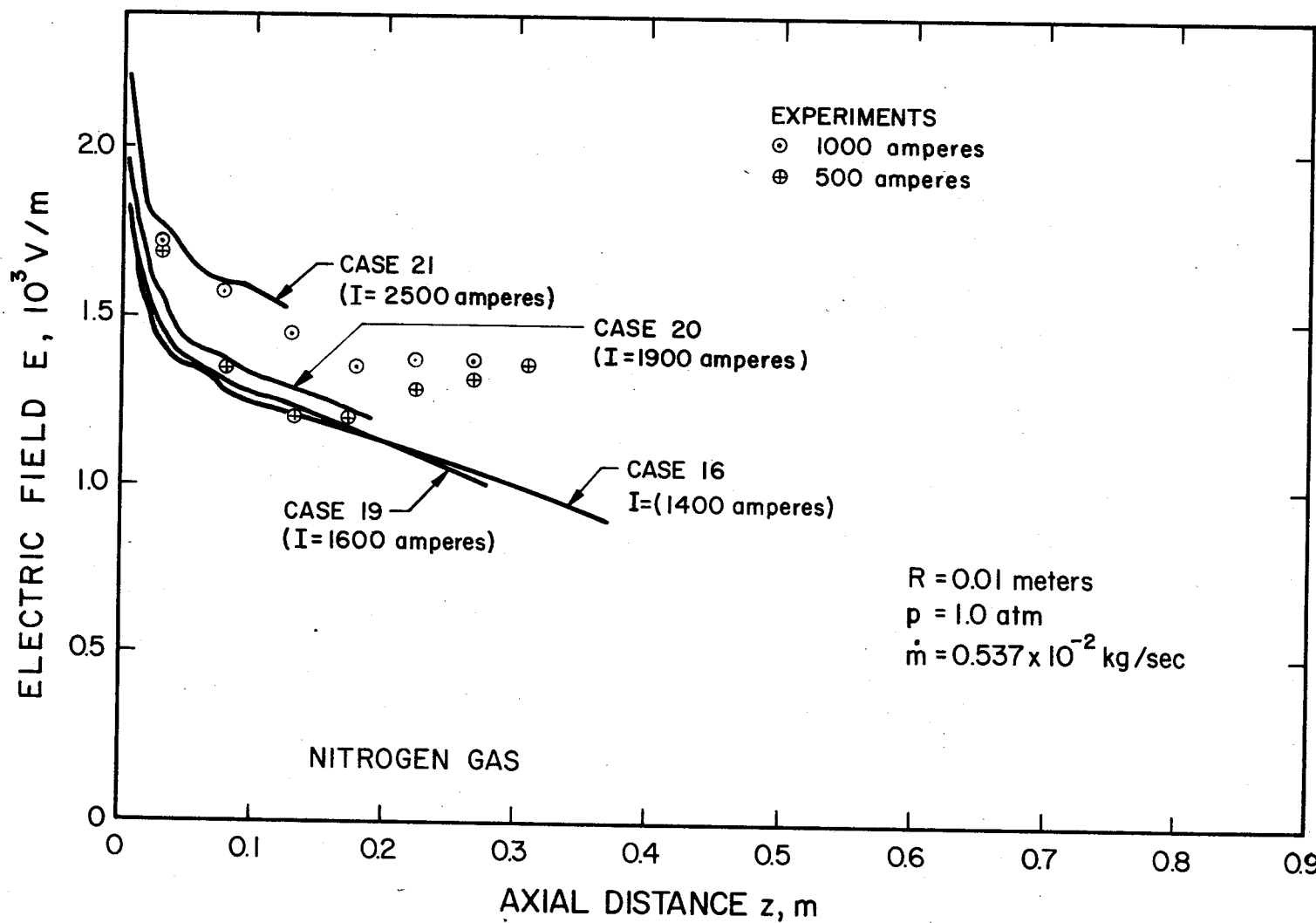


FIG. 3-14 CALCULATIONS SHOWING CURRENT DEPENDENCE OF ELECTRIC FIELD FOR A 2.0-cm-DIAMETER CONSTRICTOR

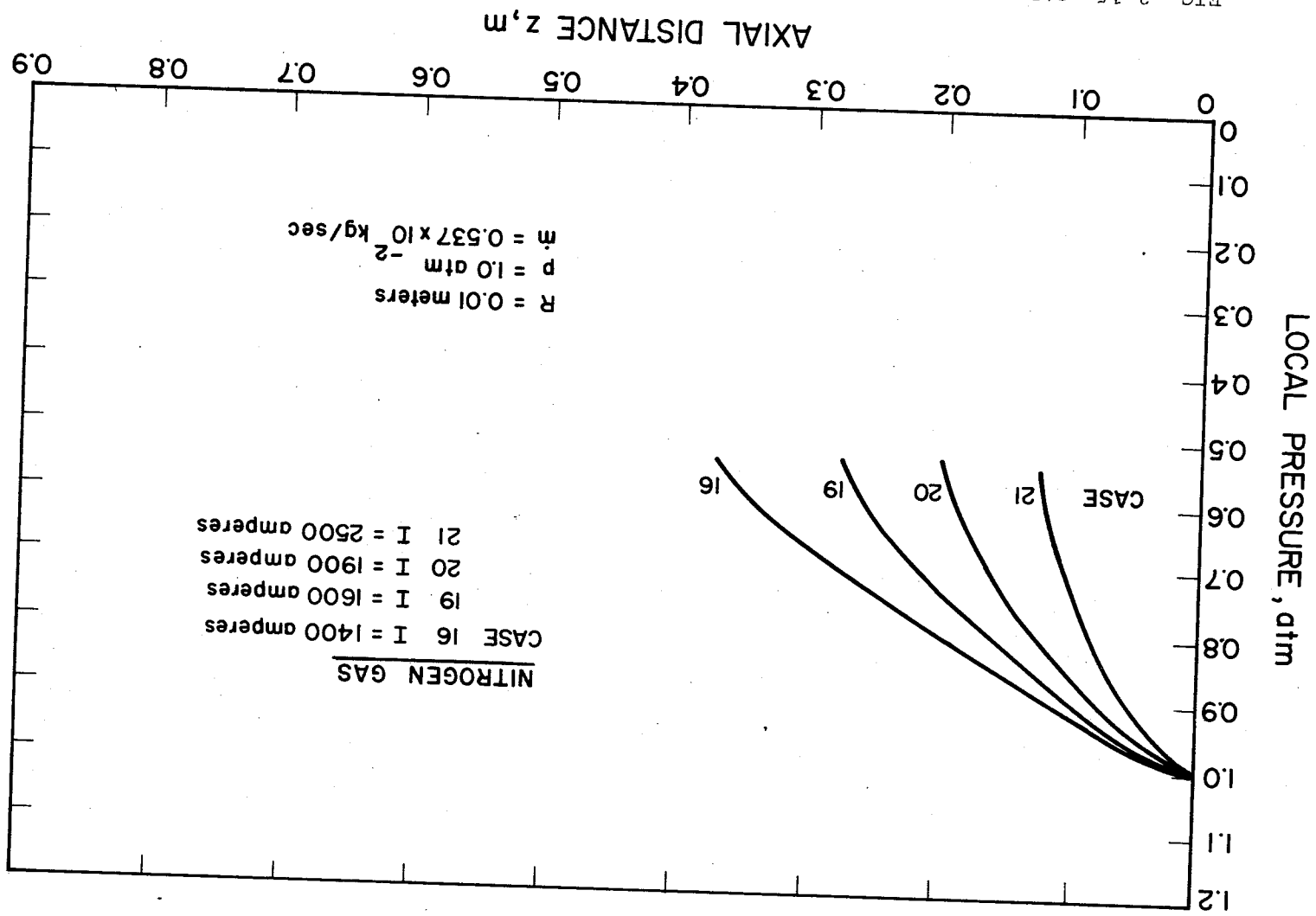


FIG. 3-15 CALCULATIONS SHOWING CURRENT DEPENDENCE OF LOCAL PRESSURE FOR A 2.0-cm-DIAMETER CONSTRICTOR

3.3 Calculations for a Large High-Power Device

Case 23 (listed on Table 3-1) is a trial calculation for an arc heater of much higher power with roughly the same mass-averaged enthalpy as a 2.0 cm device. When mass-averaged enthalpy is held constant in scaling, Ref. 3. Section 6 offers a convenient method of determining the various "scaled" parameters (radius, current, mass-flow, etc.). This method was used quite successfully; first, to determine the input and then to predict the results of the case 23 computer calculation.

Figure 3-16 shows that the very high initial values of radiation suppress the usual fast initial rise in mass-averaged enthalpy. Figure 3-17 shows that conduction (the difference between the two curves) is an insignificant component of wall heat transfer in this device. Figure 3-18 shows that the electric field is quite similar to the electric field in the smaller 2.0 cm device. The reason is that, from simple theory (Ref.

$$E \propto \frac{1}{R} (1 + \underbrace{\text{Const } R^2}_{\text{Radiation Term}})^{1/2}$$

When the radius and pressure are high enough for the radiation term to dominate, the electric field becomes insensitive to radius.

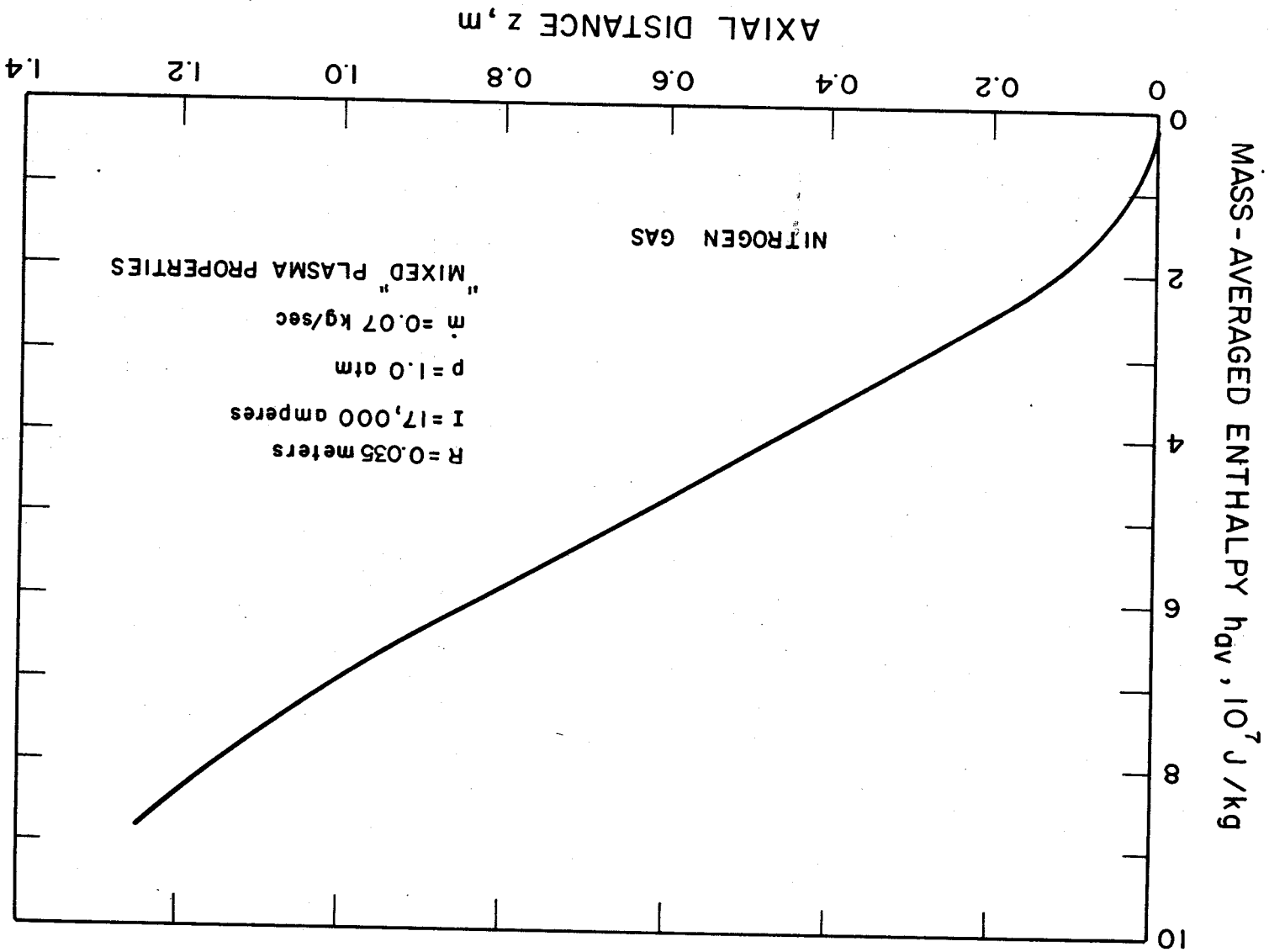


FIG. 3-16 MASS-AVERAGED ENTHALPY CALCULATIONS FOR A LARGE HIGH-POWER DEVICE

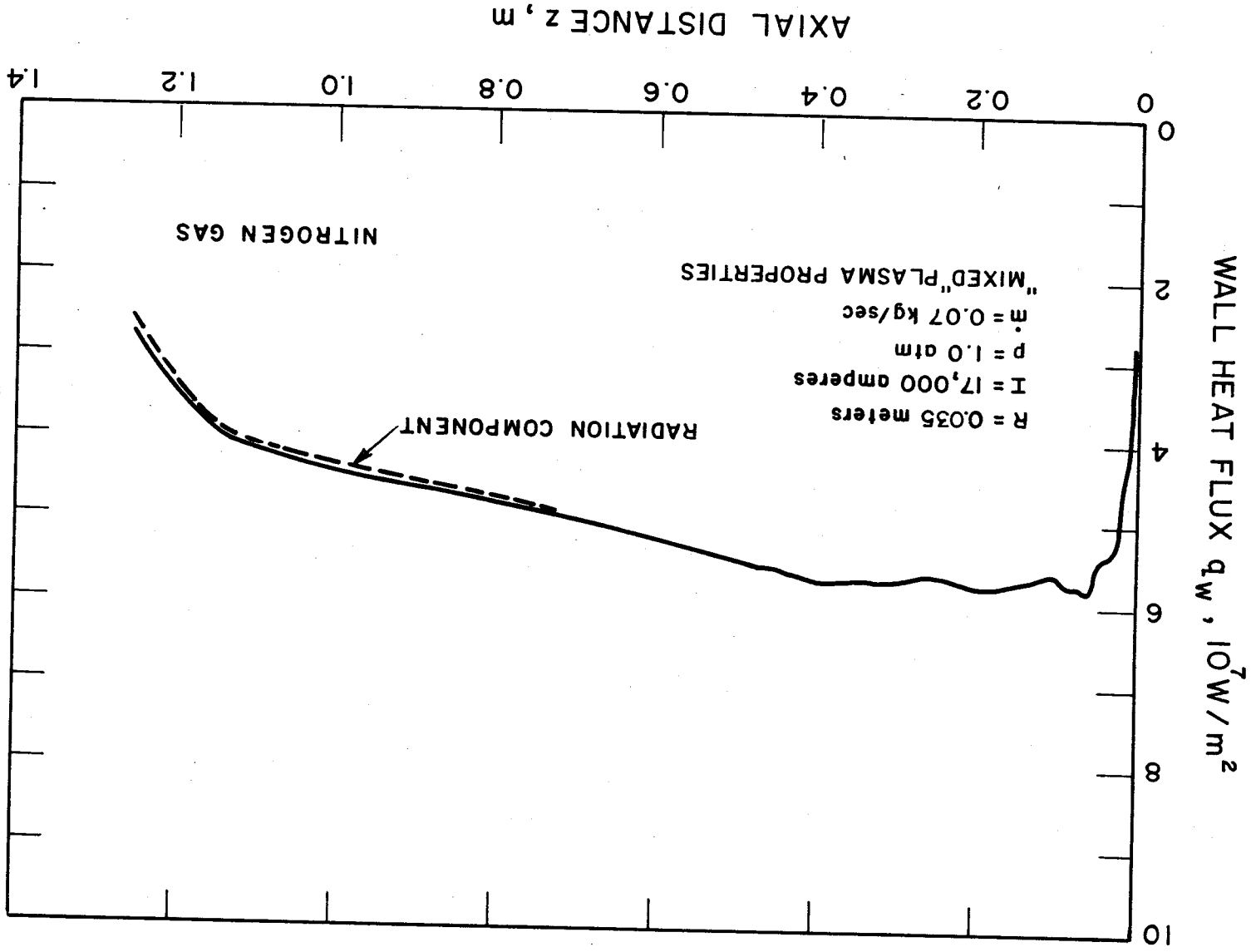


FIG. 3-17 WALL HEAT FLUX CALCULATIONS FOR A LARGE HIGH-POWER DEVICE

3-24

6320-20-1

73618315

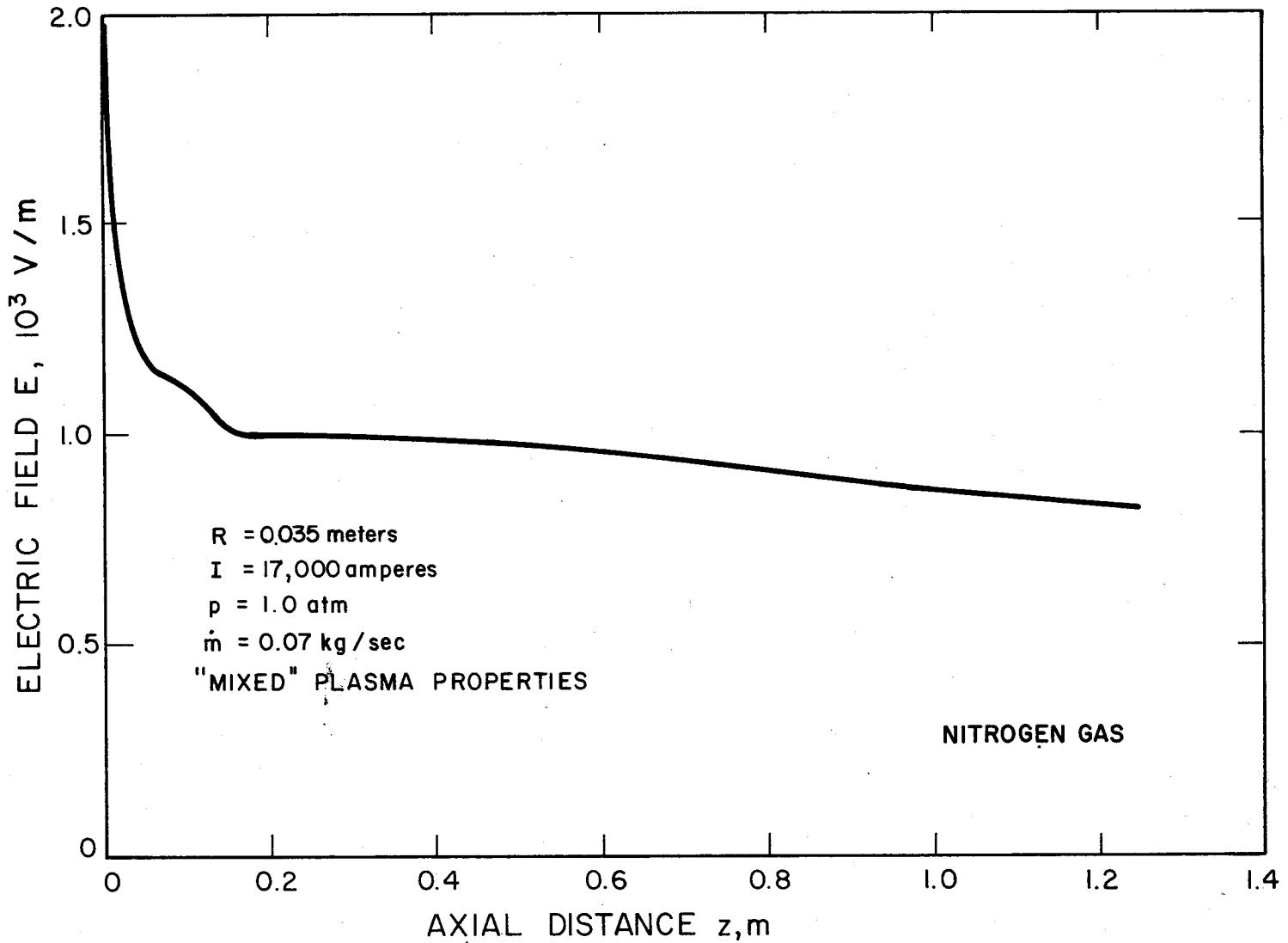


FIG. 3-18 ELECTRIC FIELD CALCULATIONS FOR A LARGE HIGH-POWER DEVICE

4. ONE MEGAWATT HEATER - BRIEF REVIEW OF PERFORMANCE DATA

The experimental procedures used and the detailed discussion of the results obtained will be given elsewhere*. In this report, primarily those empirical performance curves and other results are summarized which are utilized in the semi-empirical design procedure and performance estimates for the 10 mw High Enthalpy Heater.

The correlations given here are predominantly empirical, and are based on very consistent test data. Some of the trends which were established experimentally agree with simple theoretical relations discussed earlier. While the simple analytical and scaling rules are used to cross correlate and later extrapolate the data, the absolute levels of the curves all are based on the measurements rather than on purely theoretical results.

4.1 Correlation Between Total Enthalpy, Constrictor Exit Pressure, and Mass Flow Rate for Choked Flow Conditions

The following relations all apply to the case where the arc heater exhausts directly into a vacuum tank, without an intervening mixing chamber or "second" nozzle throat. For this case, a correlation between the total enthalpy, the static pressure at the exit of the constrictor, and the total mass-flow rate can be found if one makes the following assumptions for the condition at the constrictor exit:

1. One-dimensional flow, i.e., uniform velocity and enthalpy distribution, no frictional effects
2. "Chemical" (species distribution) and thermodynamic equilibrium
3. Sonic flow conditions

With these assumptions one can write

$$\frac{\dot{m}}{A p^*} \approx \frac{v^* \rho^*}{p^*} = f(h_T \text{ only}) \quad (4-1)$$

* Bimonthly Progress Reports and Final Technical Report

where $v^* = f(h, p^*) =$ throat (sonic) velocity
 $\rho^* = f(h, p^*) =$ throat (sonic) density

and the total enthalpy is

$$h_T = h + \frac{v^{*2}}{2}$$

The approximate relation (Eq. 4-1) was verified for both nitrogen and air up to very high temperatures ($\sim 15,000^\circ\text{K}$), by using the equilibrium thermodynamic properties of these gases given respectively in Ref. 13 and Ref. 14. All plots of ρ^*v^*/p^* vs h_T for different pressures (0.1 to 10 atmospheres) all fall on the same curve, with engineering accuracy. The curve for nitrogen is shown in Fig. 4-1. Moreover, for a very wide range of enthalpies, the mean slope of the mass-flow parameter came out -0.492, while for a perfect gas it would be constant and -0.50. Thus, we have

$$\frac{\rho^*v^*}{p^*} (h_T)^{.5} = \text{constant (for perfect gas)}$$

\approx weak function of h_T only (for one-dimensional flow of equilibrium nitrogen)

The wavy curve which accurately represent the simple one-dimensional flow of equilibrium nitrogen (or air) was then compared with experimental data from a 1/2-inch diameter constricted arc heater at NASA Ames Research Center.* The Ames data were given in terms of the upstream stagnation pressure, p_{T0} . Measured throat pressures were not then available for that heater. However, from calculations, as well as other measurements, it was known that the relation between throat pressure and upstream stagnation pressure

$$\frac{p^*}{p_{T0}} \approx .53 (\pm .02) \tag{4-2}$$

is valid for air or nitrogen over a wide range of conditions. A throat pressure calculated with this relation was used for the correlation.

*Furnished to this project by C. Shepard and H. Stine (Head)
 Magnetoplasmdynamics Branch

FIG. 4-1 ANALYTICAL CORRELATION BETWEEN THE CRITICAL FLOW PARAMETER AND THE TOTAL ENTHALPY

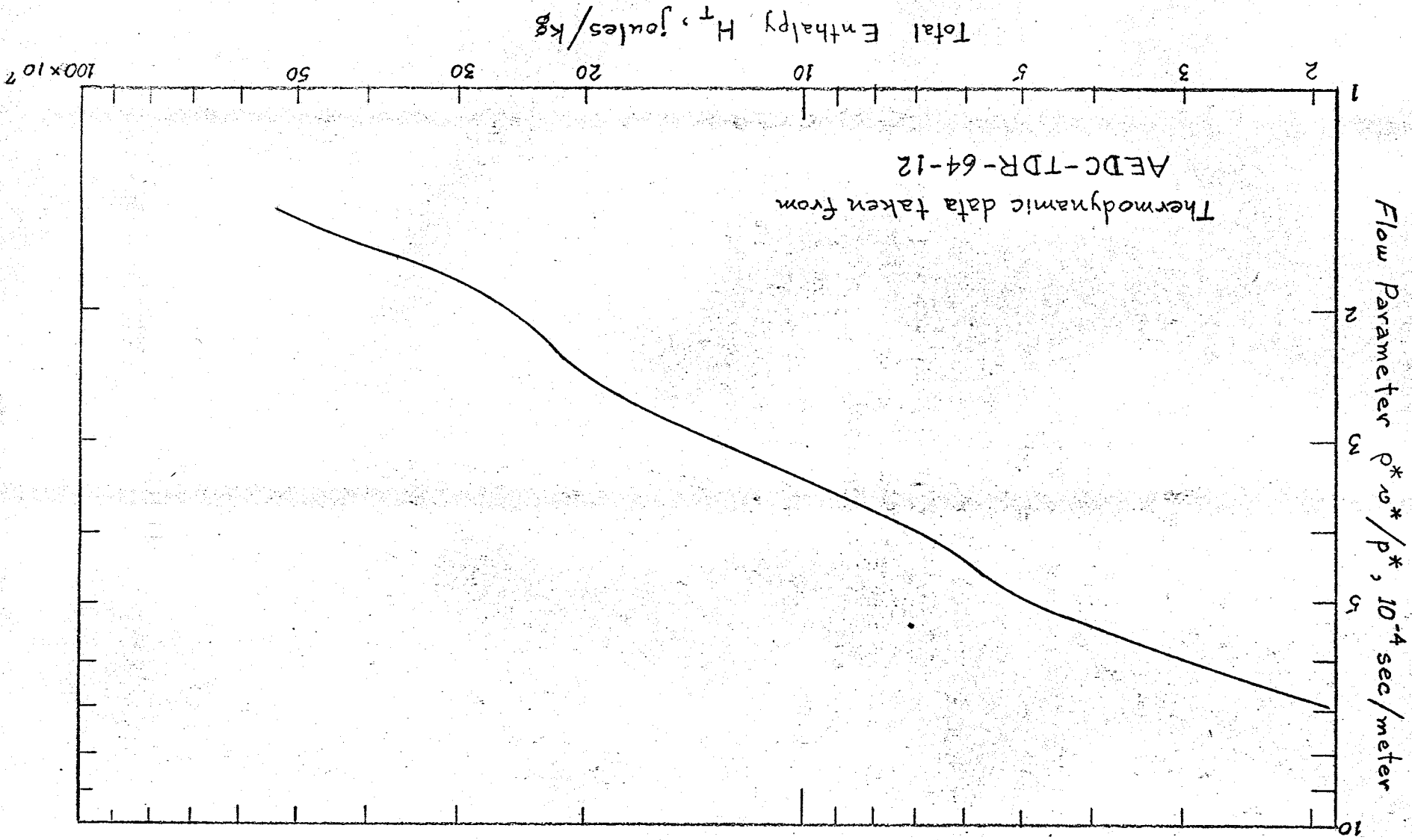
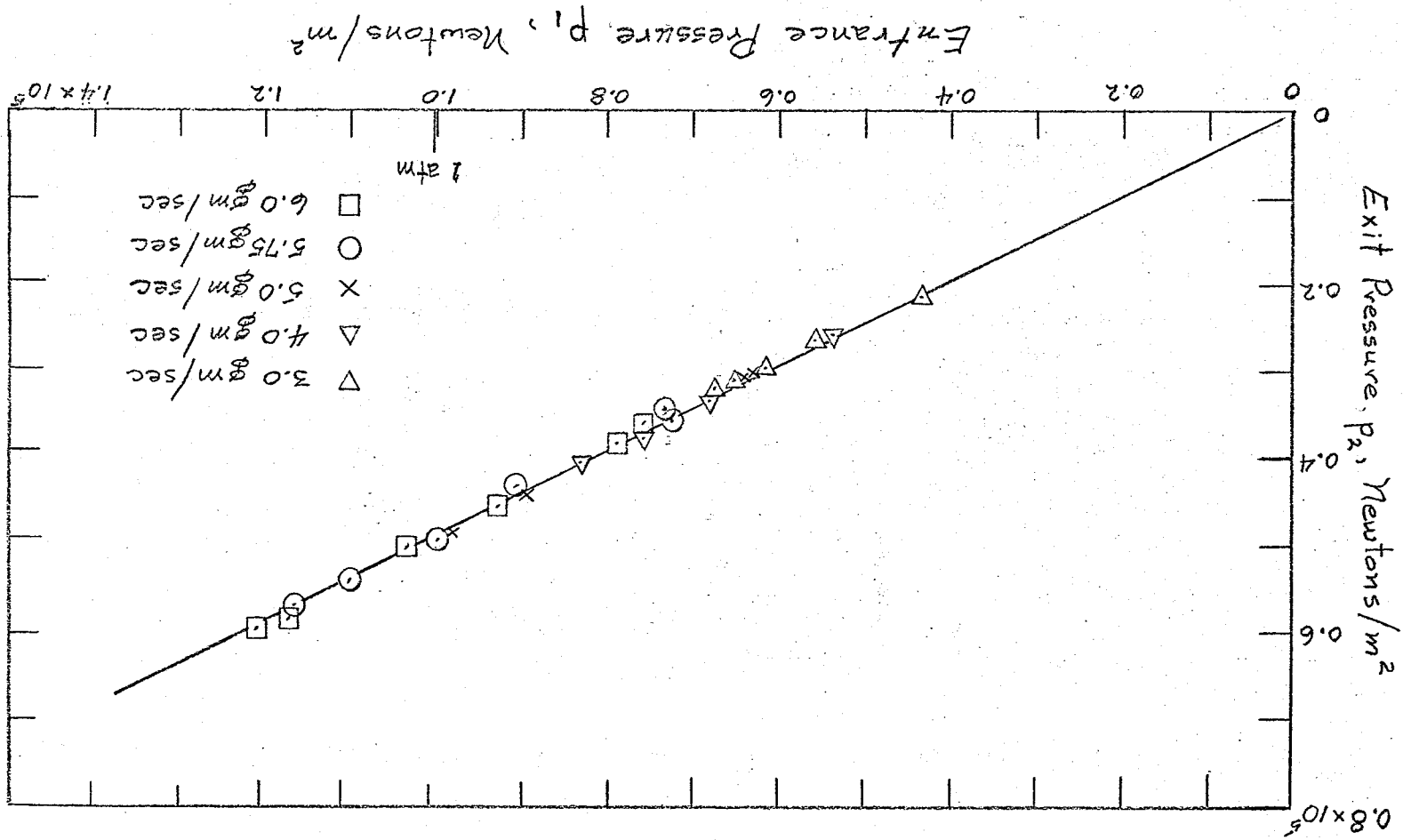


FIG. 4-2 CORRELATION BETWEEN THE PRESSURE AT THE ENTRANCE AND THE PRESSURE AT THE EXIT OF THE 2-cm-DIAMETER CONSTRICTED ARC HEATER FOR FIVE MASS FLOW RATES AND CRITICAL EXIT CONDITIONS



The precise value chosen (within a few percent) is not critical because any error can be absorbed in the final empirical correlation factor (see below). The validity of using a constant for the pressure ratio p^*/p_{T0} was later verified by measurements such as those shown in Fig. 4-2. This correlation shows that the ratio of the measured pressures at the first segment, p_1 (which is slightly lower than p_{T0}), to that of the exit segment, p_2 , remained constant at a value of 0.49. The important fact is that neither enthalpy, flow rates nor absolute pressure level have any appreciable effect on the sonic throat to inlet pressure ratio of the constrictor.

The Shepard mass-flow data were thus converted to $h_T = f\left(\frac{1}{0.53} \frac{\dot{m}}{p_{T0} A^*}\right)$, and compared with the one-dimensional analytic values (Fig. 4-3). It was found that the mean curve through the converted test data runs parallel and quite close to the simple one-dimensional curve. This indicated that the experimental data could be closely approximated by the one-dimensional analytic curve times a small constant correction factor. This correction factor lumps together all the effects neglected in the simple one-dimensional flow model, i.e., nonuniform enthalpy and velocity distribution, friction (boundary layer), etc. The factor chosen for the 1 MW heater design and performance correlations was 0.936, giving the following assumed relation:

$$\dot{m}_{\text{Heater}}(p^*, \overline{h_T}) = 0.936 \text{ (one-dimensional value nitrogen flow)} \quad (4-3)$$

For larger heaters in which boundary layer effects are smaller and the enthalpy becomes more uniform (higher Reynolds numbers) the correction factor may approach unity.

The thus established mass flow relation (Eq. 4-3) is utilized to choose the heater constrictor (or throat) diameter for a given design mass flow, enthalpy, and pressure. The 1 MW heater was designed on this basis. It also permits the construction of a heater operating map for a given constrictor size in terms of the same variables. Such a map, for a 2 cm diameter constrictor, is shown in Fig. 4-4. Finally, the same

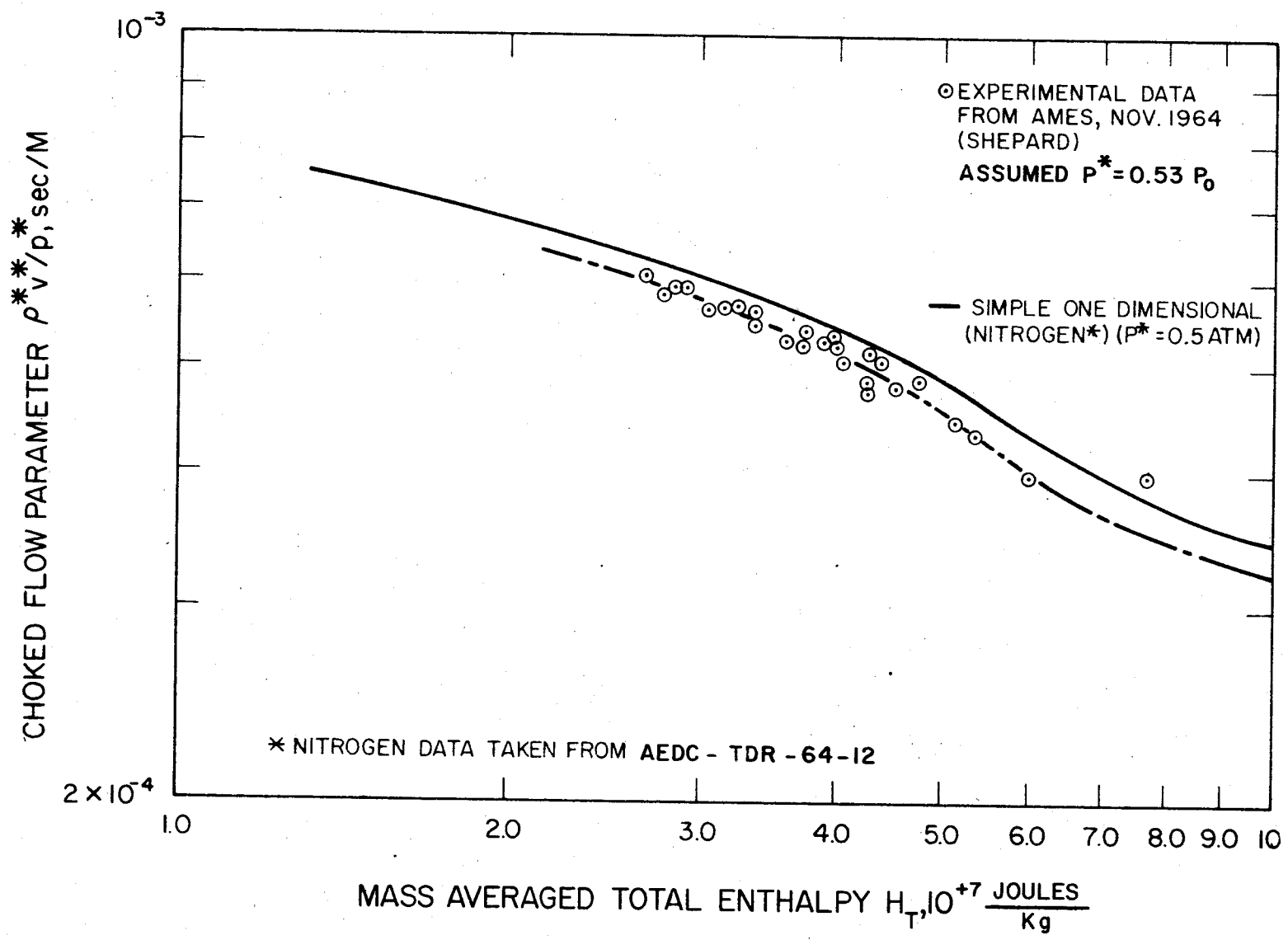


FIG.4-3 CORRELATION OF THE CHOKED FLOW PARAMETER WITH THE MEAN TOTAL ENTHALPY (NITROGEN)

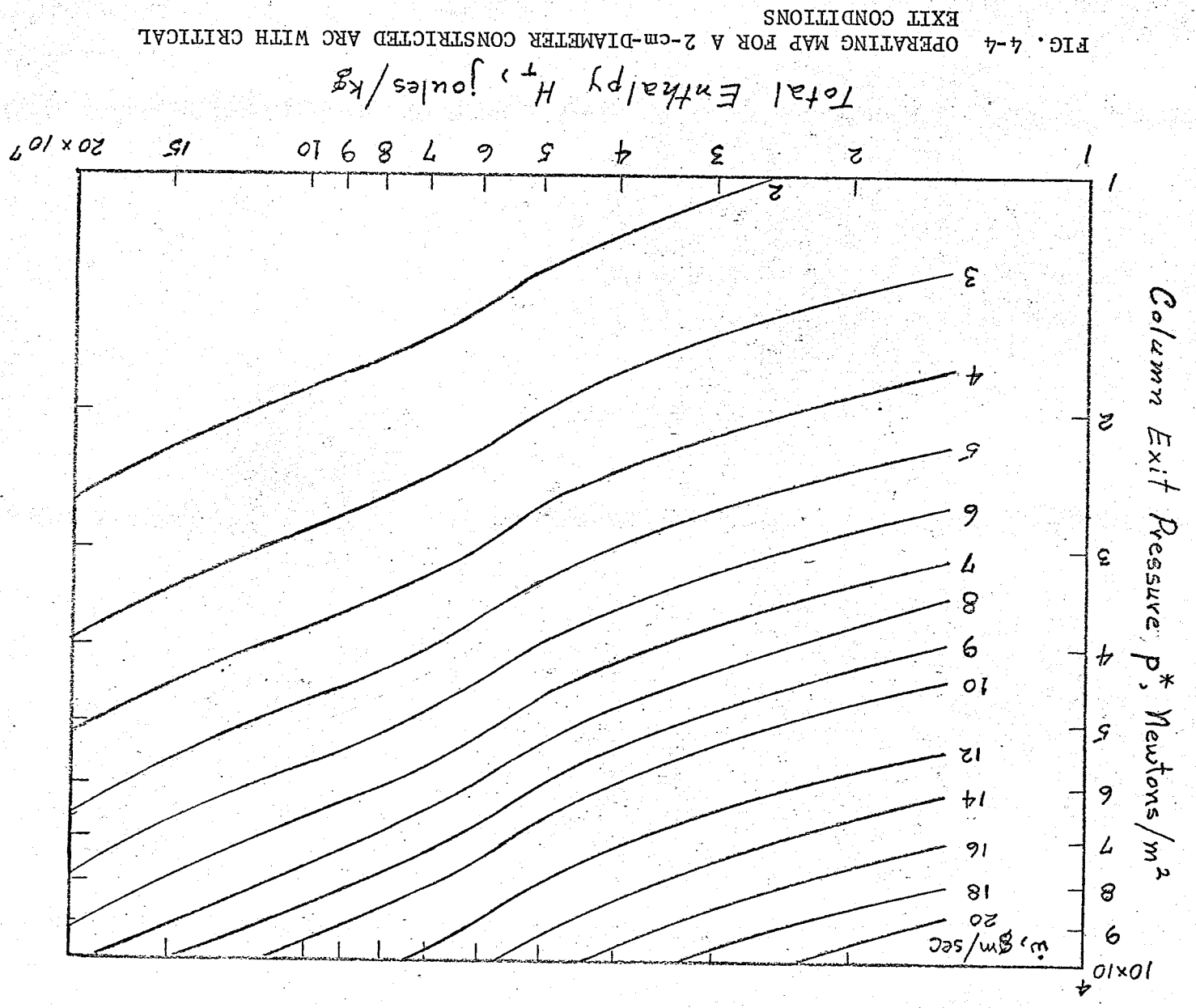


FIG. 4-4 OPERATING MAP FOR A 2-cm-DIAMETER CONSTRICTED ARC WITH CRITICAL EXIT CONDITIONS

map can be used to quickly estimate the heater throat enthalpy from the measured throat pressure and mass flow. This is very useful because the directly determined enthalpy based on the energy balance is not always readily available (e.g., for short runs or during a run). In addition, this method furnishes an independent simple check on the energy balance. The good consistency between the "throat pressure" enthalpy or "choked flow" enthalpy and the enthalpy determined directly from the energy balance is shown in Fig. 4-5. The scatter is within the experimental accuracy.

A map similar to that of Fig. 4-4, but with the power in gas (instead of the mass flow rate) as a parameter, can easily be drawn. On these maps, the possible operating range for a given heater in terms of maximum pressure versus enthalpy for given gas power can be sketched out.

4.2 Electric Parameters

The next task is the correlation of arc voltages and currents with the gas dynamic parameters and the constrictor dimensions.

The total voltage of the heater is given by the relation:

$$V_T = \int_0^L E dz + \phi_c + \phi_A + V_{BR} \quad (4-4)$$

where

V_T = total heater potential, (volt)

L = length of arc, (cm)

E = electric field, (volt/cm)

ϕ_c = cathode drop voltage, (volt)

ϕ_A = anode drop voltage, (volt)

V_{BR} = ballast resistor voltage (if applicable), (volt)

z = distance along the constrictor, (cm)

and the arc voltage is being considered to be represented by the term

$$V_A = \int_0^L E dz = \int_0^L E dz \quad \text{constrictor} \quad + \quad \int E dz \quad \text{nozzle} \quad (4-5)$$

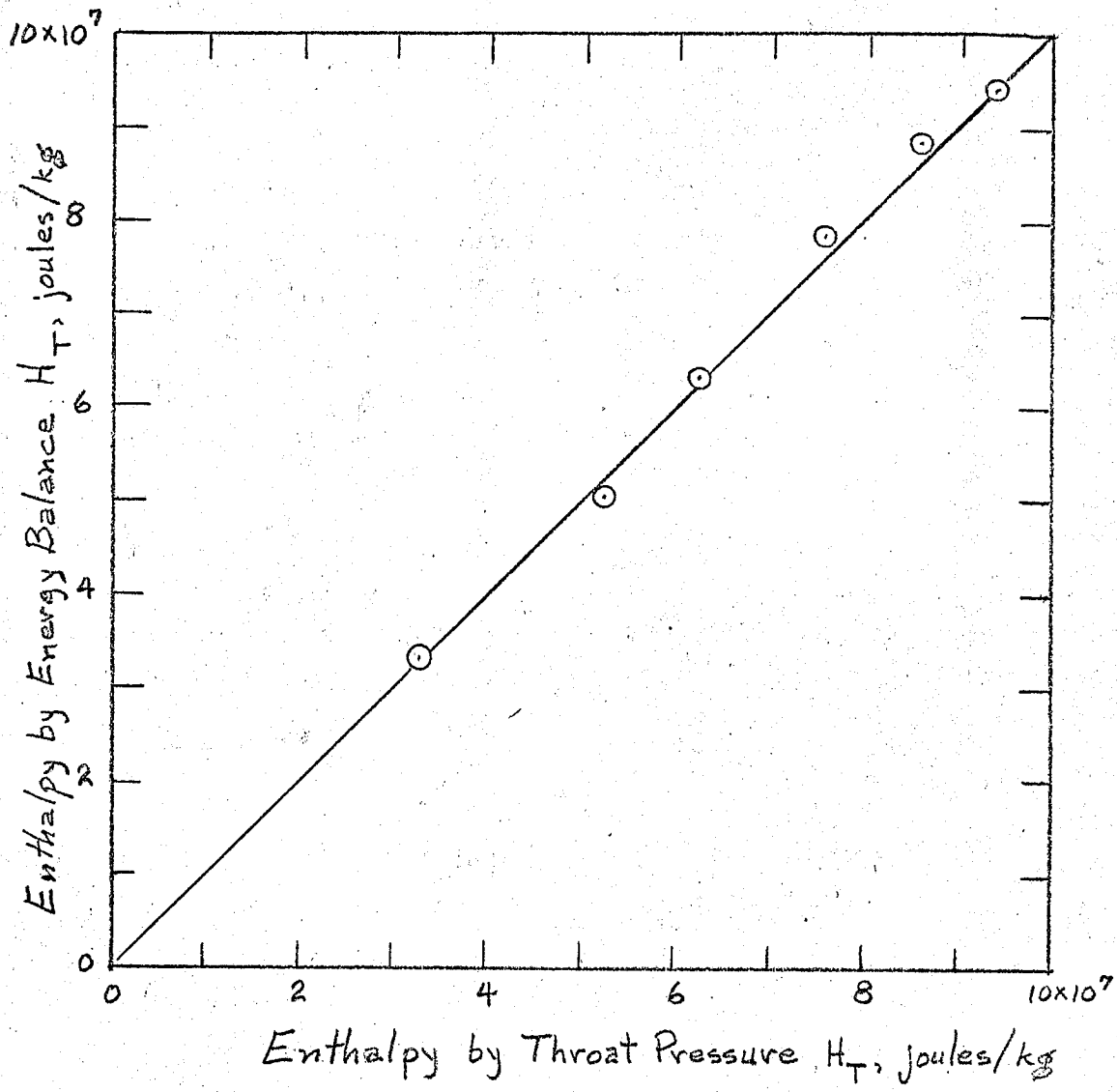


FIG. 4-5 COMPARISON BETWEEN THE ENTHALPY DETERMINED BY ENERGY BALANCE AND THE ENTHALPY DETERMINED BY THROAT PRESSURE MEASUREMENT FOR THE 2-cm-DIAMETER CONSTRICTED ARC HEATER WITH CRITICAL EXIT CONDITIONS

The latter breakdown is desirable when the design and optimization of the constrictor is discussed.

In Fig. 4-6 the total heater voltage is plotted vs current with mass flow as a parameter as measured during the test. In Fig. 4-7 the arc voltage alone (as defined above) is shown as a function of the arc current and the mass flow rate. The total heater voltage rises more steeply with current than the arc voltage because of the anode ballast resistors. The arc voltage rise with increasing current at constant mass flow is a pressure effect, as will be shown. In Fig. 4-8 the total heater input power is given as a function of the arc current and flow rate. The throat pressure as a function of arc current and flow rate is presented in Fig. 4-9.

In Fig. 4-10 the enthalpy is correlated with the arc current, with constant mass flow values as the parameter. The enthalpy curves have a slope of 1.0 while the pressure curves in Fig. 4-9 have a slope of roughly 0.5. These slopes agree with the results of the simple analytic relations (Section 2).

Gross correlation of all the presented data yields a result of great practical importance and of theoretical significance also. The arc voltages were plotted against the throat pressure, first with the enthalpy and then with the arc current as the constant parameter. The very significant result found (Fig. 4-11) is that the voltage is substantially a function only of the pressure, and is nearly independent of all the other parameters. This is true within the range of the parameters covered and within the accuracy required for design calculations. This result is expressed by

$$V_A \approx k \left(\frac{p^*}{p_a} \right)^{1/2} \quad (4-6)$$

where p_a is atmospheric reference pressure. It is evident that plotting the arc voltage against the inlet pressure would have yielded a similar correlation different only in the constant factor k .

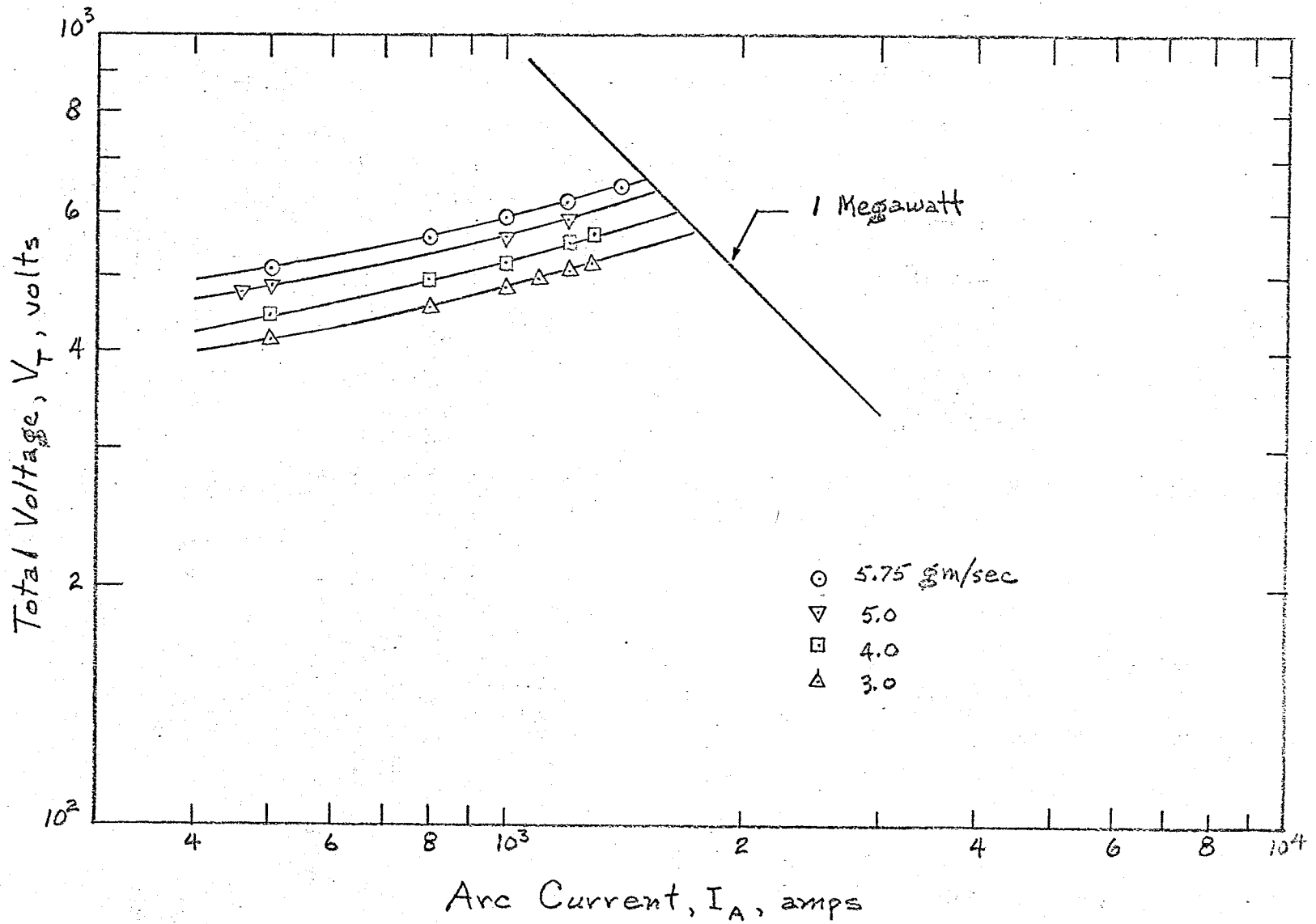


FIG. 4-6 CORRELATION BETWEEN TOTAL VOLTAGE AND ARC CURRENT FOR THE 2-cm-DIAMETER CONSTRICTED ARC HEATER

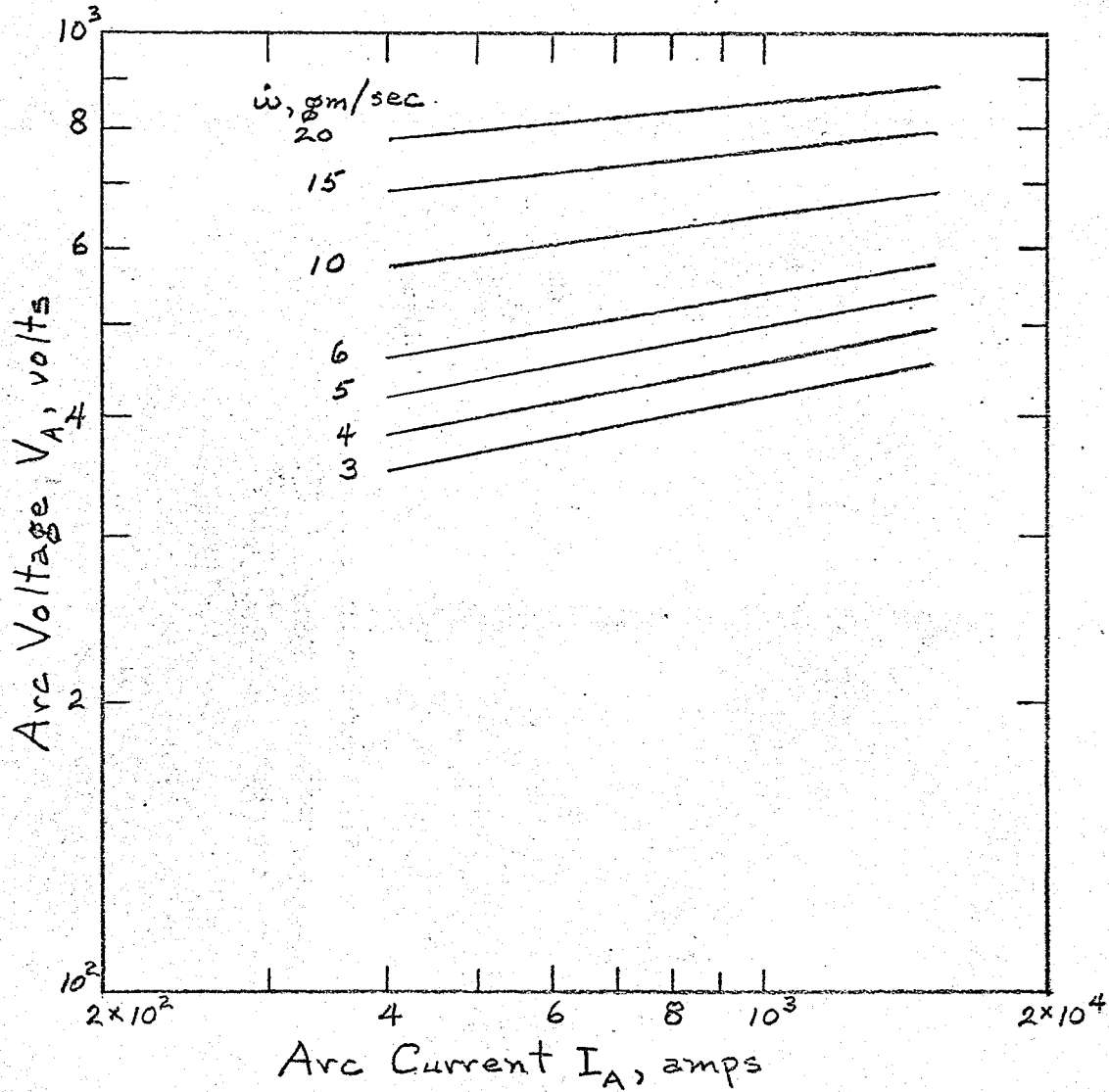


FIG. 4-7 CORRELATION BETWEEN ARC VOLTAGE AND ARC CURRENT FOR THE 2-cm-DIAMETER CONSTRICTED ARC HEATER

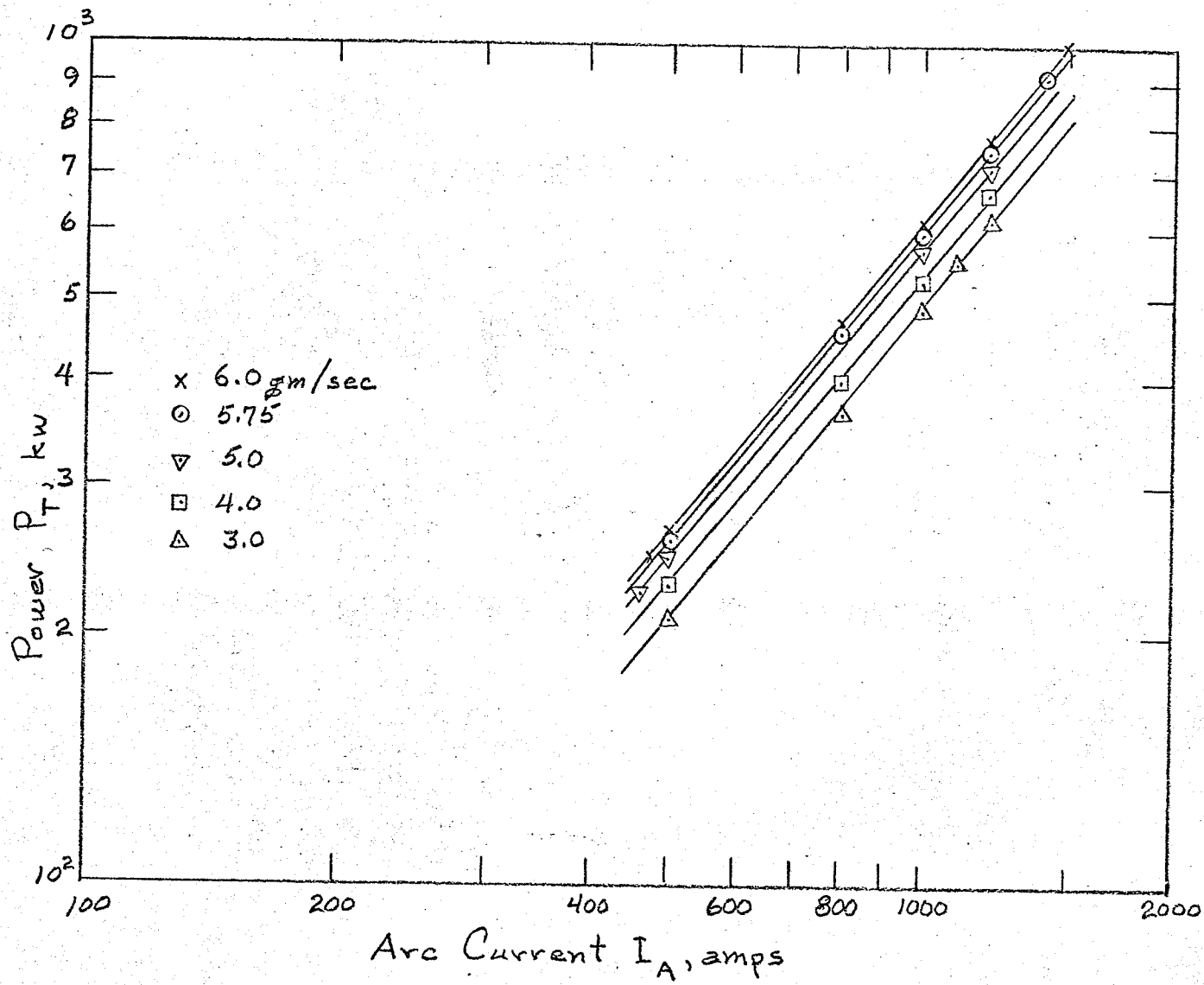


FIG. 4-8 CORRELATION BETWEEN TOTAL POWER AND ARC CURRENT FOR THE 2-cm-DIAMETER CONSTRICTED ARC HEATER

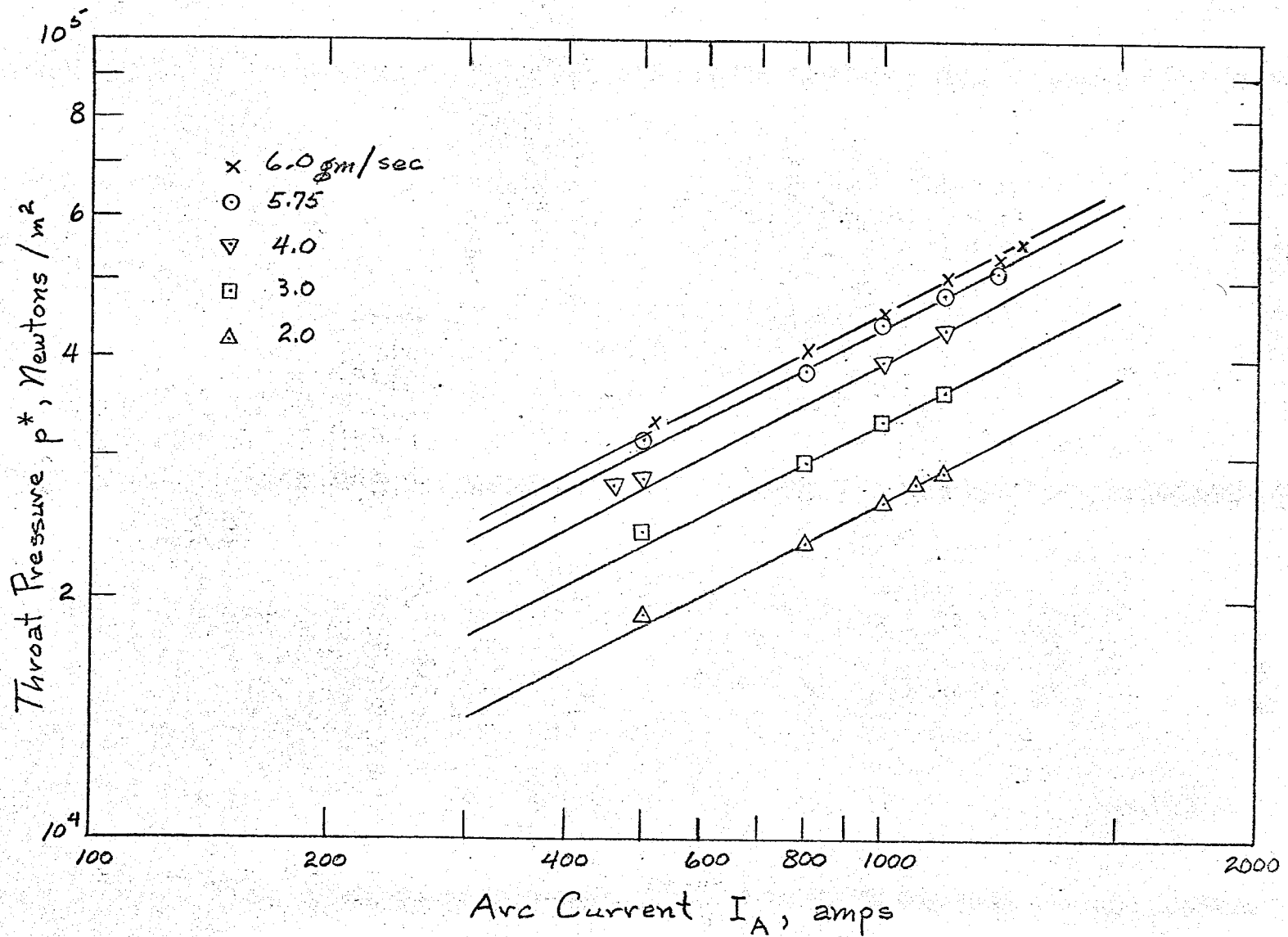


FIG. 4-9 CORRELATION BETWEEN THROAT PRESSURE AND ARC CURRENT FOR THE 2-cm-DIAMETER CONSTRUCTED ARC HEATER

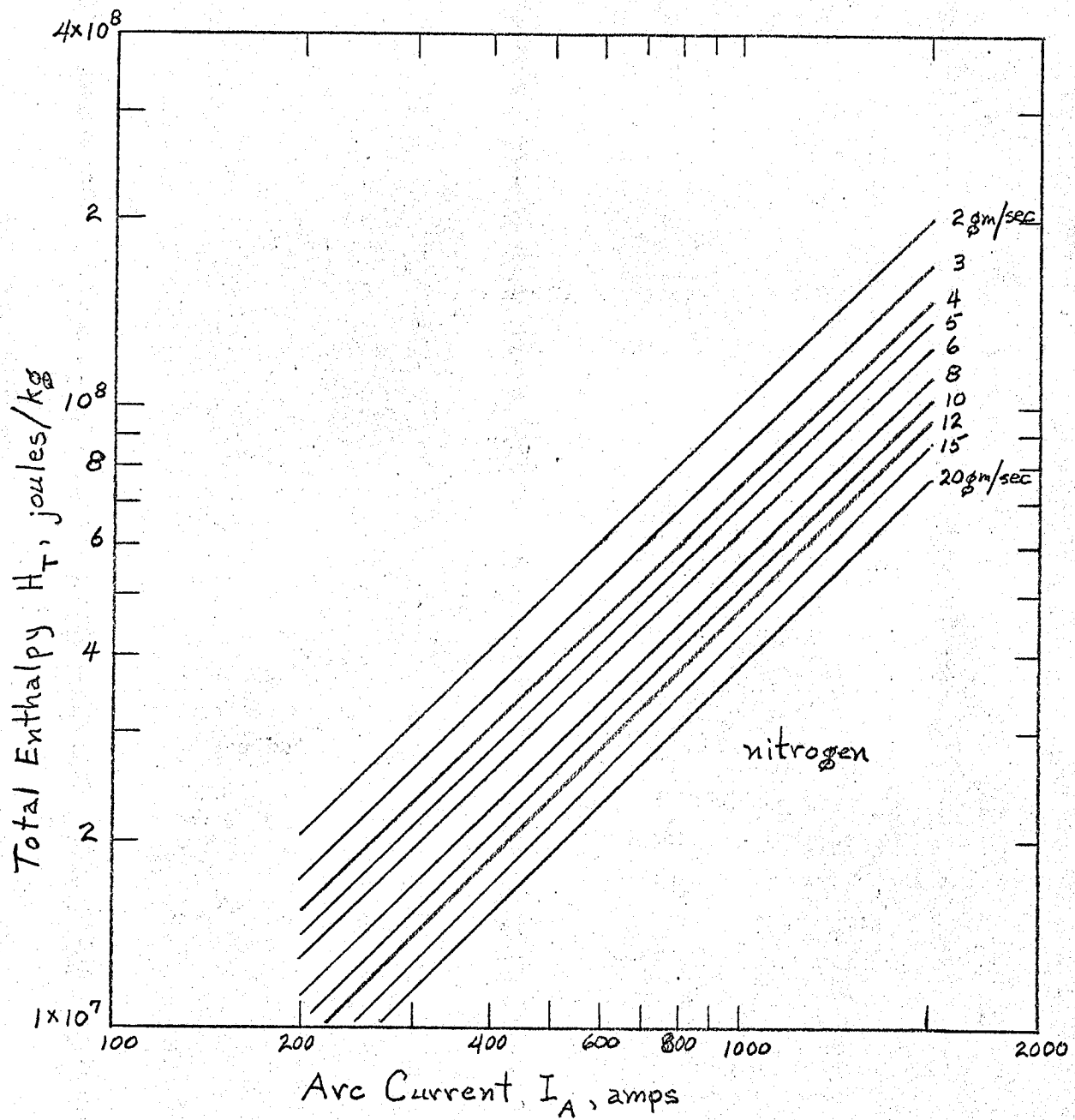


FIG. 4-10 CORRELATION BETWEEN TOTAL ENTHALPY AND ARC CURRENT FOR THE 2-cm-DIAMETER CONSTRICTED ARC HEATER

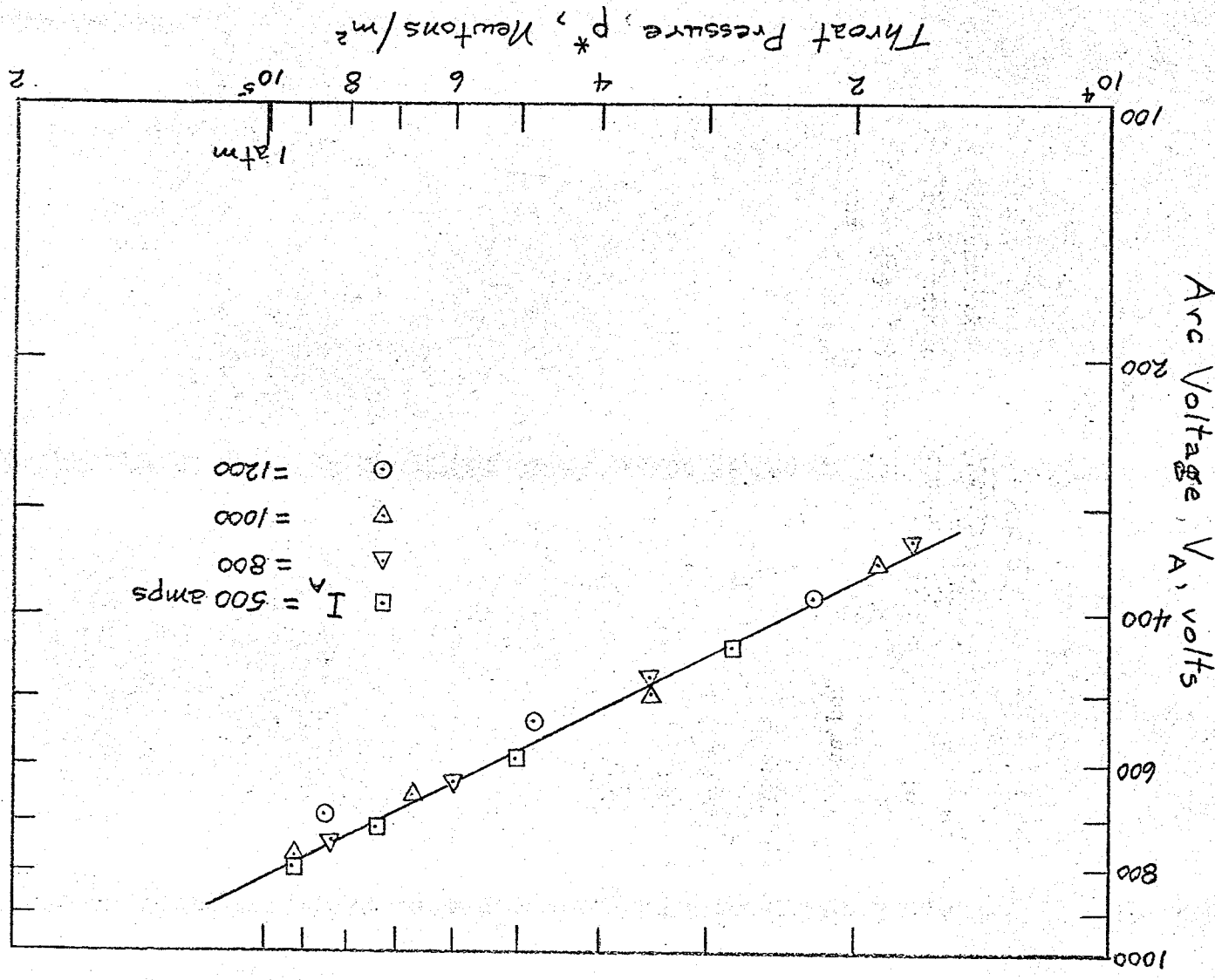


FIG. 4-11 CROSS-CORRELATION OF TEST DATA MEASURED WITH THE 2-CM-DIAMETER CONSTRICTED ARC HEATER

Since all pressures along the constrictor are proportional to the throat pressure, we can immediately conclude that the potential gradient, E , along the constrictor has the same functional dependence on the pressure, namely:

$$E(z) \approx k \left(\frac{p(z)}{p_0} \right)^{1/2} \quad (4-7)$$

This result agrees surprisingly well with the results of a very simple approximate analysis of large open arcs (Ref. 15, see also Section 2) and with many experimental data on open arcs. The simple theory for large open arcs gives $E \approx \sqrt{u/\sigma}$ which, at high temperatures (or high currents) is substantially a function only of the pressure and the gas type.

The same pressure dependence can be obtained from the detailed potential gradients along the constrictor of one single operating point. Fig. 4-12 shows the potential and voltage gradients along the constrictor at a current of 1008 A and a mass flow rate of 6g/sec of nitrogen. The gradients range from ~ 18.8 V/cm near the inlet to ~ 13.6 V/cm near the outlet. The ratio is almost precisely $\sqrt{2}$, i.e., the square root of the pressure ratio. This would indicate that, even in the inlet region of the heater near the cathode, the voltage gradients appear to be largely dependent only on the pressure.

Measurements along the constrictor, like those of Fig. 4-12, can furnish the constant $k_E = E(p) / (p/p_a)^{1/2}$ directly. This constant can also be obtained from the relation between arc voltage and pressure are shown in Fig. 4-11. Because of the almost linear pressure drop along the constrictor, one can write

$$\frac{p(z)}{p^*} \doteq 2 - \frac{z}{L} \quad (4-8)$$

Then the relation between measured arc voltage and throat pressure is

$$V_A = \int_0^L E(z) dz = \int_0^L k \left(\frac{p}{p_a} \right)^{1/2} (z) dz \quad (4-9)$$

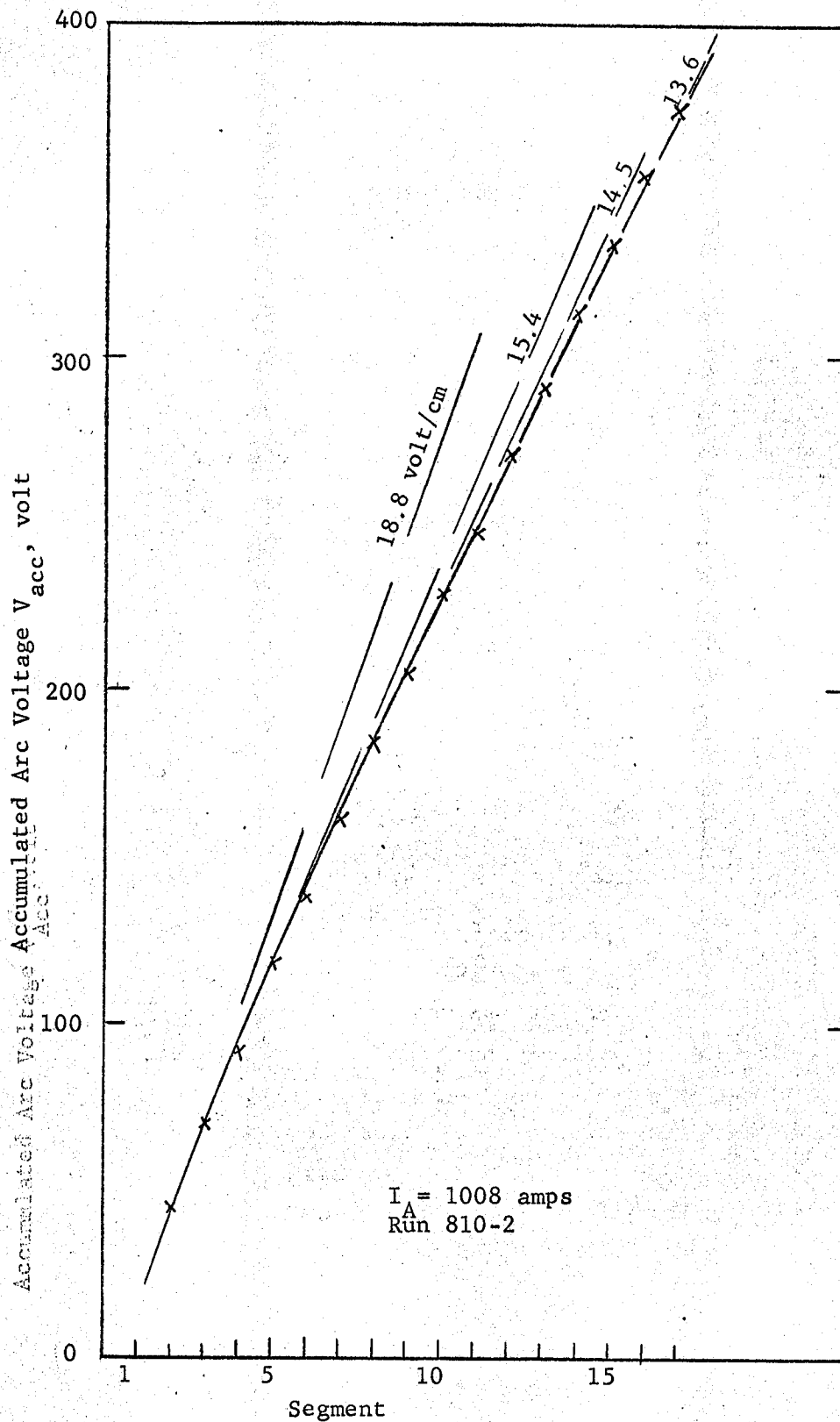


FIG.4-12 ACCUMULATED ARC VOLTAGE ALONG THE 2-cm DIAMETER CONSTRICTED ARC HEATER

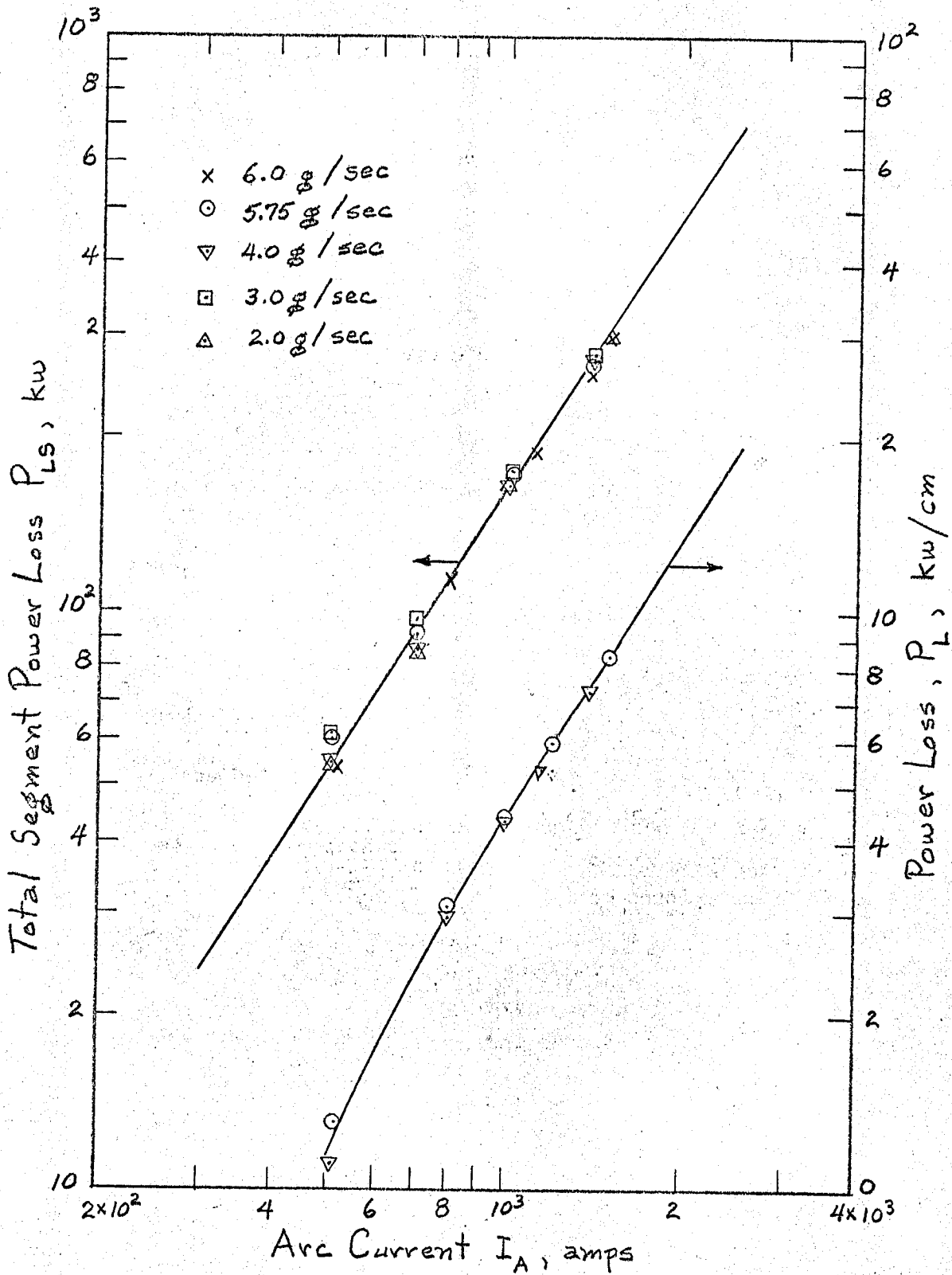


FIG. 4-13 CORRELATION OF ENERGY TRANSFER TO CONSTRICTOR WALL FOR THE 2-cm-DIAMETER CONSTRICTED ARC HEATER

Inserting Eq. 4-8 into Eq. 4-9 and setting $Z/L = \xi$,

$$V_A = k_E \left(\frac{p_a^*}{p_a} \right)^{1/2} L \int_0^1 (2 - \xi)^{1/2} d\xi \quad (4-10)$$

one finds

$$k_E = 0.807 \frac{V_A}{L} \left(\frac{p_a}{p_a^*} \right)^{1/2} \quad [V/m] \quad (4-11)$$

From the correlation of the test results, the constant k_E was found to be

$$k_E = 1.804 \times 10^3 \quad [V/m] \quad (4-12)$$

4.3 Energy Transfer to the Constrictor Wall

In large arc heaters, a most difficult quantity to comprehend analytically and to predict with any accuracy is the heat transfer to the constrictor wall. At the same time, this quantity is critical for the prediction of the attainable enthalpy-pressure performance envelope as well as the heater efficiency.

The complete energy transfer to the constrictor wall depends on a large number of parameters and conditions. Some of the more important ones are the temperature profile across the constrictor, the radiant emission and self absorption properties of all gas layers, the reflectivity, reactivity, and roughness of the constrictor wall surface, the magnitude of turbulent energy and mass transport (reacting species), the heat conduction and molecular recombination near the wall, and the symmetry and stability of the discharge and the flow. None of these can be reliably predicted yet by analytical means. Only for the limiting case of small, fully laminar, and conduction-governed arc columns with simple gases is there hope for achieving fairly reliable analytic predictions.

For the 1 MW size now under development, radiation is expected to dominate the energy transfer to the constrictor wall, but conduction and turbulent convection could still play an important part, especially near the constrictor outlet. The numerical computer calculations by Watson, which assume purely laminar flow, still predicted about half

of the heat transfer near the outlet to come from conduction (see Section 3). Unfortunately, the energy transfer rates produced by these computer calculations neither agree in magnitude nor in axial distribution with those measured in the 2 cm diameter constricted arc heater. We are therefore forced to rely to a large extent upon purely empirical correlations at this stage.

The important empirical discovery was made that the heat losses to the constrictor wall depend substantially only on the current, especially at the higher currents. This correlation is shown in Fig. 4-13, for the whole constrictor as well as for a group of 3 individual segments. These test results suggest an energy transfer dependency for the 2 cm diameter heater with current of the form

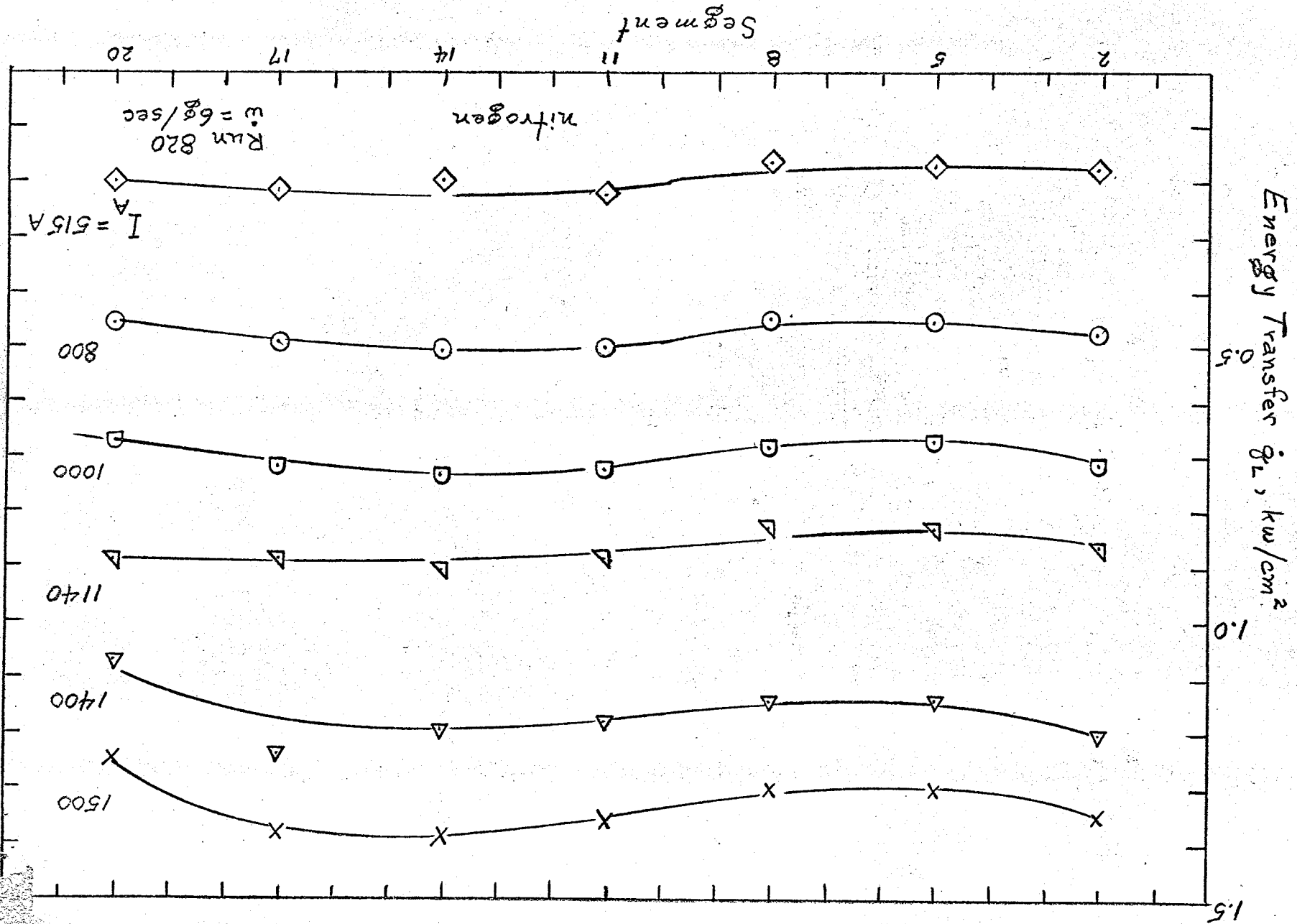
$$\dot{Q}_L \approx K_L I^n \quad (4-13)$$

where $n \sim 1.62$.

The same dependency must hold, of course, for the wall heat load of this heater. Thus, whatever effect pressure, mass flow, and enthalpy have on the energy transfer to the wall, these effects seem to appear only in such a combination as to be proportional to a simple power of the current, at least for a given arc constrictor which operates with choked outlet flow.

The first test of this is to look at the heat load distribution along the constrictor for different currents. This is shown in Fig. 4-14. Indeed, these heat load distributions are rather flat, and they are quite different from those predicted by the computer calculations (Section 3). Since the enthalpy increases while the pressure decreases along the length of the constrictor, the dependence of the energy transfer on these two parameters individually must somehow cancel out. The correlation of the wall heat loss with the enthalpy alone, which was a very good one for the small 1/2 cm research cascade, fails here, as is shown in Fig. 4-15. Such a correlation would be typical for a strongly conduction-governed or convection-governed energy transfer process.

FIG. 4-14 ENERGY TRANSFER TO CONSTRICTOR WALL OF THE 2-cm-DIAMETER CONSTRICTED ARC HEATER



The experimental wall heat loads on the 1 MW constrictor are seen (Fig. 4-14) to be moderate. Typically, they are ~ 1.3 to 1.4 KW/cm^2 for the 1500A runs, and proportionately lower at lower currents.

4.4 Heater Efficiency

With the empirical correlations which were found for the electric field and the energy transfer to the constrictor wall, it is now possible to arrive at a correlation between the operating parameters of the heater and the efficiency.

The total electric power consumed in the constricted arc heater is

$$P_T = I \left\{ \int_0^L E \, dz + \phi_A + \phi_C + R_B I \right\}$$

Inserting now the relation for the arc voltage from Eq. 4-11, solved for V_A ,

$$V_A = \int_0^L E \, dx = 1.239 \times L k_E \left(\frac{P^*}{P_a} \right)^{1/2} \quad (4-14)$$

The total power is then

$$P_T = I \left\{ 1.239 \times L k_E \left(\frac{P^*}{P_a} \right)^{1/2} + \phi_A + \phi_C + R_B I \right\} \quad (4-15)$$

The power in the gas is the difference between the total electric power and the total loss. The total loss is comprised of the electrode losses due to the electrode voltage drop, $I(\phi_A + \phi_C)$; the power into the ballast resistance, $R_B I^2$; and the energy transfer to the constrictor wall, which was found to be $L K_L I^n$. The efficiency of the heater is, therefore,

$$\begin{aligned} \eta &= \frac{P_T - P_L}{P_T} \\ &= 1 - \frac{L K_L I^{n-1} + (\phi_A + \phi_C + R_B I)}{1.239 \times L k_E \left(\frac{P^*}{P_a} \right)^{1/2} + (\phi_A + \phi_C + R_B I)} \end{aligned} \quad (4-16)$$

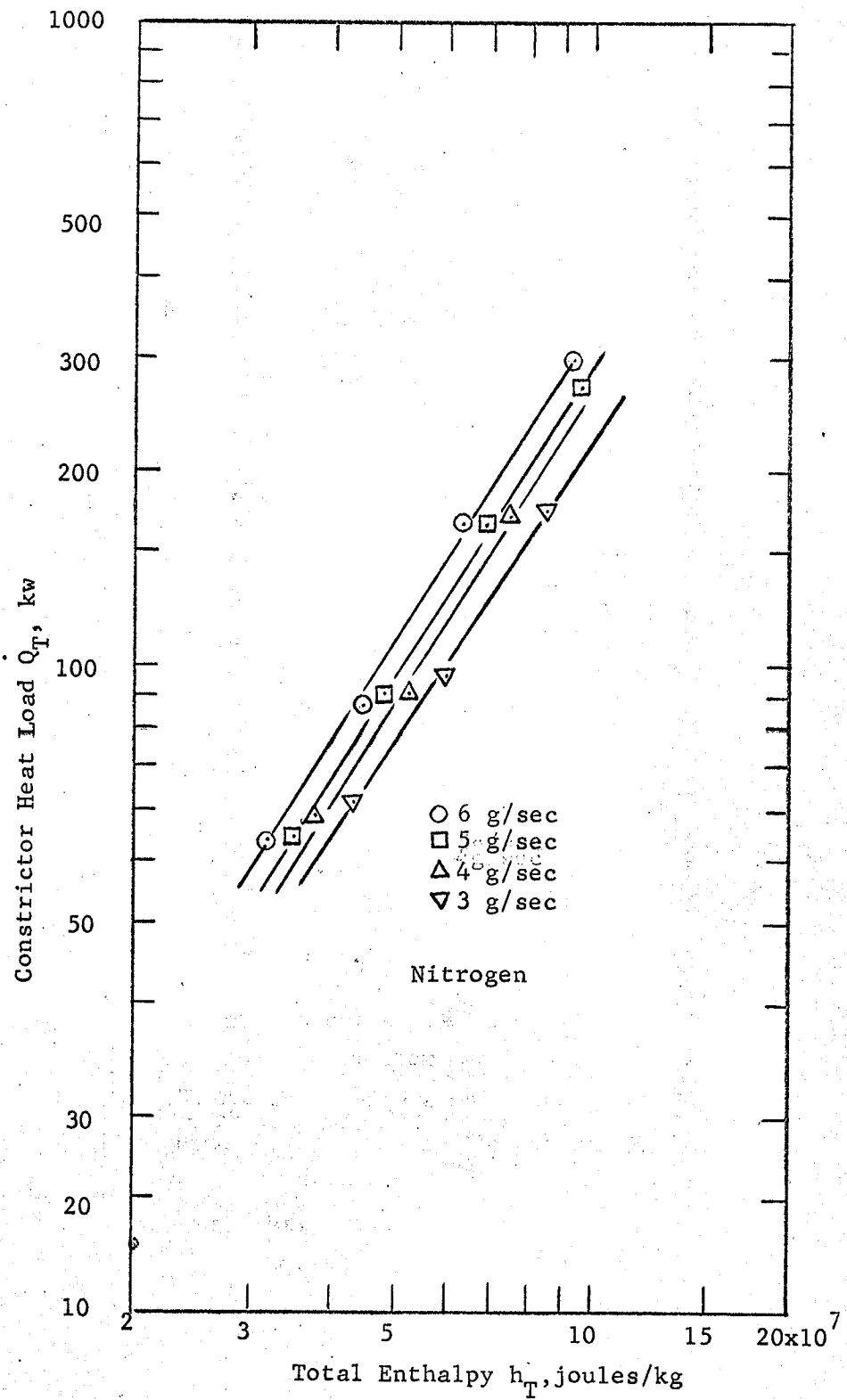


FIG.4-15 TOTAL POWER LOSS TO THE CONSTRICTOR WALL OF THE 2-cm DIAMETER CONSTRICTED ARC HEATER

From Eq. 4-16 one can recognize the dependency of the efficiency on the arc current. This agrees with the test results, which are shown in Fig. 4-16 and Fig. 4-17 as measured. In Fig. 4-18, the test data are cross-plotted with the correlations between throat pressure and arc current, which were shown in Fig. .

The semi-empirical equation (Eq. 4-16) and the test results show that the efficiency decreases somewhat with increasing current (at fixed p^*), and increases with increasing throat pressure (or mass flow) at fixed current.

FIG. 4-16 EFFICIENCY OF THE 2-cm-DIAMETER CONSTRICTED ARC HEATER AS A FUNCTION OF ARC CURRENT AND MASS FLOW RATE

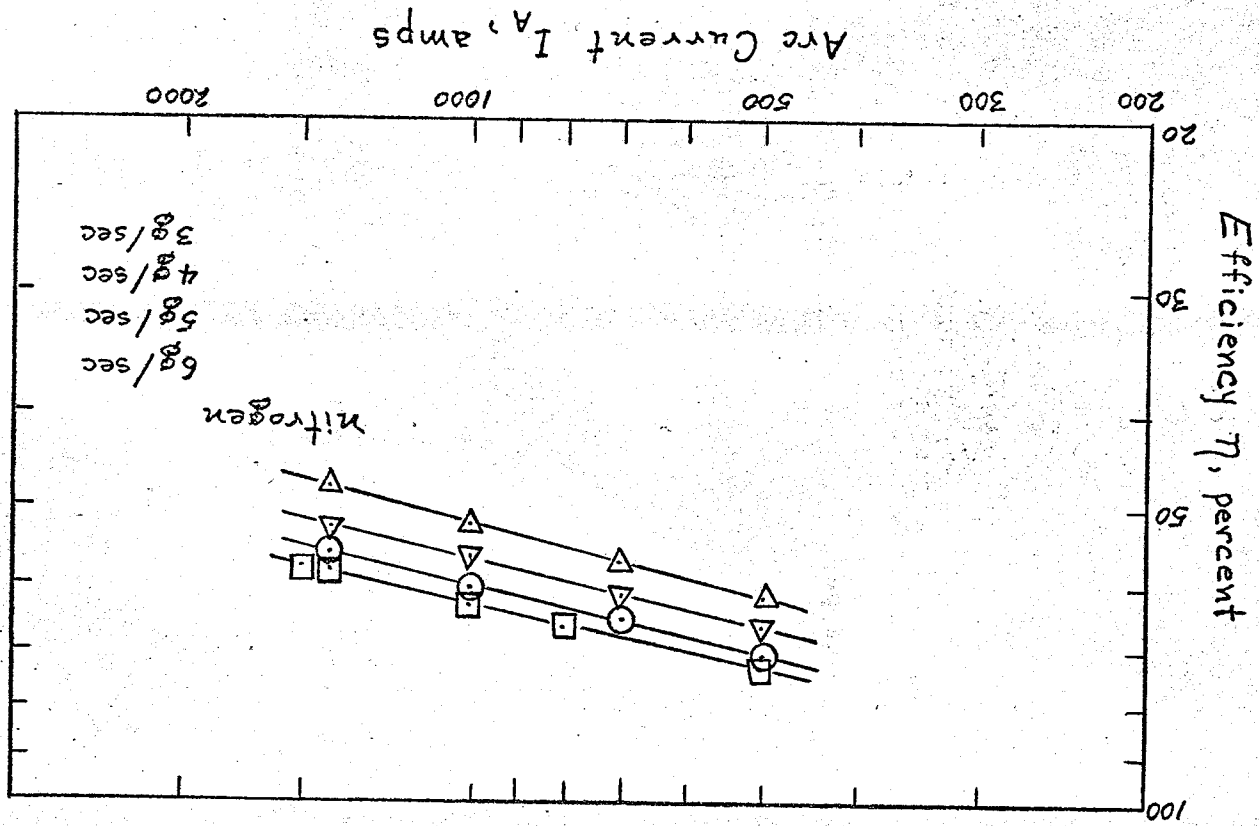


FIG. 4-17 EFFICIENCY OF THE 2-cm-DIAMETER CONSTRICTED ARC HEATER AS A FUNCTION OF TOTAL ENTHALPY AND MASS FLOW RATE

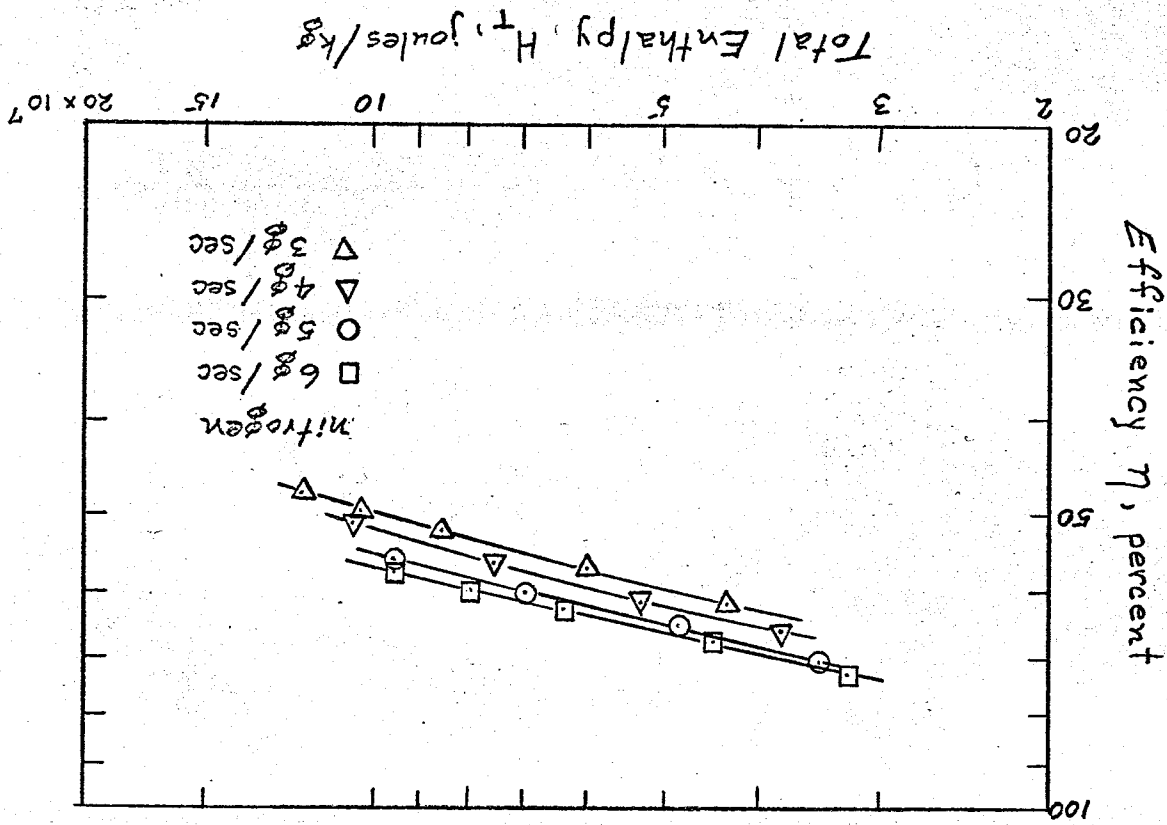
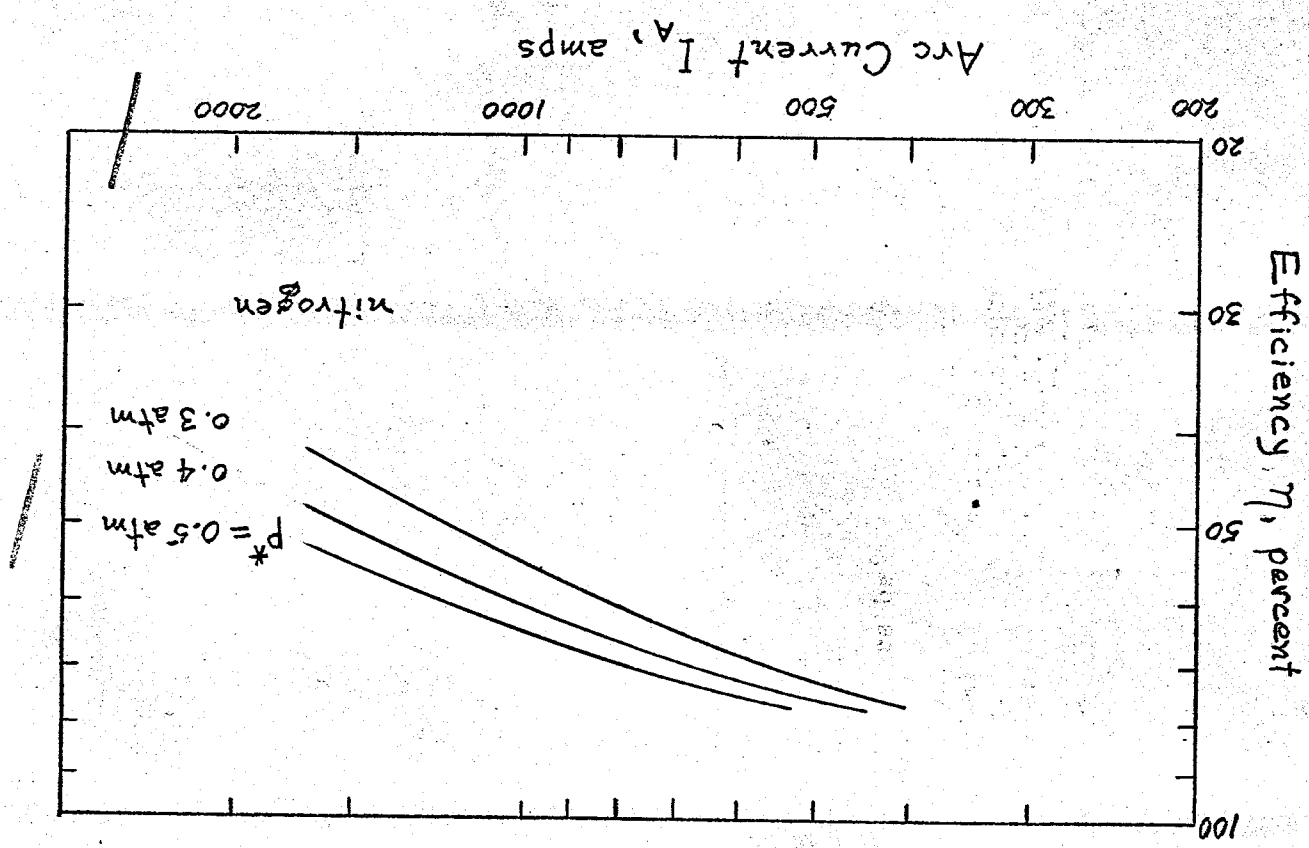


FIG. 4-18 EFFICIENCY OF THE 2-cm-DIAMETER CONSTRICTED ARC HEATER AS A FUNCTION OF ARC CURRENT AND THROAT PRESSURE



5. EXTRAPOLATION TO LARGE SIZE CONSTRICTED ARC HEATERS

The test results and the empirical relations established between all operating parameters for the 2 cm diameter constricted arc heater enable us to design constricted arc heaters of this size for a broad range of operating conditions and to predict their performance. The test results have furnished two "constants" for this size; which, however, must be assumed to be functions of the constrictor radius: the heat loss constant K_L and the electric field constant K_E .

The choked flow relations of Section 4.2 are considered valid and sufficiently accurate for the design of any contemplated heater size. This will establish the proper constrictor size for a given mass flow, enthalpy and throat pressure.

To carry out design calculations and performance predictions for larger heaters than the 1 MW, two additional relations are needed: one for the electric field along the constrictor, and one for the heat loss to the wall. With these two relations all necessary design and performance information can be obtained, such as:

- i) Constrictor length and voltage vs current, for given outlet gas conditions
- ii) Constrictor wall heat load distribution, and heating efficiency, vs current.

From these curves all other necessary heater calculations can be made except those for the electrodes which are still in the "black art" stage.

To obtain the necessary electric field and constrictor wall heat load relations, we must find the manner in which the corresponding relations from the 1 MW heater will scale with size. Based on the general considerations of Section 2 and other experience it is reasonable to postulate that the dependences of the electric field and the wall heat loss on the current and the pressure will remain valid, so that the size dependence will be only in the factors $K_L(R)$ and $K_E(R)$. This amounts to a "separation of variables" concept which is justified, at least to first order, from the nature of the pertinent equations. Thus we postulate

that expressions of the form

$$Q_L = K_L (R) \cdot f_L (I, \phi)$$

and

$$E = K_E (R) f_E (I, p)$$

will be adequate for our scaling, where f_L and f_E will be the same as those found for the 1 MW heater. The validity of this is really based on the assumptions that the 1MW and the 10 MW heater are in the same regime, namely predominantly governed by radiation rather than thermal conduction. Because of this we assume $f_L = f_L(I \text{ only})$ and $f_E = f_E(p \text{ only})$ as indicated above, because these dependencies were found to hold for the 1 MW heater over the range tested. The validity of this approach will be "checked" by appearing to the rather general (though complicated) scaling rules of Ref. 3. These rules have been numerically fitted to correlate the theoretical asymptotic arc column results of Yos, as is briefly described in Section 3.

The essential assumption made here is that the theoretical arc column results, even though they are not yet trustworthy for absolute values, should give us the size and pressure dependencies to a sufficient accuracy. In the past this has been borne out, as far as it has been tested.

Eventually, research tests with several heater sizes larger than 1 MW and over a wide range of pressures will have to be carried out and compared with more theoretical calculations, to verify the scaling rules and to gain better understanding of the high powered arcs. It is hoped that this can be carried out during the next phase of this project.

5.1 A Combined Analytical and Experimental Approach to the Design of Large Diameter Constricted Arc Heaters

Because of the lack of experimental data from large diameter constricted arcs and the lack of a complete analysis of the constricted arc column for this regime, the approximate dependency of the "constants"

K_A and K_E on the constrictor size has to be found from analytical considerations given in Ref. 3. The results of Ref. 3 are scaling rules which correlate the numerical arc column integrations of Yos (Ref. 1) and we will assume that these rules will be valid also for the arc heater case.

In Fig. 11 of Ref. 3 it is shown that for high currents, the electric field is a very weak function of the arc current and can therefore be expressed by

$$\frac{E R}{(1 + \xi)^{1/2}} p^{s/2} \approx C_1 \quad (5.1)$$

where from Fig. 13 of the same reference the relation for the function ξ can be found to be

$$\xi \approx C_2 R^2 p^t = \frac{\text{radiative heat loss}}{\text{conductive heat loss}} \quad (5.2)$$

For large diameters

$$\xi \gg 1$$

so that

$$1 + \xi \approx \xi$$

Inserting relation 5.2 into equation 5.1, one can find

$$\frac{E R p^{s/2}}{C_2^{1/2} R p^{t/2}} = C_1 \quad (5.3)$$

or

$$E = C_E p^{(t/2-s/2)} \quad (\text{see also Section 2}) \quad (5.4)$$

From Fig. 16 of Ref. 3

$$t \approx 1.31$$

$$s \approx 0.31$$

which finally results in an electric field dependency of

$$E \approx C_E p^{.50} \quad (5.5)$$

Thus, the scaling rules of Ref.3 agree at least in this important respect with both the 1 MW experimental data, with open arc experience and with the very simple "zero order" equations and scaling rules of Section 2. All the evidence therefore states that in the "high powered arc" regime, the potential gradient E should be independent of the size R or of the current, and depend substantially only on the pressure and the gas type. It also states that in this respect the 1 MW heater falls well into this regime (which previously was open to question).

Next we look for the scaling rule which applies to the wall heat loss calculation. From Fig 14 of Ref.3 we have

$$\frac{\dot{q}_A R}{(1 + \xi)} = f \left(\frac{I}{R(1 + \xi)^{1/2} p^{s/2}} \right) \quad (5.6)$$

But from the 1 MW experimental results we established that for a fixed radius of 1 cm

$$\dot{q}_A = K_A I^n \quad (5.7)$$

combining these two results gives

$$\frac{\dot{q}_A R}{1 + \xi} = C_3 \frac{I^n}{R^n (1 + \xi)^{n/2} p^{ns/2}} \quad (5.8)$$

If we assume again that $\xi \gg 1$ and remains roughly constant over a range

then

$$\begin{aligned} \dot{q}_A &= C_3 I^n \frac{(C_2 R^2 p^t)^{1-n/2}}{(R^{n+1})^{ns/2}} \\ &= C_3 C_2^{(1-n/2)} \frac{I^n}{R^{2n-1}} \times p^{t(1-n/2)-ns/2} \end{aligned} \quad (5.9)$$

From the 1 MW experimental results the exponent on the current dependence was

$$n = 1.617$$

so that, for $t \approx 1.31$ and $s \approx 0.31$, the exponent on the pressure becomes

$$t(1-n/2) - ns/2 = 1.31 \times .1915 - \frac{1.617 \times 0.31}{2} = \underline{0}$$

and the exponent of the radius R

$$2n-1 = \underline{2.234}$$

The complete relation for the energy transfer \dot{Q}_A is then

$$\dot{q}_A = C_Q \frac{I^{1.617}}{R^{2.234}} \quad \left[\text{kw/m}^2 \right] \quad (5.10)$$

Again we find with this relation a good agreement between test data and the derived approximation. The analytical relations indicate that there should not exist any dependence between energy transfer to the constrictor wall and the pressure. This was completely borne out by the test results. The interesting fact is that in relation 5.10 the constrictor radius exponent is actually solely determined by the experimentally found value of n, and the theoretical scaling rules. Comparing relation 5.7 with relation 5.10, the factor K_A is found to be the following function of the constrictor radius

$$K_A(R) = \frac{C_Q}{R^{2.234}} \quad (5.11)$$

where C_Q is a function of the gas.

From the test results for nitrogen we conclude that

$$C_{Q_{N_2}} = 3.38 \times 10^{-6} \quad \boxed{\text{MKS}} \quad (5.12)$$

Relations have now been established between the operating parameters and the physical parameters of constricted arcs in nitrogen. These relations are based on combinations of analytical and experimental correlations. They can now be employed in the design of constricted arc heaters of larger size. The procedure for this design and performance prediction will be outlined in the next subsection.

5.2 Design and Performance Calculations for a 10 Megawatt Constricted Arc Heater

The procedure for designing any size constricted arc heater in the Megawatt regime will be demonstrated in this section. From what has been said previously it is clear that there exists no unique design for any size heater. The design of a heater will generally be governed by several factors which are important in different cases. Some of these factors are: the required enthalpy-pressure envelope, the maximum power, current and voltage envelopes available, the required jet size and hence lowest allowable efficiency, the maximum heat load on the constrictor wall, the test gases to be used, and the required service life between overhauls.

For the 10 Megawatt constricted arc heater we tentatively establish the following design limits

Total input power P_T	10 Megawatt
Constrictor-Exit pressure p^*	0.5 atm
Gas	Air (Nitrogen)
Ballast resistance voltage drop V_B (if used)	70 volt

With these conditions given the following relations can be used to prepare design charts from which a specific design can be selected. From the relations:

$$V_T = V_A + \phi_A + \phi_C + V_B \quad (5.14)$$

and

$$V_T = P_T / I$$

and the arc voltage relation

$$V_A = L \left[1.239 k_E \left(\frac{p^*}{p_a} \right)^{\frac{1}{2}} \right] \quad (5.15)$$

a correlation between arc current I_A and constrictor length L is obtained which will result in a heater family of the chosen input power:

$$L = \left[\frac{P_T}{I_A} - \phi_A + \phi_C + V_B \right] / \left[1.239 k_E \left(\frac{p^*}{p_a} \right)^{\frac{1}{2}} \right] \quad (5.16)$$

This correlation is shown in Fig. 5.1.

With the energy transfer coefficient which is given by equation 5.12 and the constant given by relation 5.13 inserted into equation 5.16 we can find the efficiency to be

$$\eta = 1 - \frac{\frac{C_{Q_{N_2}}}{R} I_A^{0.617} \times 10^{+3} \frac{\phi_A + \phi_C + V_B}{L}}{1.239 k_E \left(\frac{p^*}{p_a} \right)^{\frac{1}{2}} + \frac{\phi_A + \phi_C + V_B}{L}} \quad (5.17)$$

The efficiency can be plotted using relation 5.16 for the elimination of the length parameter. This plot is shown in Fig. 5.2. The third design chart is constructed from the relation between the total enthalpy and the critical flow parameters

$$h_T = f \left(\frac{\dot{W}}{\pi R^2 p^*} \right)$$

which is given in Fig. 4.1 and the simple efficiency relation

$$\eta P_T = \dot{W} h_T$$

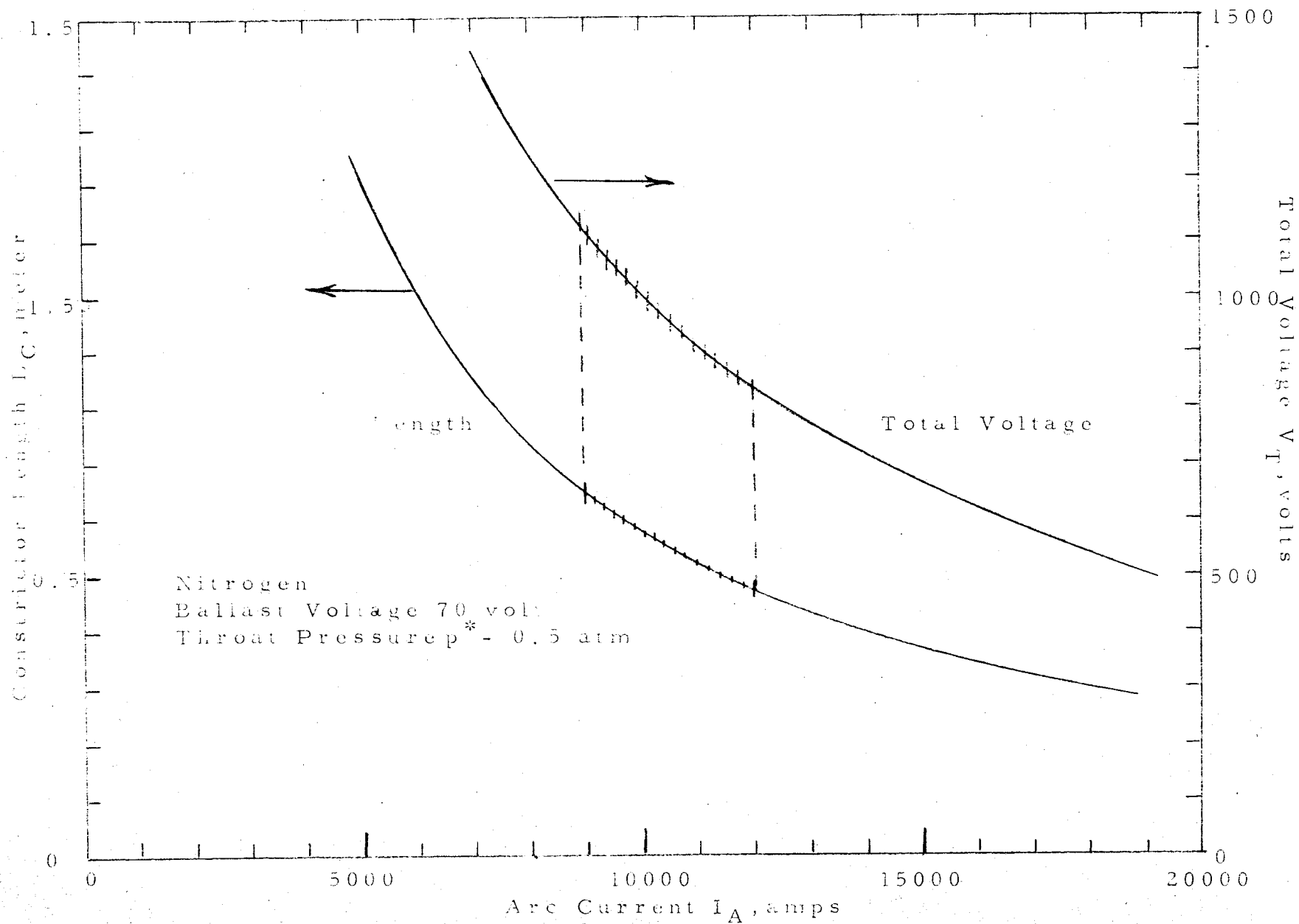


Fig. 5.1 Correlation Between Arc Current, Total Voltage, and Constrictor Length

For a 10 Megawatt Constricted Arc Heater

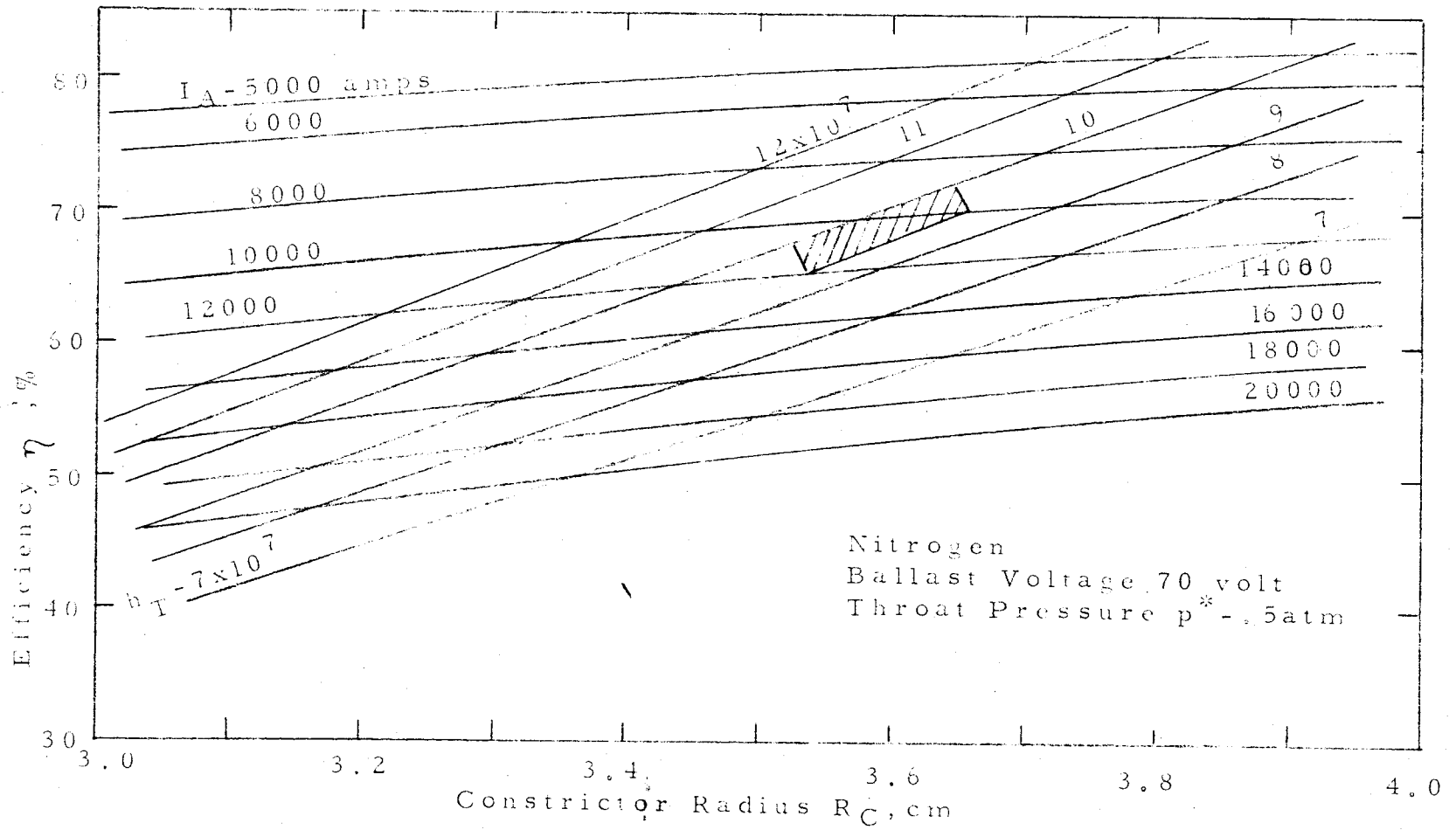


Fig 5.2 Design Chart for a 10 Megawatt Constricted Arc Heater
(Efficiency, Constrictor Radius, and Arc Current)

This plot is shown in Fig. 5.3. The final design chart correlates the heat load on the constrictor wall, Q_A , with the arc current I_A and the constrictor radius R_c . (Fig. 5.4)

Because of the use of boron nitride in the constrictor the general philosophy for the 10 megawatt heater design should be to hold the constrictor wall heat load to a minimum. From Fig. 5.4 this would indicate a low current and large constrictor diameter design. From Fig. 5.1 indications are that the arc current should fall into a range between 9000 to 12000 amps. From Fig 5.2 one can expect a heater efficiency of 65 to 72 %. For a total enthalpy between $9.3 \times 10^{+7}$ joules/kg to $10 \times 10^{+7}$ joules/kg we find from Fig. 5.3 a flow rate of 69.0 to 77.5 g/sec and a constrictor radius of 3.525 cm to 3.65 cm. From Fig. 5.4 the heater can be designed for a constrictor wall heat load between 1.2 kw/cm^2 to 2.4 kw/cm^2 . The constrictor length would be between 47 cm and 65 cm. The area enclosed by the above limits for the 10 megawatt constricted arc heater design has been mapped into Figs. 5.1, 5.2, 5.3 and 5.4.

The results of these new, semi-empirical heater design charts should now be compared with other possible ways of calculating the 10 MW heater, especially with the Ames computer results. This comparison is not yet complete.

As far as a comparison can be made, i.e., on the constrictor voltage and the wall heat load, the present design charts do agree with the scaling rules of Ref 3, as they should.

For the first computer run at Ames on the 10 MW level a set of assumed input variables was chosen which differ from the design region now believed to be near the optimum. By scaling up the 1 MW heater (as pointed out in Section 3) the current for the computer run was chosen at 17,000A. The results of this run do agree well with the design charts, but the 17,000A design would result in wall heat loads of about $6 \text{ to } 7 \text{ kw/cm}^2$, and in a somewhat lower efficiency than the design regime now considered best ($\sim 9000 - 12000 \text{ A}$). It was only after the empirical wall heat load and efficiency dependence on the current became available that it was clear that lower currents should be used. Therefore the results of the

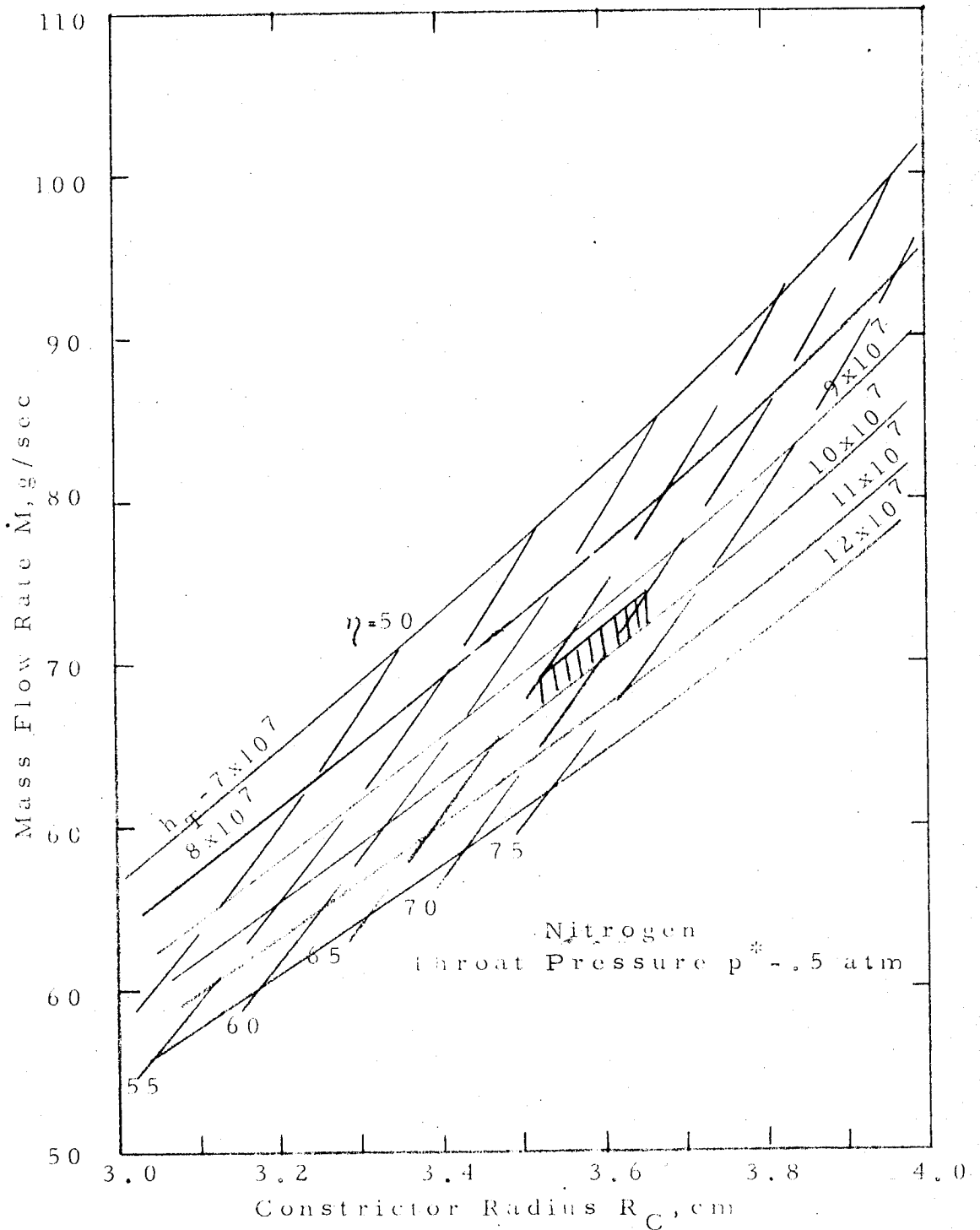


Fig. 5.3 Design Chart for a 10 Megawatt Constricted Arc Heater (Mass Flow Rate, Constrictor Radius, Total Enthalpy, and Efficiency)

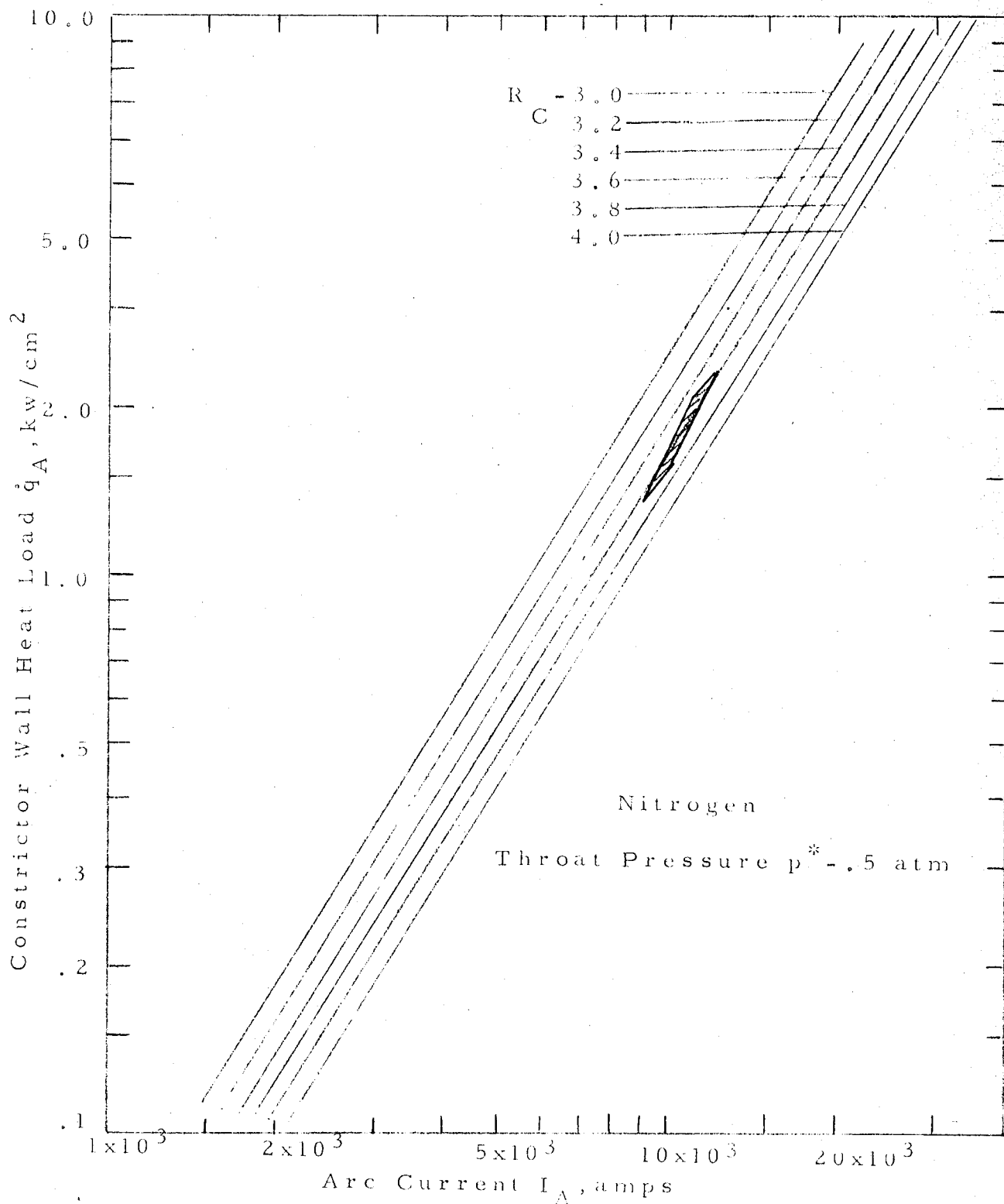


Fig. 5.4 Design Chart For A 10 Megawatt Constricted Arc Heater (Constrictor Wall Heat Load, Arc Current, and Constrictor Radius)

first 10 MW computer run do not fall into the now most interesting current regime. Additional computer runs in the 9000-12000A region should now be planned. It is gratifying, however, that the computer results do appear to agree quite well with the semi-empirical design charts, as far as we can tell at present.

The new design results and performance predictions make the 10 MW high enthalpy heater much more feasible and promising than did the numbers previously estimated for the higher current designs. The wall heat loads of about 2 kw/cm^2 along the constrictor should present no severe problems for either the segments or the insulators, even in regions where there is a high oxygen concentration.

The anode(s) should present no insurmountable problems, since they can be both scaled to higher currents and subdivided. Only at much higher pressures will the anodes become critical.

The cathode does present a definite problem for the 10,000 + ampere regime. Here the pressure must be at least of the order of one atmosphere, and subdividing is generally more difficult. However, a 10,000 ampere cathode should not be an impossible task at the 1-2 atmosphere level. Also, it can be hoped that studies on cathodes now in progress in several laboratories will contribute to the solution.

Thus the 10 MW high enthalpy heater now looks generally feasible and potentially efficient. The development of such a heater can now be planned with a good probability of success.

6. CONCLUSIONS

1. The 1 mw laboratory model high enthalpy heater performed very well, over the range of currents (500-1500 A) and mass flow values (3-12 gm/sec) tested. The efficiencies and enthalpies exceeded the design values slightly. The highest segment heat loads were below the estimated values.

2. The anodes, constrictor, and nozzle segments performed without appreciable erosion or damage through many hours of operation, except for two early runs during which a few anode pins and one constrictor were accidentally damaged.

The cathode did, however, suffer some measurable erosion. It is expected that it will meet the five hour life requirement. Some of the erosion was due to oxygen injection too close to the cathode. This problem has been corrected.

3. After early cathode problems were resolved, all subsequent experimental points from the heater cross correlated on perfectly smooth curves, and were repeatable within measurement accuracy.

4. Three important correlations were obtained:

a) The mass flow vs enthalpy and pressure correlated very closely with one dimensional choked flow calculations for equilibrium nitrogen, multiplied by an empirical correction factor (.936).

b) The total energy loss to the constrictor wall was found to be a function of the current only, within a narrow band of scatter ($\dot{Q}_L = K_L \times I^{1.617}$)

c) The arc potential gradient was found to be dependent only on the pressure, for the full range of currents and

and mass flow values tested ($E = K_E \times (p^*/p_a)^{.5}$)

5. The theoretical (computer) results did not, in general, agree with the measured data either in absolute values or in general shape. With the "Maecker like" transport properties the predicted constrictor wall heat loads were too low.

With the "Mixed" (Maecker-Yos) properties the calculated radiation heat loads came close to the total measured values in both value and axial distribution, but the calculated corrective component appears much too large. The calculated electric fields were low in most cases, by about 20 per cent, and the length to the choking point deviated greatly from the experiments.

However, the calculated results show the observed voltage dependence on the pressure only.

6. A design and performance calculation method and charts for larger heaters (10 MW) were evolved from the semi-empirical correlations of the 1 mw heater results, together with scaling rules based on theoretical calculations to include the effect of heater size.

7. The design calculations for a 10 mw high enthalpy heater based on these charts indicate this heater to be entirely feasible and promising. The most severe engineering problem likely to be encountered will be on the cathode. The calculated efficiencies run higher than those of the present 1 mw size heater at the same enthalpies and pressures, they are generally 85 per cent or higher. The constrictor wall heat loads

($\sim 2 \text{ kw/cm}^2$) are quite moderate and are considerably lower than initially estimated. Both the higher efficiencies and the lower wall heat loads resulted from lowering the current and increasing the heater length.

8. Based on the findings it is recommended that a development program for a 10 mw high enthalpy materials test heater be initiated.

REFERENCES

1. AVCO, RAD Division, Theoretical and Experimental Investigation of Arc Plasma Generation Technology, Part II, Vol. 2, ASD-TDR-62-729, Sept. 1963 (U)
2. L. A. King, "The Voltage Gradient of the Free Burning Arc for Air or Nitrogen," Proceedings of the Fifth International Conference on Ionization Phenomena in Gases, Vol. 1, North-Holland Publication Company, Amsterdam, 1962
3. G. L. Marlotte, et al., "Basic Research on Gas Flows Through Electric Arcs - Phase III: Studies of the Inlet Region," Electro-Optical Systems, March 1965, USAF Contract AF 33(657)-7940, Project 70192, to be issued as Aerospace Research Laboratories Report
4. H. Stine, V. Watson, "Theoretical Enthalpy Distribution of Air in Steady Flow Along the Axis of a Direct-Current Electric Arc," NASA Technical Note TN D-1331, August 1962
5. G. L. Cann, R. D. Buhler, R. H. Harder and R. A. Moore, "Basic Research on Gas Flows through Electric Arcs Hot Gas Containment Limits," Aerospace Research Laboratories Report No. ARL 64-49, March, 1964
6. J. G. Skifstad and S. N. B. Murthy, "Analysis of Arc-Heating Phenomena in a Tube," Vol. NS 11, IEEE Trans. Nucl. Sci., (1) pp. 92-103, 1964; also J. G. Skifstad, "Analysis of the Flow and Heat Transfer Processes in a Tube Arc for Heating a Gas Stream," AIAA Journal (TN) Vol. I, No. 8, pp 1906-1909, August 1963
7. H. E. Weber, "Growth of an Arc Column in Flow and Pressure Fields," AGARD Specialist Meeting on Arc Heaters and MHD Accelerators for Aerodynamic Purposes, Rhode-Saint Genese, Belgium, September 1964. Published as AGARDograph No. 84, pp 845-881
8. H. A. Stine, V. R. Watson and C. E. Shepard, "Effect of Axial Flow on the Behavior of the Wall Constricted Arc," (paper presented at the AGARD Specialists Meeting on Arc Heaters and MHD Accelerators for the Aerodynamic Purposes, Rhode-Saint-Genese, Belgium, 21-23 Sept. 1964)
9. V. R. Watson, "Comparison of Detailed Numerical Solutions with Simplified Theories for the Characteristics of the Constricted Arc Plasma Generator" (paper presented at 1965 Heat Transfer and Fluid Mechanics Institute, University of California, Los Angeles, California, 21-23 June 1965)

REFERENCES (Contd)

10. Electro-Optical Systems, Inc., Basic Research on Gas Flows Through Electric Arcs - Measurement Techniques and Analytical Procedures, by G. L. Marlotte and M. L. Dalton, ARL 64-208, Contract AF 33(657)-7940, Pasadena, California, Nov. 1964
11. J. Uhlenbusch, "Berechnung der Materialfunktionen eines Stickstoff und Argonplasmas aus gemessenen Bogendaten," Z. Physik, Vol. 179, 1964, pp. 347-366
12. Electro-Optical Systems, Inc., High Enthalpy Gas Heater, by R. Richter and R. D. Buhler, First and Second Bi-Monthly Reports on Contract NAS 9-3564, Pasadena, Calif., 14 January 1965 and 12 March 1965, respectively
13. K. S. Drellishak, D. P. Aeschlman, Ali Bulent Cambel, "Tables of Thermodynamic Properties of Argon, Nitrogen, and Oxygen Plasmas" AEDC-TDR-64-12, January 1964
14. J. Hilsenrath and M. Klein, "Tables of Thermodynamic Properties of Air from 90 to 15,000^oK" AEDC-TDR-61-103, August 1961
15. R. D. Buhler, "Simple Scaling Relations for a High Current Arc in a Parallel Gas Flow," Technical Note on Contract AF 33(657)-7940, to be published